

Glass beads as model carrier in dry powder inhalers

Dissertation

to obtain the academic degree of “Doktorin der Naturwissenschaften” at
Graz University of Technology

Mag.pharm. Sarah Zellnitz

Research Center Pharmaceutical Engineering GmbH

Graz, Austria

2014

Sarah Zellnitz

Glass beads as model carrier in dry powder inhalers

Dissertation

First assessor and supervisor

Prof. Mag. Dr.rer.nat. Nora Anne Urbanetz

Research Center Pharmaceutical Engineering GmbH

Second assessor

Prof. Mag. Dr.phil.nat. Andres Zimmer

Department of Pharmaceutical Technology

University of Graz

Copyright ©2014 by Sarah Zellnitz

All rights reserved. No part of the material protected by this copyright notice may be reproduced or utilized in any form or by any means, electronically or mechanical, including photocopying, recording or by any information storage and retrieval system with written permission from the author.

Deutsche Fassung:
Beschluss der Curricula-Kommission für Bachelor-, Master- und Diplomstudien vom 10.11.2008
Genehmigung des Senates am 1.12.2008

EIDESSTÄTLICHE ERKLÄRUNG

Ich erkläre an Eides statt, dass ich die vorliegende Arbeit selbstständig verfasst, andere als die angegebenen Quellen/Hilfsmittel nicht benutzt, und die den benutzten Quellen wörtlich und inhaltlich entnommenen Stellen als solche kenntlich gemacht habe.

Graz, am

.....
(Unterschrift)

Englische Fassung:

STATUTORY DECLARATION

I declare that I have authored this thesis independently, that I have not used other than the declared sources / resources, and that I have explicitly marked all material which has been quoted either literally or by content from the used sources.

.....
date

.....
(signature)

Acknowledgments

I would never have been able to finish my dissertation without the guidance of my supervisor, help from friends, and support from my family.

First of all I want to express my gratitude to my supervisor Nora Urbanetz for granting me the possibility to conduct my PhD thesis, for her guidance, her caring, her patience, and for the nice moments we shared at conferences and meetings.

I thank Johannes Khinast for the opportunity to work at the Institute of Process and Particle Engineering for two years and also Thomas Klein for giving me the chance to finish my thesis at the RCPE.

Further thank goes to my collaboration partner Martin Sommerfeld, although the meetings were limited, I have greatly benefited from our scientific discussions. I also received generous support from Michael Kappl, who guided me through the AFM measurements. Furthermore I would like to show my greatest appreciation to Zinaida Kutelova for supporting me with the silanization of my glass substrates. I also would like to thank Jakob Redlinger-Pohn for the great work he did regarding physical surface modification and many laughs. Moreover, I want to thank my student assistants for lightening my workload in the lab.

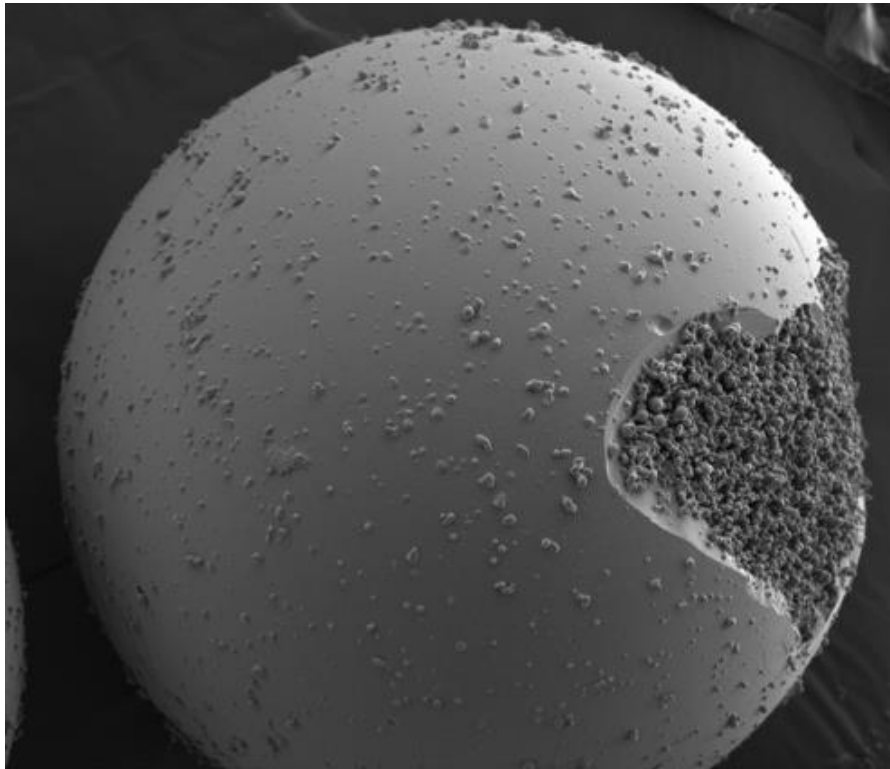
Special thanks also to Michael Piller and Christoph Neubauer for different measurements and support in the laboratory, Viktoria Marko for performing the HPLC analysis and Michaela Cibulka, Adela Roller and Silvia Houben for organizational assistance.

In my daily work I have been blessed with a friendly and cheerful working environment. Therefore I want to thank all my colleagues from RCPE and IPPT, for their support, many interesting and inspiring discussion, the nice coffee breaks and lunch times at the institute or at ZAPO. Especially, I want to thank Stefan and Eva who were always there for me and helped me with scientific problems, but also for the nice and funny moments we shared.

I would like to offer my special thanks to Josef, who always believed in me, encouraged me and helped me with his positivity in so many situations during the last years.

To all my friends, thank you for listening, offering me advice, supporting me through this entire process and being there whenever I needed a friend.

Finally I want to thank all my family, my parents Helga & Gert, my brother Stefan and my sister Lisa for believing in me and supporting me emotionally in any imaginable way. I am especially grateful to my parents and grandparents, who in addition to the emotional support also supported me generously with some “spending money”.



Thank you!

Abstract

In order to reach the deep lung, active pharmaceutical ingredient (API) particles have to exhibit an aerodynamic diameter of 1 μ m to 5 μ m. Particles of this size however are rather cohesive and possess poor flow properties, what challenges reproducible dosing in dry powder inhalers (DPIs), which is carried out volumetrically. To still guarantee reproducible dosing carrier based formulations, where the small API particles are attached to larger carrier particles with adequate flowability, have been invented. But in order to reach their target site, the deep lung API particles must be detached again from the carrier during inhalation. Thus, interparticle interactions play a crucial role in carrier based formulations for dry powder inhalers. Interparticle interactions on the one hand have to be high enough that the API is attached onto the carrier during handling, transport and dosing, and on the other hand low enough that drug detachment during inhalation is guaranteed. As the surface properties of carrier and API particles largely affect interparticle interactions, the aim of the present work is tailoring interparticle interactions via the surface modification of glass beads used as model carriers. Glass beads were chosen as model carrier because they allow various prospects of chemical and physical surface modification, without affecting other properties that may also influence interparticle interactions like particle size and shape. By this means the changes in interparticle interactions between API and carrier and thus drug detachment can be attributed solely to the surface properties of the glass beads used. In that way glass beads should help to bring the development of DPIs on a scientific level.

Kurzfassung

Damit Wirkstoffpartikeln bei der Inhalation über die Lunge aufgenommen werden können, müssen sie eine Partikelgröße zwischen $1\mu\text{m}$ und $5\mu\text{m}$ aufweisen. Partikel dieser Größe sind jedoch kohäsiv und fließen schlecht, was sich negativ auf die Reproduzierbarkeit der Dosierung auswirken kann, da diese in Pulverinhalatoren meist volumetrisch erfolgt. Um dennoch eine gleichmäßige Dosierung zu gewährleisten, werden die Wirkstoffpartikel in einem Mischprozess auf einen gröberen Träger, der gute Fließeigenschaften aufweist, aufgebracht. Damit der Wirkstoff während der Inhalation die Lunge erreichen kann, muss er sich während der Inhalation wieder vom Träger ablösen. Demnach spielen interpartikuläre Kräfte eine sehr große Rolle in diesen trägerbasierten Formulierungen für Pulverinhalatoren. Die interpartikulären Kräfte zwischen Wirkstoff und Träger müssen einerseits so groß sein, dass der Wirkstoff auf dem Träger während des Herstellungsprozesses und dem Dosierprozess haftet, andererseits jedoch so klein, dass er sich bei Inhalation wieder löst und in die Lunge gelangt. Es ist bekannt, dass die Oberflächeneigenschaften der wechselwirkenden Partner von entscheidender Bedeutung für die interpartikulären Kräfte zwischen Wirkstoff und Träger sind. Ziel dieser Forschungsarbeit ist daher die Steuerung dieser interpartikulären Wechselwirkungen über die Modifizierung der Oberflächeneigenschaften von Glaskugeln als Träger. Glaskugeln wurden als Träger verwendet, weil Glas die Modifizierung seiner Oberfläche durch physikalische und chemische Maßnahmen in einem sehr weiten Bereich erlaubt, ohne dass andere, die interpartikulären Wechselwirkungen ebenfalls beeinflussende Faktoren, wie Partikelgröße oder -form, angetastet werden. Dies erlaubt die eindeutige Zuordnung des Einflusses der Oberflächenmodifizierung auf die interpartikulären Wechselwirkungen zwischen Träger und Wirkstoff und in weiterer Folge auf die Lungengängigkeit des Wirkstoffs, was die Entwicklung von Pulverinhalatoren auf eine wissenschaftliche Basis stellt.

Table of content

1	Introduction.....	4
1.1	Pulmonary drug delivery	4
1.2	Interparticle interactions in dry powder inhalers.....	5
1.3	Glass beads as model carrier in dry powder inhalers.....	8
2	Aim of the work.....	12
3	Spray drying of aqueous salbutamol sulfate solutions using the Nano Spray Dryer B-90 – The impact of process parameters on particle size	15
4	Preparation and characterization of physically modified glass beads used as model carriers in dry powder inhalers	24
5	Influence of surface coverage on the fine particle fraction: investigating surface modified glass beads as model carriers in dry powder inhalers.....	32
5.1	Introduction	33
5.2	Materials and methods	37
5.2.1	Materials	37
5.2.2	Preparation of surface modified carrier particles	37
5.2.3	Characterization of the carrier particles.....	38
5.2.3.1	Surface roughness.....	38
5.2.3.2	Contact angle	39
5.2.4	Spray drying of the API.....	39
5.2.5	Preparation of adhesive mixtures	39
5.2.6	Determination of the actual surface coverage from the mixing homogeneity.....	41
5.2.7	Determination of the true surface coverage based on the recovered dose from NGI experiments	41
5.2.8	Scanning electron microscopy	42
5.2.9	Assessment of fine particles – fine particle fraction (FPF), emitted dose (ED), fine particle dose (FPD).....	42
5.2.10	HPLC analysis	44
5.3	Results and discussion.....	44
5.3.1	Characterization of the carrier particles.....	44

5.3.2	SEM images of adhesive mixtures.....	45
5.3.3	Actual surface coverage from mixing homogeneity experiments	46
5.3.4	True surface coverage from NGI experiments	48
5.3.5	Assessment of fine particles – Influence of surface coverage on aerodynamic behavior	49
5.3.6	Conclusion	55
6	Influence of surface characteristics of modified glass beads as model carriers in dry powder inhalers (DPIs) on the aerosolization performance	59
6.1	Introduction	60
6.2	Materials and methods	63
6.2.1	Materials	63
6.2.2	Sample preparation	63
6.2.3	Characterization of the modified glass beads	63
6.2.3.1	Surface roughness.....	63
6.2.3.2	Specific surface area	64
6.2.4	Spray drying of the API.....	64
6.2.5	Preparation of adhesive mixtures	65
6.2.6	Actual surface coverage	66
6.2.7	True surface coverage	67
6.2.8	Scanning electron microscopy	67
6.2.9	Aerodynamic assessment of fine particles	68
6.2.10	HPLC analysis	69
6.3	Results and discussion.....	69
6.3.1	Characterization of the modified glass beads	69
6.3.2	Correlation of actual and calculated surface coverage.....	71
6.3.3	SEM micrographs of adhesive mixtures with untreated and modified glass beads.....	73
6.3.4	True surface coverage	73
6.3.5	Assessment of aerodynamic behavior.....	74
6.3.6	Correlation of surface characteristics and aerodynamic behavior	75
6.3.6.1	Surface roughness.....	76
6.3.6.2	Surface area	77
6.4	Conclusion.....	78
7	Towards the optimisation and adaptation of dry powder inhalers	82

8	Summary	96
9	Conclusion and outlook.....	100
10	Appendix	102
10.1	Curriculum vitae	102
10.2	List of publications	104
10.2.1	Research papers	104
10.2.2	Application notes	104
10.2.3	Conference proceedings	104
10.2.4	Conference participation – invited oral presentations	106
10.2.5	Conference participation –oral presentations.....	106
10.2.6	Conference participation - poster presentations.....	106

1

Introduction

1.1 Pulmonary drug delivery

Pulmonary drug delivery is a common route of administration for the treatment of respiratory diseases such as asthma or chronically obstructive pulmonary disease (COPD). As the lung provides an enormous surface area and a relatively low enzymatic, controlled environment for systemic absorption of medications [1], it is the ideal target for the local treatment of respiratory diseases. Since compared to oral administration, the first pass effect in pulmonary application is missing, the onset of action is much faster and only a fraction of the oral dose is needed to cause a therapeutic effect. For the administration of active pharmaceutical ingredient (API) particles to the lung, different types of inhalers including nebulizers, pressurized metered-dose inhalers (pMDIs), non-pressurized metered-dose inhalers (MDIs) and dry powder inhalers (DPIs) can be used. Formulations used in nebulizers, pMDIs and MDIs are liquid whereas solid formulations are used in DPIs.

Advantages of the use of solid formulations and thus of DPIs are the avoidance of propellants, high patient compliance, high dose carrying capacity, high drug stability and reduced risk of microbial contamination compared to liquid formulations [2]. Moreover DPIs are small, cheap, more or less easy to use and do not require a coordination of actuation and inhalation. One weakness of some DPIs is that the amount of drug that can reach the lung varies and depends on the inspiration flow rate of the patient.

APIs for pulmonary drug delivery must have an aerodynamic diameter of $1\mu\text{m} - 5\mu\text{m}$ [3,4]. Particles that are larger cannot follow the air stream and will impact in the throat. Particles that are smaller however, will travel deeper into the lung and will be deposited mainly in the alveolar region or exhaled again due to their slow settling velocity, which depends on the particle size. Thus, both too large and too small particles will have no access to the bronchiolar

region and will consequently not be useful for the treatment of asthma and COPD.

A common method to generate particles with the desired aerodynamic diameter is milling of the API, alternatively, like in this study, spray drying can be used. The resulting micron sized particles are rather cohesive and possess poor flow properties, which lead to difficulties concerning dosing that is carried out volumetrically in DPIs. To overcome this problem, carrier based formulations, where the API is attached to the surface of larger carrier particles (50 μ m – 200 μ m) of adequate flowability, were developed. Together the coarse carrier and the API form a so called adhesive mixture [5]. These adhesive mixtures enhance the flowability of the drug and thus the dosing accuracy.

1.2 Interparticle interactions in dry powder inhalers

Interparticle interactions play a crucial role in carrier based dry powder inhalers. On the one hand it is important, that they are high enough so that the formulation is stable during transport, handling and dosing. On the other hand they need to be low enough so that drug detachment during inhalation can occur. Drug particles that are not detached during inhalation will impact together with the coarse carrier in the mouth or the upper airways and will not reach their target site, the bronchiolar region of the lung. When developing DPI formulations the choice of carrier and API is mainly based on trial and error and thus rather time consuming, expensive and by no means scientific. The reason therefore might be the complexity that goes hand in hand with interparticle interactions.

Interparticle interactions are affected by various factors like physicochemical properties, in figure 1 highlighted in yellow (surface energy, electric properties, crystallinity, chemical structure and hygroscopicity), factors that are related to either the carrier or the API particles, highlighted in red (deformation, surface topography, particle shape and particle size) and factors that are related to the formulation itself, highlighted in green (preparation, excipients and API/carrier ratio). Furthermore altering one of these factors often affects and changes one or more other factors influencing interparticle interactions.

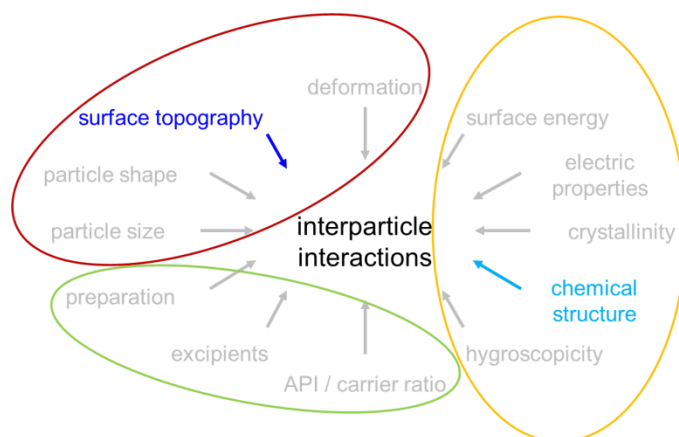


Figure 1 Factors influencing interparticle interactions.

According to literature one major factor influencing interparticle interactions is the carrier surface topography [6,7]. Therefore different attempts to modify the surface topography of commonly used carrier particles like lactose or mannitol were performed with the main goal to increase drug detachment from the carrier particles. Such attempts include crystallization of lactose particles from different media and under different crystallization conditions [8–12] and particle smoothing by coating lactose particles with aqueous lactose solutions [13,14]. Another attempt to smoothen particles is dispersing the carrier material in a dispersion media and subsequent elimination of the dispersion media [15–20]. Spray drying was described to be a suitable method to generate mannitol particles with modified surface roughness [21–23]. Other attempts implement the effect of mechanical stress on lactose surface properties e.g. wet smoothing in a high shear mixer [24], particle smoothing with a high speed mixer in the presence of a small amount of wetting solvent [25], surface processing with a high speed elliptical-rotor type powder mixer [26] as well as milling lactose with various mill speeds to avoid batch to batch variability and to make the carrier particle surface homogenous [27]. However, in most of these cases beside the surface topography also other properties impacting interparticle interactions, like particle size or shape of the carrier particles, were altered. For example, recently, Maas reported carrier surface modification of mannitol by spray drying at different conditions [28]. Spray drying changed the surface roughness, however, the particle shape changed as well.

When changing the surface topography or roughness of the carrier the contact area between carrier (black) and API (pink) can either be increased (figure 2b) or decreased (figure 2c and 2d) and thus interparticle interactions can also either increase or decrease. Only when a surface roughness is introduced that is smaller with respect to the API particle size the acting adhesion forces are decreased and further drug detachment facilitated. By contrast, when a surface roughness is introduced that is larger compared to the API particle size, the API particles might be entrapped in these cavities and thus drug detachment is hindered. So, the shade of surface roughness compared to the size and shape of the API largely impacts interparticle interactions and thus drug detachment.

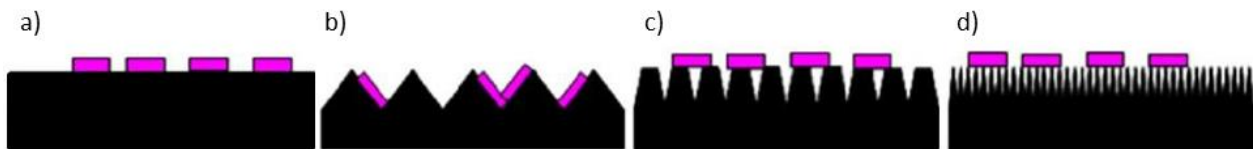


Figure 2: Schematic of potential API carrier adhesion scenarios. Modified from Young P.M., Roberts D., Chiou H., Rae W., Chan H.-K., Traini, D., Composite carriers improve the aerosolization efficiency of drugs for respiratory delivery, *Journal of Aerosol Science*, 39, 82-93, 2008.

That is also why there are different and contradictory findings related to the correlation of particle roughness and the detachment of the API particles from the carrier surface during inhalation often expressed as the fine particle fraction (FPF). The FPF gives the percentage of API particles that are detached from the carrier during inhalation and that have an aerodynamic particle size smaller than $5\mu\text{m}$ and thus are able to reach the deep lung. Therefore the FPF may be defined as the main parameter describing the performance or efficiency of a DPI carrier system. For example Kawashima documented that the rougher the carrier particles the lower the FPF [3]. The surface roughness in that study resulted from crevices on the lactose surface. By contrast, Chan reported that rougher lactose carrier particles lead to a higher fine particle fraction [13]. In that study the surface roughness resulted from the presence of immobilized lactose fine particles on the surface that lead to microscopic undulations on the lactose surface rather than to crevices. These contradictory findings illustrate that it has to be differentiated between roughnesses and that in order to increase the FPF the right kind of surface roughness has to be introduced.

1.3 Glass beads as model carrier in dry powder inhalers

The fact that by modifying the surface topography/roughness of lactose or mannitol particles, not only the surface topography, but also other factors influencing interparticle interactions are altered, makes lactose and mannitol unsuitable as carriers to study the influence of surface topography on the performance of DPIs. That is why glass beads are used as model carriers in DPI formulations in the present study. Glass beads have ideal geometry, they are available in different sizes and, most importantly, they allow various prospects of surface modification, without affecting other properties like particle size and shape. This allows the attribution of changes of DPI performance solely to the surface topography of the differently modified glass beads used. Thereby glass beads should help to bring the development of DPIs on a scientific level, and to avoid trial and error due to better knowledge about the relation of surface topography, interparticle interactions and DPI performance.

However it has to be mentioned that glass beads are neither typical carrier particles nor safe for inhalation from a medical point of view. In this study glass beads are used as model carriers to understand how the surface topography of carrier particles in DPIs should ideally be to get a high deposition of API particles in the lung. For the application of glass beads containing dry powder inhalates to humans, a grid has to be implemented in the inhaler device retaining the carrier particles in the inhaler device.

References

- [1] N.R. Labiris, M.B. Dolovich, Pulmonary drug delivery. Part I: Physiological factors affecting therapeutic effectiveness of aerosolized medications, *Br. J. Clin. Pharmacol.* 56 (2003) 588–599.
- [2] M.B. Chougule, B.K. Padhi, K. a Jinturkar, A. Misra, Development of dry powder inhalers., *Recent Pat. Drug Deliv. Formul.* 1 (2007) 11–21.
- [3] Y. Kawashima, T. Serigano, T. Hino, H. Yamamoto, H. Takeuchi, Effect of surface morphology of carrier lactose on dry powder inhalation property of pranlukast hydrate, *Int. J. Pharm.* 172 (1998) 179–188. 6.
- [4] D.I. Daniher, J. Zhu, Dry powder platform for pulmonary drug delivery, *Particuology.* 6 (2008) 225–238.
- [5] Hersey J A, Ordered Mixing: A New Concept in Powder Mixing Practice, *Powder Technol.* 11 (1974) 41–44.
- [6] P.M. Young, D. Roberts, H. Chiou, W. Rae, H.-K. Chan, D. Traini, Composite carriers improve the aerosolization efficiency of drugs for respiratory delivery, *J. Aerosol Sci.* 39 (2008) 82–93.
- [7] M. Lohrmann, *Adhäsionskräfte in interaktiven Mischungen für Pulverinhalatoren*, Duesseldorf, 2005.
- [8] H. Larhib, G.P. Martin, C. Marriott, D. Prime, The influence of carrier and drug morphology on drug delivery from dry powder formulations, *Int. J. Pharm.* 257 (2003) 283–296.
- [9] X.M. Zeng, G.P. Martin, C. Marriott, J. Pritchard, The influence of crystallization conditions on the morphology of lactose intended for use as a carrier for dry powder aerosols., *J. Pharm. Pharmacol.* 52 (2000) 633–643.
- [10] X.M. Zeng, G.P. Martin, C. Marriott, J. Pritchard, Crystallization of lactose from carbopol gels., *Pharm. Res.* 17 (2000) 879–886.

- [11] X.M. Zeng, G.P. Martin, C. Marriott, J. Pritchard, The use of lactose recrystallised from carbopol gels as a carrier for aerosolised salbutamol sulphate., *Eur. J. Pharm. Biopharm.* 51 (2001) 55–62.
- [12] X.M. Zeng, G.P. Martin, C. Marriott, J. Pritchard, Lactose as a carrier in dry powder formulations: the influence of surface characteristics on drug delivery., *J. Pharm. Sci.* 90 (2001) 1424–1434.
- [13] L.W. Chan, L.T. Lim, P.W.S. Heng, Immobilization of fine particles on lactose carrier by precision coating and its effect on the performance of dry powder formulations., *J. Pharm. Sci.* 92 (2003) 975–984.
- [14] K. Iida, H. Todo, H. Okamoto, K. Danjo, H. Leuenberger, Preparation of dry powder inhalation with lactose carrier particles surface-coated using a Wurster fluidized bed., *Chem. Pharm. Bull. (Tokyo)*. 53 (2005) 431–434.
- [15] B.H.J. Dickhoff, a H. de Boer, D. Lambregts, H.W. Frijlink, The effect of carrier surface treatment on drug particle detachment from crystalline carriers in adhesive mixtures for inhalation., *Int. J. Pharm.* 327 (2006) 17–25.
- [16] D. El-Sabawi, R. Price, S. Edge, P.M. Young, Novel temperature controlled surface dissolution of excipient particles for carrier based dry powder inhaler formulations., *Drug Dev. Ind. Pharm.* 32 (2006) 243–251.
- [17] K. Iida, Y. Hayakawa, H. Okamoto, K. Danjo, H. Leuenberger, Evaluation of flow properties of dry powder inhalation of salbutamol sulfate with lactose carrier., *Chem. Pharm. Bull. (Tokyo)*. 49 (2001) 1326–30.
- [18] K. Iida, Y. Hayakawa, H. Okamoto, K. Danjo, H. Leuenberger, Preparation of dry powder inhalation by surface treatment of lactose carrier particles., *Chem. Pharm. Bull. (Tokyo)*. 51 (2003) 1–5.
- [19] N. Islam, P. Stewart, I. Larson, P. Hartley, Lactose Surface Modification by Decantation : Are Drug-Fine Lactose Ratios the Key to Better Dispersion of Salmeterol Xinafoate from Lactose-Interactive Mixtures? , *Pharm. Res.* 21 (2004) 492–9.

- [20] N. Islam, P. Stewart, I. Larson, P. Hartley, Effect of carrier size on the dispersion of salmeterol xinafoate from interactive mixtures., *J. Pharm. Sci.* 93 (2004) 1030–8.
- [21] E.M. Littringer, A. Mescher, H. Schroettner, L. Achelis, P. Walzel, N. A. Urbanetz, Spray dried mannitol carrier particles with tailored surface properties - The influence of carrier surface roughness and shape., *Eur. J. Pharm. Biopharm.* 82 (2012) 194 –204.
- [22] E.M. Littringer, A. Mescher, S. Eckhard, H. Schröttner, C. Langes, M. Fries, et al., Spray Drying of Mannitol as a Drug Carrier—The Impact of Process Parameters on Product Properties, *Dry. Technol.* 30 (2012) 114–124.
- [23] S.G. Maas, G. Schaldach, E.M. Littringer, A. Mescher, U.J. Griesser, D.E. Braun, et al., The impact of spray drying outlet temperature on the particle morphology of mannitol, *Powder Technol.* 213 (2011) 27–35.
- [24] F. Ferrari, D. Cocconi, R. Bettini, F. Giordano, P. Santi, M. Tobyn, et al., The surface roughness of lactose particles can be modulated by wet-smoothing using a high-shear mixer., *AAPS PharmSciTech.* 5 (2004) 1–6.
- [25] P.M. Young, D. Cocconi, P. Colombo, R. Bettini, R. Price, D.F. Steele, et al., Characterization of a surface modified dry powder inhalation carrier prepared by “particle smoothing,” *J. Pharm. Pharmacol.* (2002) 1339–1344.
- [26] K. Iida, Y. Inagaki, H. Todo, H. Okamoto, K. Danjo, H. Luenberger, Effects of surface processing of lactose carrier particles on dry powder inhalation properties of salbutamol sulfate., *Chem. Pharm. Bull. (Tokyo).* 52 (2004) 938–942.
- [27] H. Steckel, P. Markefka, H. TeWierik, R. Kammelar, Effect of milling and sieving on functionality of dry powder inhalation products., *Int. J. Pharm.* 309 (2006) 51–59.
- [28] S.G. Maas, Optimierung trägerbasierter Pulverinhalate durch Modifikation der Trägeroberfläche mittels Sprühtrocknung, 2009.

2

Aim of the work

According to the introduction the aim of this work is the preparation of surface modified carrier particles to tailor interparticle interactions and thus drug detachment from the carrier surface, finally leading to the optimum DPI performance.

Chapter 3 deals with the preparation of the model API used in this study, salbutamol sulphate. To generate spherical shaped salbutamol sulphate particles of appropriate size and suitable for inhalation, the Nano Spray Dryer B-90 was used. Spherical API particles are favored in this work, since when using spherical glass beads as carrier and spherical salbutamol sulphate particles as API, the factor of shape is eliminated when investigating interparticle interactions and drug detachment. In order to choose appropriate spray drying conditions, which result in the formation of particles with the desired characteristics, a 3^3 full factorial design was used to investigate the influence of process parameters like mesh size, feed concentration, and drying air temperature on the particles, the amount of product produced per time, and product yield.

Chapter 4 treats the preparation of surface modified glass beads used as model carriers by physical means and their characterization. Therefore mechanical treatment of the glass beads in a ball mill with different grinding materials and different grinding times was applied. The resulting surface modified rough carrier particles were characterized with respect to particle size (laser diffraction), shape (image analysis) and surface topography (gas adsorption and atomic force microscopy (AFM)). Furthermore, techniques to characterize changes of surface topography were evaluated regarding their applicability, advantages and disadvantages as well as the benefits of combining several techniques to obtain a full surface characterization were discussed.

Chapter 5 focuses on the preparation of adhesive mixtures of surface modified glass beads as carrier particles and spray dried salbutamol sulphate as API particles. As besides surface roughness also surface chemistry influences interparticle interactions, in addition to physically modified glass beads, which have already been introduced in chapter 4, chemically modified glass beads were used to investigate the mixing behavior of surface modified glass beads. In this context, the relationship between the amount of API particle weighed in for each mixture (calculated surface coverage), the amount of API particles present on the glass beads surface after mixing (actual surface coverage) and the amount of API particles present on the glass beads surface when carrying out the analysis of the in vitro respirable fraction often referred to as fine particle fraction (FPF), was investigated. Additionally the influence of surface coverage on the fine particle fraction and thus the performance of DPI formulations, containing surface modified glass beads and spray dried salbutamol sulphate was discussed.

Chapter 6 deals with the effect of surface characteristics (surface roughness and specific surface area) of surface modified glass beads on the FPF of salbutamol sulphate. A prerequisite for comparing the differently modified glass beads with each other, are the same actual and true surface coverage for all the carrier particles investigated and compared. For that reason, first the preparation of mixtures with same actual and true surface coverage by the correlation of calculated and actual surface coverage was described. Subsequently, the correlation of the FPF for mixtures with same surface coverage but different surface characteristics of the modified glass beads was examined.

Chapter 7 presents the development of Lagrangian drug powder detachment models that are meant to form the basis for the numerical prediction of inhaler performance and efficiency that shall further assist in the optimisation of inhaler geometry and dry powder inhaler formulation. Therefore the flow field through the entire inhaler device (here the Cyclohaler®) was calculated numerically using OpenFOAM and the fluid dynamic stresses acting on the carrier particles were recorded and statistically analyzed (macro simulations). Furthermore, micro-scale simulations based on the Lattice-Boltzmann method

(LBM) were conducted for a fixed carrier particle covered with API particles. These simulations were carried out and described by the research group of Prof. Sommerfeld. The possibility of API particle detachment from the carrier was determined based on measured van der Waals forces, friction coefficients and other contact properties like adhesion surface energy. Therefore experimental measurements of van der Waals forces acting between untreated and surface modified glass beads and salbutamol sulphate particles via AFM, friction coefficient measurements with a FT4 Powder Rheometer, and adhesion surface energy measurements of untreated and physically modified glass beads were described. The validation of the micro simulations with the data obtained from the experimental measurements is also part of this chapter.

3

Spray drying of aqueous salbutamol sulfate solutions using the Nano Spray Dryer B-90 – The impact of process parameters on particle size

Eva Maria Littringer, Sarah Zellnitz, Kerstin Hammernik, Verena Adamer, Herwig Friedl, Nora Anne Urbanetz

Drying Technology 31(2013), 1346–1353.

Drying Technology, 31: 1346–1353, 2013
Copyright © 2013 Taylor & Francis Group, LLC
ISSN: 0737-3937 print/1532-2300 online
DOI: 10.1080/07373937.2013.793701



Spray Drying of Aqueous Salbutamol Sulfate Solutions Using the Nano Spray Dryer B-90—The Impact of Process Parameters on Particle Size

E. M. Littringer,¹ S. Zellnitz,¹ K. Hammernik,¹ V. Adamer,² H. Friedl,³ and N. A. Urbanetz¹

¹Research Center Pharmaceutical Engineering GmbH, Graz, Austria

²Department of Pharmaceutical Technology, University of Innsbruck, Innsbruck, Austria

³Institute of Statistics, Graz University of Technology, Graz, Austria

In order to prepare spherical salbutamol sulfate particles of adjustable size, a Nano Spray Dryer B-90 was employed. A 3³ full-factorial design was used to investigate the influence of process parameters (mesh size, feed concentration, and drying air temperature) on particle size (median size and width of the particle size distribution), amount of product produced per time, and product yield. The median particle size was significantly influenced by all three factors of the statistical design. Within the design space studied, particle sizes of 1.0 to 6.4 μm were obtained. The width of the particle size distribution (span) increased with increasing mesh sizes. All particles with a particle size greater than 2.4 μm showed a bimodal particle size distribution. Generally, larger mesh sizes as well as higher concentrations led to an increase in the amount of product prepared per time. The corresponding values observed were from 0.4 to 75.8 mg/min. The product yield was independent of the process parameters studied. All products were amorphous after spray drying and were stable up to a relative humidity of 60% at a temperature of 25°C.

Keywords Dry powder inhaler (DPI); Nano spray dryer B-90; Particles size; Product produced per time; Product yield; Salbutamol sulfate; Span; Spray drying

INTRODUCTION

Dry powder inhalers are widely used in the treatment of respiratory diseases like asthma bronchiale and chronic obstructive pulmonary disease. In such formulations, which usually consist of an excipient that ensures sufficient flowability and the active pharmaceutical ingredient (API), the dry powder is directly administered to the lung. However, in order to reach the targeted regions of the lung, the bronchioles, the API must have an aerodynamic particle size in the range of 1 to 5 μm.^[1–3] Particles that are

too large cannot follow the air stream. They will impact in the throat and will have no access to the bronchiolar region. However, if the particle size is below 1 μm, the particles will travel deeper into the lungs during inhalation and will be deposited mainly in the alveolar region.

The preparation of particles in the low micrometer range usually involves micronization. The disadvantages of this procedure are the need for high energy input and the high variability in the morphology of the obtained single particles, leading to unpredictable dry powder inhaler performance. For this reason, narrowly size-distributed, isometric, spherical particles would be desirable. A rather easy and widely used technique to prepare spherical particles with a narrow size distribution is spray drying. There are several studies that show the suitability of spray drying for the preparation of API particles for pulmonary drug delivery.^[4–6] Therefore, the aim of this work is the preparation of spherical salbutamol sulfate particles as a model API with adjustable particle size.

Instead of a conventional spray dryer, the recently launched Nano Spray Dryer B-90 (Buchi Labortechnik AG, Flawil, Switzerland) was used in the present study.^[7] The droplet generation as well as particle collection of this spray dryer differs from a conventional one. A vibrating mesh, which is piezoelectrically driven, enables droplet generation. Further, instead of using the cyclone technology, particles are collected with an electrostatic particle collector.^[8,9] Several studies have been performed using this novel spray dryer. For example, protein solutions were dried by Bürki et al.^[10] and Lee et al.^[8] Cyclosporin A and dexamethasone were encapsulated by Schafroth et al.^[11] In addition, potential wall materials for encapsulation (arabic gum, whey protein, polyvinyl alcohol, modified starch, and maltodextrin) were investigated.^[12] However, to the best of the authors' knowledge, there have been no thorough investigations of the impact of process parameters of the Nano Spray Dryer B-90 on the particle size

E. M. Littringer and S. Zellnitz contributed equally to this work.

Correspondence: E. M. Littringer, Research Center Pharmaceutical Engineering GmbH, Inffeldgasse 13, Graz 8101, Austria; E-mail: eva.littringer@gmail.com

(median, width of the particle size distribution), the mass of product generated per time, and yield of a low-molecular-weight compound, here salbutamol sulfate, spray dried from aqueous solutions.

EXPERIMENTAL SETUP, MATERIALS, AND METHODS

Materials

Salbutamol sulfate (USP25 quality) was provided by Selectchemie (Zurich, Switzerland). Aqueous salbutamol sulfate solutions used for spray drying were prepared with purified water (TKA MicroPure UV UltraPure Water System, TKA Wasseraufbereitungssysteme GmbH, Niederelbert, Germany) equipped with a capsule filter (0.2 μm).

Spray Drying

The spray-dried products were prepared on a Nano Spray Dryer B-90 equipped with the long version of the drying chamber (height 150 cm, diameter 55 cm). Drying air flow rate (110 L/h) and spray rate (30%) were constant and the same for all experiments. Atomizer mesh size, feed concentration, and drying air temperature were varied according to the experimental design (see below and Table 1). After spray drying, the product was replaced from the collection electrode with a particle scraper and stored desiccated at room temperature over silica gel until further required.

Statistical Design

The influence of atomizer mesh size (4.0, 5.5, 7.0 μm), feed concentration (1.0, 7.5, 15.0% [m/m]), and drying air inlet temperature (80, 100, 120°C) on the median particle size, the amount of product spray dried per time, and product yield was studied using a 3^3 full-factorial design (Tables 1 and 2). Statistical analysis was carried out using Modde 9.0 software (Umetrics AB, Umeå, Sweden). In order to obtain normally distributed data, the responses median particle size and amount of product spray dried per time were logarithmically transformed prior to statistical analysis. Only significant terms were considered in the model. A significance level of 0.05 was used.

TABLE 1

Process parameters used in the 3^3 full-factorial design

Parameter	Factor level			Unit
	1	2	3	
Mesh size	4.0	5.5	7.0	μm
Feed concentration	1.0	7.5	15.0	% (m/m)
Drying air temperature	80	100	120	°C

Particle Size Distribution

The particle size distribution of the spray-dried products was determined by laser light diffraction (Helos/KR, Sympatec, Clausthal-Zellerfeld, Germany). A dry dispersing system (Rodas/L, Sympatec) and a vibrating chute (Vibri, Sympatec) were used for powder dispersion. A dispersion pressure of 2.0 bar was applied. Evaluation of the data was performed using the software Windox 5 (Sympatec). The volumetric median particle size and particle span (span = $(X_{90.3} - X_{10.3})/X_{50.3}$) were obtained from the analysis.

Amount of Product Produced per Time

The amount of product spray dried per time was calculated by dividing the mass of product collected after spray drying by the time that was required to produce the product.

Product Yield

Product yield was determined as the ratio of spray-dried mass by the initial mass of salbutamol sulfate used for the preparation of the feed solution.

Particle Surface Investigations

The powder samples were examined using a scanning electron microscope (SEM) (Zeiss Ultra 55, Zeiss, Oberkochen, Germany) operating at 5 kV. The particles were sputtered with gold-palladium prior to analysis.

Water Sorption Analysis

The moisture sorption isotherms were recorded with an SPS-11 moisture sorption analyzer (Projekt Messtechnik, Ulm, Germany) at a temperature of $25 \pm 0.1^\circ\text{C}$. The measurement cycle was started at 0% relative humidity (RH), increased in two 5% steps to 10% RH, further increased up to 90% RH in 10% steps, and from 90 to 95% RH in one step. Subsequently, the RH was decreased again to 90% RH and further decreased in 10% steps to 10% RH and in two 5% steps to 0% RH. The equilibrium condition for each step was set to a mass constancy of $\pm 0.001\%$ over 60 min. Two hundred forty milligrams of the spray-dried product was used for analysis.

X-Ray Powder Diffraction Analysis

X-ray powder diffraction (XRPD) patterns were obtained with an X'Pert PRO diffractometer (PANalytical, Almelo, The Netherlands) equipped with a theta/theta-coupled goniometer in transmission geometry, programmable XYZ stage with well plate holder, Cu-K α 1,2 radiation source (wavelength 0.15419 nm) with a focusing mirror, a 0.5° divergence slit, a 0.02° soller slit collimator, and a 0.5° antiscattering slit on the incident beam side, a 2-mm antiscattering slit, a 0.02° soller slit collimator, an Ni filter, and a solid state PIXcel detector on the diffracted

TABLE 2
Design matrix of the 3³ full-factorial design and the data collected from the analyses

Sample ID	Factor			Response			
	Mesh size (μm)	Concentration (% w/w)	Temperature ($^{\circ}\text{C}$)	Size (μm)	Span	Mass per time (mg/min)	Product yield (%)
1	7.0	15.0	120	6.4	1.8	75.8	90.4
2	7.0	15.0	100	6.4	2.0	36.7	70.3
3	7.0	15.0	80	5.4	2.1	20.3	73.0
4	7.0	7.5	120	5.4	2.1	42.0	83.8
5	7.0	7.5	100	4.9	2.0	15.1	72.2
6	7.0	7.5	80	4.0	1.9	3.7	75.4
7	7.0	1.0	120	2.0	2.0	2.3	46.4
8	7.0	1.0	100	3.1	1.7	4.4	82.7
9	7.0	1.0	80	2.3	2.1	1.8	57.1
10	5.5	15.0	120	3.4	1.7	3.2	86.1
11	5.5	15.0	100	3.5	1.7	4.9	51.4
12	5.5	15.0	80	3.1	1.7	7.5	70.8
13	5.5	7.5	120	2.9	1.8	4.4	82.7
14	5.5	7.5	100	2.8	1.7	4.0	48.3
15	5.5	7.5	80	2.7	1.6	6.8	65.2
16	5.5	1.0	120	1.4	1.6	3.9	49.6
17	5.5	1.0	100	1.6	1.7	0.6	59.1
18	5.5	1.0	80	1.2	1.8	0.7	78.1
19	4.0	15.0	120	2.4	1.7	0.8	71.7
20	4.0	15.0	100	2.3	1.6	4.1	41.2
21	4.0	15.0	80	2.4	1.6	4.6	73.8
22	4.0	7.5	120	2.3	1.5	6.1	61.9
23	4.0	7.5	100	2.3	1.6	4.4	61.2
24	4.0	7.5	80	1.9	1.5	9.1	63.1
25	4.0	1.0	120	1.2	1.7	3.0	72.2
26	4.0	1.0	100	1.0	1.9	0.6	56.0
27	4.0	1.0	80	1.1	1.7	0.4	57.2

beam side. The patterns were recorded at a tube voltage of 40 kV and tube current of 40 mA, applying a step size of $0.013^{\circ} 2\theta$ with 40 s per step in the angular range of 2 to $40^{\circ} 2\theta$.

RESULTS AND DISCUSSION

In order to study the influence of mesh size, feed concentration, and drying air inlet temperature on the median particle size, width of the particle size distribution (span), product produced per time, as well as the product yield when spray drying aqueous salbutamol sulfate solutions using the Nano Spray Dryer B-90, a 3³ full-factorial statistical design was used. Table 1 shows the three factor levels of the statistical design. The mesh sizes used (4.0, 5.5, and 7.0 μm) were the three sizes that are available for the nano spray dryer. The high level of the drying air inlet temperature (120 $^{\circ}\text{C}$) was the highest temperature at which the nano

spray dryer can be operated (corresponding outlet temperature 50 $^{\circ}\text{C}$). In order to allow complete drying of the aqueous solutions, the lower level was set to 80 $^{\circ}\text{C}$ (corresponding outlet temperature 40 $^{\circ}\text{C}$). The high level of the feed concentration was 15.00% (m/m), which is close to the solubility of salbutamol sulfate at room temperature ($\approx 18.00\%$ [m/m]).

In order to keep the number of experiments at a reasonable level, drying air flow rate (110 L/h) and spray rate (30%), which were both expected not to impact particle size, were kept constant.

For a conventional spray dryer, a change in the drying air flow rate might alter the deposition efficiency of the cyclone. Via this mechanism, the particle size could change. However, this was not expected for the nano spray dryer because particle collection relies on electrostatic deposition.

When using conventional atomizers (rotary as well as nozzles), a change in the atomizing conditions (e.g., spray

rate) may influence the droplet size and, consequently, the particle size.^[13] However, for the novel vibrating mesh spray technology, an increase in the spray rate increases the oscillation frequency of the mesh. The higher oscillation frequency results in the formation of more droplets per time. However, the size of the droplets should not change.

Drying air flow rate as well as spray rate impact the drying temperature. Via a change in drying temperature, the two factors might change the particle size. However, preliminary experiments showed that the change in drying air temperature was small compared to the temperature range studied within the experimental design (80–120°C).

Particle Size

Within the design space studied, particles with a median size of 1.0 to 6.4 µm (Table 2) were observed. All of the three factors studied significantly influenced the size of the spray-dried products (Fig. 1). In addition to the three main factors, the quadratic terms Concentration × Concentration and Mesh size × Mesh size as well as the interaction term Mesh size × Concentration significantly impacted particle size (Fig. 1). The complex interplay of these terms and their effect on particle size at intermediate temperature (100°C) is graphically displayed in Fig. 2. In this contour plot, factor settings where particles of the same size were obtained are displayed by regions of equal color. Because of the fact that the influence of drying air temperature was small, the impact of this factor is not graphically displayed.

For all mesh sizes studied, an increase in feed concentration from 1 to 12% led to an increase in particle size. The correlation between feed concentration and particle size was already described by Masters^[14] and was explained by Elversson and Millqvist-Fureby^[15] for a spray-drying process with a conventional spray dryer. Lee et al.^[8] observed the same impact, albeit less pronounced, when spray drying protein solutions using the Nano Spray Dryer B-90. Although the nano spray dryer relies on atomization

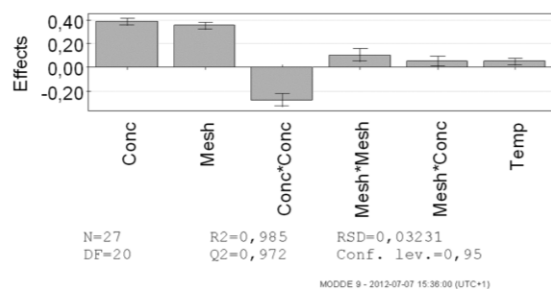


FIG. 1. Effect plot displaying the influence of process parameters on the median particle size.

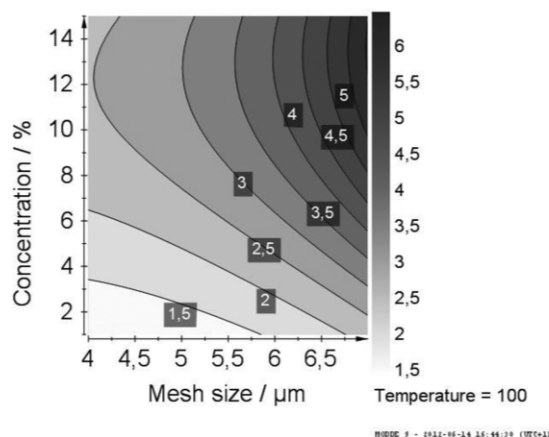


FIG. 2. Contour plot of the influence of feed concentration and mesh size on the median particle size (µm) of the spray-dried products.

and particle collection principles different from conventional ones and is therefore a novel spray dryer, the mechanism of drying of the droplets once generated is the same. A liquid feed is dispersed into small droplets. Those droplets are then dried in the tower and are collected after drying at the bottom of the dryer. In order to understand the influence of feed concentration, the progress of droplet drying should be understood. As soon as the droplet enters the tower, evaporation of water at the droplet surface takes place. Due to the evaporation of water, the concentration of salbutamol sulfate at the droplet surface increases. When the concentration exceeds the solubility, solidification starts. With higher concentration, the concentration where solidification starts is reached at an earlier point of time when the droplet is comparably larger. Therefore, higher feed concentrations lead to larger particle sizes.

Figure 2 shows that the increase in particle size was more pronounced with larger mesh size; hence the larger the droplets generated. A further increase in feed concentration from 12 to 15% resulted in a slight decrease in particle size. One explanation for this might be that the impact of feed concentration on particle size is more pronounced at comparably lower concentrations. For example, a change in feed concentration from 1 to 2% led to a greater change in particle size than an increase from 14 to 15%. This correlation was also described by Elversson and Millqvist-Fureby^[15] when spray drying carbohydrate solutions. Therefore, the higher the concentration, the sooner the solidification will start and the change in volume and, hence, size is comparably smaller. Additionally, the particles of larger size exhibited a corrugated surface (Fig. 3), which may result in a slightly lower particle size detected with laser diffraction.

1350

LITTRINGER ET AL.

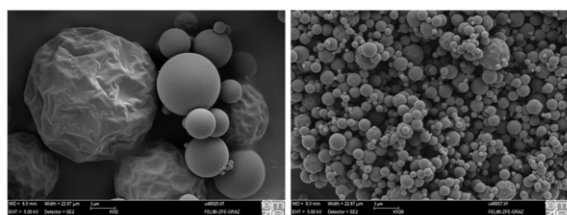


FIG. 3. SEM micrographs of the products with the largest (sample 2, left) and smallest (sample 26, right) particle sizes.

For all concentrations studied, an increase in mesh size resulted in the formation of larger particles. This was not much of a surprise because with larger mesh sizes the size of the droplets generated increases.^[9] Consequently, the larger the droplets, the larger the size of the solidified particles.

In addition, drying air temperature was found to significantly influence the median particle size, although the impact was small compared to the effect of mesh size and feed concentration. Vehring et al.^[16] described this phenomenon with the help of the Peclet number, which is the ratio of the evaporation rate to the diffusion coefficient of the solute. During drying, the increase in solute concentration at the particle surface causes a diffusion of the solute toward the droplet center. If the diffusion is equal to the evaporation rate, there will not be any concentration gradient along the radius of the droplet. However, if the evaporation is faster than the diffusion, the concentration at the particle surface will be higher than that in the center of the droplet. With higher drying air temperatures, the evaporation rate increases and larger Peclet numbers are observed, leading to comparably higher concentrations at the particle surface. Therefore, shell formation takes place at an earlier point in time, when the droplet volume is still larger resulting in larger particles.

Chawla et al.^[5] who studied the influence of process parameters on particle size when spray drying aqueous salbutamol sulfate solutions using a conventional Mini Spray Dryer B-190, observed that none of the single process parameters studied (pump speed, aspirator level, inlet temperature, feed concentration) impacted the particle size. However, they reported that the interaction of feed concentration and aspirator level was significant. When both factors were at their highest levels, the largest particles were obtained. The authors further reported that the spray-dried particles had a median diameter of 4.4 μm . In contrast to the study performed by Chawla et al.^[5] on the Mini Spray Dryer B-190, this work shows that by using the Nano Spray Dryer B-90 the particle size can be successfully adjusted by controlling the process parameters. A greater change in particle size with the mini spray dryer might have been achieved by varying the atomizer settings.

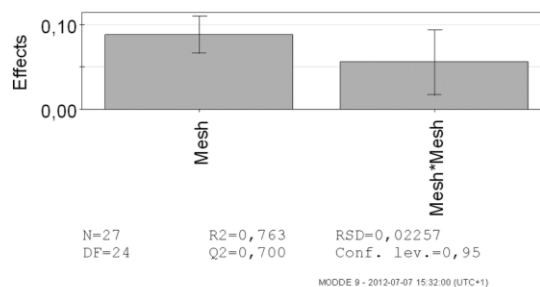


FIG. 4. Effect plot displaying the influence of process parameters on particle span.

In order to obtain an idea about the influence of process parameters on the width of the particle size distribution, the span values were evaluated too. A change in mesh size significantly altered particle span (Fig. 4). Figure 5 shows that the particle span significantly increased with increasing mesh sizes. The change was even greater the larger the mesh size (Mesh size \times Mesh size). The particle size distribution of the sample with the highest (sample 2) and the lowest (sample 26) median particle size is displayed in Fig. 6. Interestingly, all samples with a median particle size larger than 2.4 μm showed a bimodal particle size distribution (e.g., sample 2).

The increase in particle span with increasing mesh size and the change from a mono- to a bimodal distribution could be a result of secondary droplet breakup or the generation of satellite droplets during atomization, especially when larger mesh sizes are used.

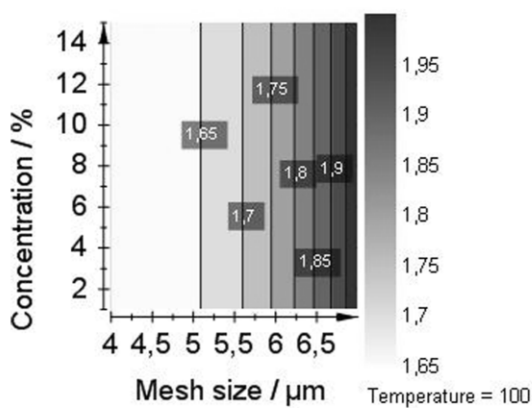


FIG. 5. Contour plot of the influence of feed concentration and mesh size on particle span of the spray-dried products.

IMPACT OF PROCESS PARAMETERS ON PARTICLE SIZE

1351

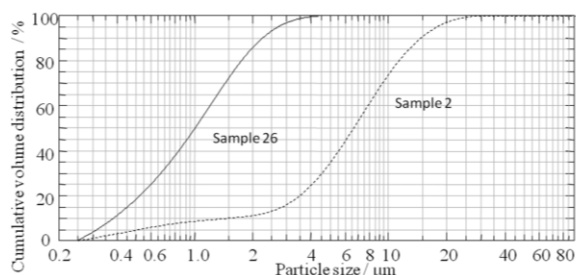


FIG. 6. Particle size distribution of products with the largest (sample 2, left) and smallest (sample 26, right) particle sizes.

Amount of Product Spray Dried Per Time

In order to get an idea regarding the time that is required to produce a certain amount of product, the influence of process parameters on the amount of product spray dried per time was investigated. Values from 0.4 to 75.8 mg/min were observed (Table 2).

Figure 7 shows that two factors, mesh size and feed concentration, as well as their quadratic terms, significantly impacted the amount of product that is produced per time. The drying air temperature had no influence on the response studied. Generally, larger mesh sizes as well as larger concentrations led to an increase in the amount of product prepared per time (Fig. 8). With larger mesh sizes there is an increase in the size of the droplets generated.^[9] Due to the higher volume those droplets contain a higher amount of dissolved salbutamol sulfate, finally leading to a higher amount of product produced per time. In addition, higher concentrations mean a higher amount of dissolved salbutamol sulfate and, consequently, a higher value of the effect studied.

Product Yield

Product yields from 41.2 to 90.4% (Table 2) were observed. The statistical analysis of the experimental

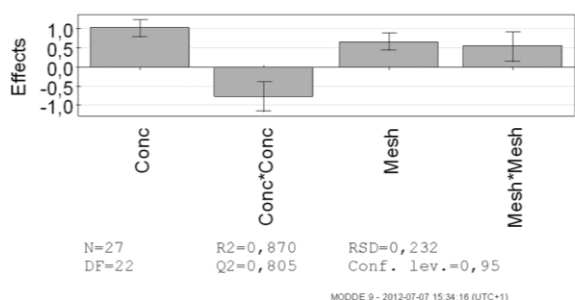
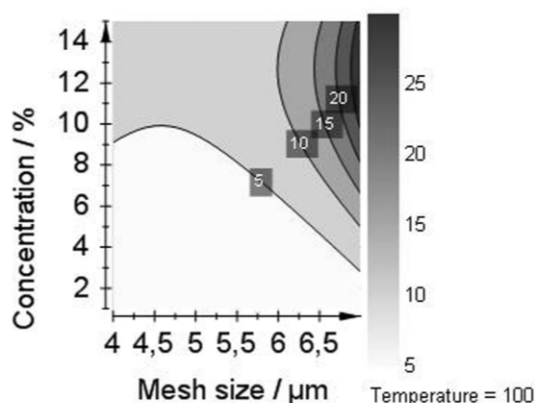


FIG. 7. Coefficient plot displaying the influence of process parameters on the product produced per time.



MODDE 9 - 2012-07-08 11:04:11 (UTC+1)

FIG. 8. Contour plot of the influence of feed concentration and mesh size on the spray-dried product produced per time (g = min).

design revealed (data not shown) that there was no correlation between the process parameters studied and the product yield. Although the result that product yield is independent of process parameters is primarily positive, the high scatter of values observed needs further understanding and will be the focus of further work.

Initially the idea was to use the same initial mass of salbutamol sulfate to prepare the feed solutions for all of the experiments. However, the experiments showed that, especially with a low feed concentration and small mesh size, the time to spray the whole feed prepared was too long. When comparably lower initial masses are used, the yield is expected to be lower due to comparably higher losses; for example, during particle collection after spray drying. In the case of losses that are attributed to the different initial masses of spray-dried salbutamol sulfate, the statistical analysis of process parameters on product yield would be invalid. In order to exclude this, the influence of initial mass on the product yield was studied. Figure 9 shows that there was no correlation between the initial mass and the product yield, indicating that the analysis of the influence of process parameters on product yield was valid.

Particle Shape

The SEM micrographs of the products revealed (Fig. 3) that all products were of spherical shape. Although the overall particle shape was spherical, the particles of larger size exhibited a corrugated surface, whereas the smaller particles showed no corrugation.

The drying history of the droplets will explain the different morphologies of the small and large particles. As described previously (see Particle Shape section), water

1352

LITTRINGER ET AL.

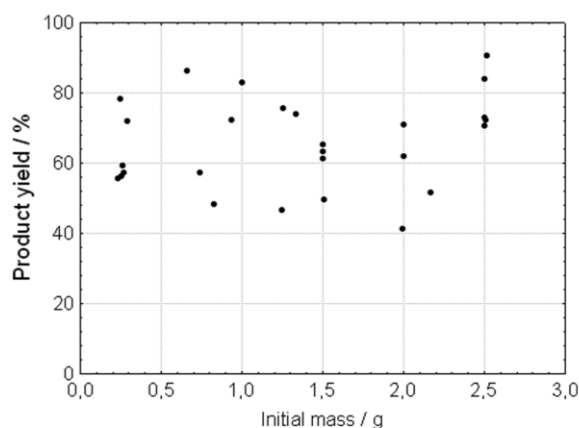


FIG. 9. Attempted correlation between the initial mass of spray-dried salbutamol sulfate and the corresponding product yield.

will evaporate at the droplet surface as soon as the droplet enters the tower. Due to the evaporation of water, there is a continuous increase in the surface concentration at the droplets surface, and once the concentration is high enough a shell will form. After the formation of the shell there is still water trapped inside the drying particle. Due to the high temperature, the water trapped inside the solidifying particles continues to vaporize and a pressure will form inside the particle. The increase in pressure leads to particle inflation. Smaller particles are more stable than larger particles. The shell of the smaller particles has sufficient mechanical stability to remain spherical, whereas the shell of the larger particles will collapse after inflation, giving the particles a corrugated surface.

Powder Crystallinity

As shown by Chawla et al.^[5] spray drying of aqueous salbutamol sulfate solutions results in the formation of amorphous products. The XRPD pattern of sample 10, which is a sample with an intermediate particle size (see Table 2), is shown in Fig. 10.

Water Vapor Sorption

In order to get an idea regarding the stability of the amorphous spray-dried products upon storage at elevated relative humidities, water vapor sorption experiments were carried out.

In Fig. 11, the moisture-induced change of mass of the spray-dried salbutamol sulfate versus relative humidity of sample 10 (see also Powder Crystallinity section) is shown. In the experiment, the relative humidity was increased from 0 to 95%. It can be seen that there was a continuous increase in mass attributed to the sorption of water in the

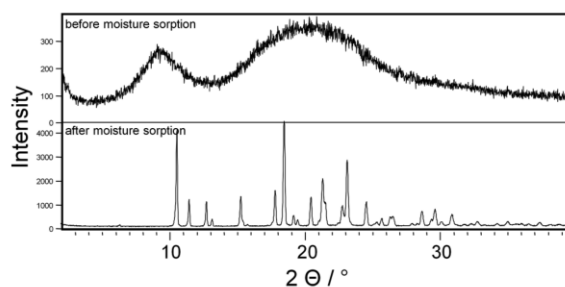


FIG. 10. XRPD pattern of sample 10 (see Table 2) before and after moisture sorption experiments.

RH range of 0 to 60%. At 60% RH the mass suddenly decreased, which was ascribed to crystallization. The water absorbed acts as a plasticizer and reduces the glass transition temperature (T_g) of the amorphous salbutamol sulfate. Once the temperature of the experiment is higher than the glass transition temperature the molecules have sufficient mobility to crystallize and vapor is expelled from the crystal lattice that forms.^[17,18] After the transformation of the amorphous material, the RH was further increased and the final water uptake at 95% RH was measured as 4% for the crystalline material. Subsequently, the humidity was reduced to 0% again, resulting in a decrease in the water content.

In order to prove that there was a change from the amorphous to the crystalline state, XRPD experiments before and after the moisture sorption were performed. Figure 10 shows that after moisture sorption, diffraction

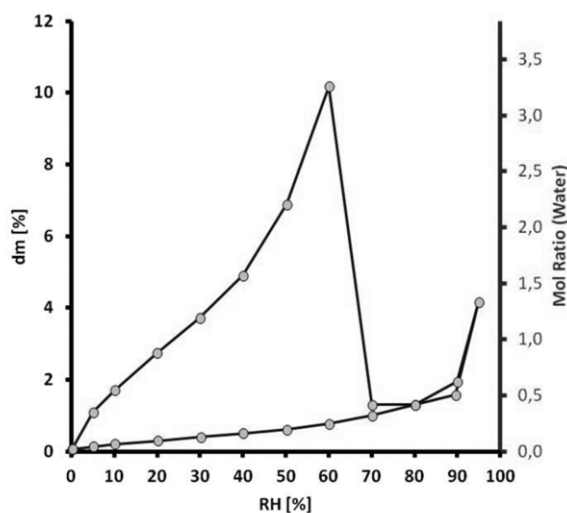


FIG. 11. Sorption isotherm of spray-dried salbutamol sulfate (sample 10; see Table 2).

peaks appeared, verifying the transition from amorphous to crystalline.

Moisture sorption experiments indicated that as long as the RH was below 60%, spray-dried salbutamol sulfate products were stable and could be used in order to study interparticle interactions in DPI formulations.

CONCLUSION

This study shows that particle size can be successfully modified by changing the process parameters of the Nano Spray Dryer B-90 when spray drying aqueous salbutamol sulfate solutions. The particle size can be tailored by adjusting the mesh size, feed concentration, as well as drying air temperature. All products were in the micrometer range (1.0 to 6.4 μm) and had an appropriate size to be used in pulmonary drug delivery. Small particles had a monomodal size distribution, whereas for particles with a mean size above 2.4 μm there was a shift to bimodal distributed sizes. The width of the particle size distribution (span) increased with increasing mesh sizes. The changes in particle size distribution might be a result of the formation of satellite droplets or secondary droplet breakup during atomization. A thorough characterization of the spray generated with the novel vibrating mesh technology is therefore necessary and will be the focus of further research. The amount of product prepared per time was observed to be from 0.4 to 75.8 mg/min. Mesh size as well as concentration significantly impacted the amount of product prepared per time. No correlation between product yield (41.2 to 90.4%) and spray-drying process parameters was observed. Further studies are suggested to identify the reasons for the high variability in product yield. Consistent with the findings of Chawla et al.^[5] who spray dried aqueous salbutamol sulfate solutions on a conventional Mini Spray Dryer B-190, all products were amorphous after spray drying. There was a change from the amorphous to the crystalline state at a relative humidity of 60% at a temperature of 25°C.

ACKNOWLEDGMENTS

The authors thank the German Research Foundation (DFG) for financial support within the priority program SPP 1423 “Prozess-Spray” and Hartmuth Schroettner (Austrian Centre for Electron Microscopy and Nanoanalysis, Graz University of Technology) for his help with SEM.

REFERENCES

1. Scheuch, G.; Zimerlich, W.C.; Siekmeier, R. Biophysical parameters determining pulmonary drug delivery. In: Luessen, H., Bechtold-peters, K. (Eds.); *Pulmonary Drug Delivery—Basics, Application and Opportunities for Small Molecules and Biopharmaceutics*; Editio Cantor Verlag: Aulendorf, Germany, 2007, 102–120.
2. Hickey, A.J. Lung deposition and clearance of pharmaceutical aerosols: What can be learned from inhalation toxicology and industrial hygiene? *Aerosol Science and Technology* **1993**, *18*(3), 290–304.
3. Weiler, C.; Egen, M.; Trunk, M.; Langguth, P. Force control and powder dispersibility of spray dried particles for inhalation. *Journal of Pharmaceutical Sciences* **2010**, *99*, 303–316.
4. Vidgrén, M.T.; Vidgrén, P.A.; Paronen, T.P. Comparison of physical and inhalation properties of spray-dried and mechanically micronized disodium cromoglycate. *International Journal of Pharmaceutics* **1987**, *35*(1–2), 139–144.
5. Chawla, A.; Taylor, K.M.G.; Newton, J.M.; Johnson, M.C.R. Production of spray dried salbutamol sulfate for use in dry powder aerosol formulation. *International Journal of Pharmaceutics* **1994**, *108*, 233–240.
6. Zhao, M.; You, Y.; Ren, Y.; Zhang, Y.; Tang, X. Formulation, characteristics and aerosolization performance of azithromycin Dpi prepared by spray-drying. *Powder Technology* **2008**, *187*(3), 214–221.
7. Arpagaus, C. A novel laboratory-scale spray dryer to produce nanoparticles. *Drying Technology* **2012**, *30*(10), 1113–1121.
8. Lee, S.H.; Heng, D.; Ng, W.K.; Chan, H.-K.; Tan, R.B.H. Nano spray drying: A novel method for preparing protein nanoparticles for protein therapy. *International Journal of Pharmaceutics* **2011**, *403*(1–2), 192–200.
9. BÜCHI Labortechnik AG. *Nano Spray Dryer B-90*; Flawil, Switzerland, 2009.
10. Bürki, K.; Jeon, I.; Arpagaus, C.; Betz, G. New insights into respirable protein powder preparation using a nano spray dryer. *International Journal of Pharmaceutics* **2011**, *408*(1–2), 248–256.
11. Schafroth, N.; Arpagaus, C.; Jadhav, U.Y.; Makne, S.; Douroumis, D. Nano and microparticle engineering of water insoluble drugs using a novel spray-drying process. *Colloids and Surfaces B: Biointerfaces* **2012**, *90*, 8–15.
12. Li, X.; Anton, N.; Arpagaus, C.; Belleleix, F.; Vandamme, T.F. Nanoparticles by spray drying using innovative new technology: The Büchi Nano Spray Dryer B-90. *Journal of Controlled Release* **2010**, *147*(2), 304–310.
13. Huntington, D.H. The influence of the spray drying process on product properties. *Drying Technology* **2004**, *22*(6), 1261–1287.
14. Masters, K. *Spray Drying*; Leonhard Hill Books: London, 1972.
15. Elvesson, J.; Millqvist-Fureby, A. Particle size and density in spray drying—Effects of carbohydrate properties. *Journal of Pharmaceutical Sciences* **2005**, *94*(9), 2049–2060.
16. Vehring, R.; Foss, W.R.; Lechuga-Ballesteros, D. Particle formation in spray drying. *Aerosol Science* **2007**, *38*, 728–746.
17. Buckton, G. Characterisation of small changes in the physical properties of powders of significance for dry powder inhaler formulations. *Advanced Drug Delivery Reviews* **1997**, *26*(1), 17–27.
18. Hancock, B.C.; Shamblin, S.L. Water vapour sorption by pharmaceutical sugars. *Pharmaceutical Science & Technology Today* **1998**, *1*(8), 345–351.

4

Preparation and characterization of physically modified glass beads used as model carriers in dry powder inhalers

Sarah Zellnitz, Jakob Dominik Redlinger-Pohn, Hartmuth Schroettner, Michael Kappl, Nora Anne Urbanetz

International Journal of Pharmaceutics 447 (2013), 132-138



Preparation and characterization of physically modified glass beads used as model carriers in dry powder inhalers

Sarah Zellnitz^{a,*}, Jakob Dominik Redlinger-Pohn^a, Michael Kappl^b, Hartmuth Schroettner^c, Nora Anne Urbanetz^a

^a Research Center Pharmaceutical Engineering GmbH, Inffeldgasse 13, Graz, Austria

^b Max Planck Institute for Polymer Research, Ackermannweg 10, Mainz, Germany

^c Austrian Centre for Electron Microscopy and Nanoanalysis, TU Graz, Steyrergasse 17/III, Graz, Austria

ARTICLE INFO

Article history:

Received 21 December 2012

Received in revised form 18 February 2013

Accepted 19 February 2013

Available online 5 March 2013

Keywords:

Glass beads

Dry powder inhaler

Carrier

Surface modification

Ball mill

ABSTRACT

The aim of this work is the physical modification and characterization of the surface topography of glass beads used as model carriers in dry powder inhalers (DPIs). By surface modification the contact area between drug and carrier and thereby interparticle forces may be modified. Thus the performance of DPIs that relies on interparticle interactions may be improved. Glass beads were chosen as model carriers because various prospects of physical surface modification may be applied without affecting other factors also impacting interparticle interactions like particle size and shape. To generate rough surfaces glass beads were processed mechanically by friction and impaction in a ball mill with different grinding materials that were smaller and harder with respect to the glass beads. By varying the grinding time (4 h, 8 h) and by using different grinding media (tungsten carbide, quartz) surfaces with different shades of roughness were generated. Depending on the hardness of the grinding material and the grinding time the surface roughness was more or less pronounced. Surface roughness parameters and specific surface area were determined via several complementary techniques in order to get an enhanced understanding of the impact of the modifying procedure on the surface properties of the glass beads.

© 2013 Elsevier B.V. All rights reserved.

1. Introduction

Dry powder inhalers (DPIs) are medical devices used in the treatment of COPD and asthma. The formulations used in DPIs typically consist of adhesive mixtures of the active pharmaceutical ingredient (API) and a carrier. In order to reach the tiny airways of the deep lung the API particles have to exhibit an aerodynamic diameter of 1–5 μm . Particles of this size are rather cohesive and show poor flow properties and dosing (Daniher and Zhu, 2008). That is why carrier based formulations, in which the API is attached to the surface of coarser carrier particles (50–200 μm), have been invented. Due to the size and adequate flowability of the carrier the adhesive mixtures of the drug and the carrier exhibit satisfactory flowability. Drug detachment from the carrier during inhalation is necessary to ensure that the drug particles reach their targeted site, the deep lung. Otherwise they will impact together with the coarse carrier on the upper airways. Therefore, interparticle interactions play a

crucial role in carrier based formulations. It is important, that they are on the one hand high enough that uniform dosing is possible and on the other hand low enough that drug detachment during inhalation is guaranteed.

The carrier particles commonly used are lactose or mannitol. As the surface topography largely affects interparticle interactions, different attempts to modify the surface topography of carrier particles to improve the performance of DPIs and increase the fine particle fraction (FPF) were reported. These attempts include crystallization of lactose particles from different media and under different crystallization conditions (Larhrib et al., 2003; Zeng et al., 2000a,b, 2001a,b), particle smoothing by coating lactose particles with aqueous lactose solutions (Chan et al., 2003; Iida et al., 2005), and dispersion of the carrier material in a dispersion media and subsequent elimination of the dispersion media (Dickhoff et al., 2006; El-Sabawi et al., 2006; Iida et al., 2001, 2003; Islam et al., 2004a,b), which is also a method to smoothen particles. Also the addition of fine carrier particles or fine ternary components was documented as a method to alter the surface topography by occupying high energy sites on the carrier or by forming multiple agglomerates (Adi et al., 2006, 2007; Guchardi et al., 2008; Iida et al., 2004a,b; Louey and Stewart, 2002; Louey et al., 2003; Podczek, 1999; Tee et al., 2000; Zeng et al., 2001b). Spray drying was described to be a suitable method to generate mannitol particles with modified

* Corresponding author. Tel.: +43 316 873 30422; fax: +43 316 873 1030422.

E-mail addresses: sarah.zellnitz@rcpe.at (S. Zellnitz), redlinger-pohn@tugraz.at (J.D. Redlinger-Pohn), kappl@mpip-mainz.mpg.de (M. Kappl), hartmuth.schroettner@felmi-zfe.at (H. Schroettner), nora.urbanetz@tugraz.at (N.A. Urbanetz).



Fig. 1. Impact of surface roughness on interparticle interactions. Depending on the shade of the surface roughness meaning the distance between the roughness peaks and valleys the contact area can be altered and thus interparticle interactions.

surface roughness (Littringer et al., 2012; Maas et al., 2011). Other attempts implement the effect of mechanical stress on lactose surface properties e.g. wet smoothing in a high shear mixer (Ferrari et al., 2004), particle smoothing with a high speed mixer in the presence of a small amount of wetting solvent (Young et al., 2002), surface processing with a high speed elliptical-rotor type powder mixer (Iida et al., 2004c), as well as milling lactose with various mill speeds to avoid batch to batch variability and to make carrier particles homogenous (Steckel et al., 2006). However, in most of these cases beside the surface topography also other properties impacting interparticle interactions, like particle size or shape of the carrier particles, are altered. For example, recently, Maas reported carrier surface modification of mannitol by spray drying at different conditions (Maas, 2009). Spray drying changed the surface roughness, however, the particle shape changed as well. In the present work glass beads are used as model carriers. Nevertheless beneath surface roughness particle shape changed as well. That is why the model carriers used in the present work are glass beads. The glass beads have ideal geometry, they are available in different sizes and, most importantly, they allow various prospects of surface modification, without affecting other properties like particle size and shape. However it has to be mentioned that glass beads are neither typical nor conventional carrier particles. They are used as model carriers and the aspect of inhalation toxicity has to be considered if applying the inhalate to the patient finally. Particles in the size of the glass beads (400–600 μm) used in this study are too big to be inhaled. Instead they will impact in the mouth and throat and will be swallowed. Nevertheless if glass beads are considered to be applied as carrier particles in DPI formulations, a new type of inhaler with a particular restraining mechanism for the glass beads has to be designed.

There are different and contradictory findings related to the correlation of particle roughness and fine particle fraction (FPF). For example Kawashima documented that the rougher the carrier particles the lower the FPF (Kawashima et al., 1998). The surface roughness in that study resulted from crevices on the lactose surface. By contrast, Chan reported that rougher lactose carrier particles lead to a higher fine particle fraction (Chan et al., 2003). In that study the surface roughness resulted from the presence of immobilized lactose fine particles on the surface that lead to microscopic undulations on the lactose surface rather than to crevices. These contradictory findings illustrate that it has to be differentiated between roughnesses and that in order to increase the FPF the right kind of surface roughness has to be introduced. As Young (Young et al., 2008) already reported and as Fig. 1 shows, the shade of surface roughness compared to the size and shape of the API largely impacts interparticle interactions and thus drug detachment and FPF. According to that, carrier particles with increased surface area and increased surface roughness pursuant to Fig. 1C lead to higher FPFs and increase the efficiency of DPIs (Kawashima et al., 1998).

Therefore the aim of the present work was to physically modify the surface roughness of glass beads intended for use as carrier particles in DPIs. Carrier particles with increased surface area and different shades of roughness were generated. Carriers were characterized with respect to particle size, shape and surface topography. The applicability, advantages and disadvantages as well as the benefits of combining several techniques of surface characterization including atomic force microscopy (AFM) will be discussed.

2. Materials and methods

2.1. Materials

Glass Beads in the size range of 400 μm to 600 μm ($X_{50} = 537.3 \pm 7.1 \mu\text{m}$) were kindly provided by SiLibeads® (SiLibeads® Glass Beads Type S, Sigmund Lindner GmbH, Warmensteinach/Germany). Sodium hydroxide, used for the cleaning procedure was purchased from Carl Roth GmbH + Co. KG, Karlsruhe/Germany. Glass slides (Standard-Objekttraeger, Carl Roth GmbH + Co. KG) as well as ammonium hydroxide, sulphuric acid and hydrogen peroxide, all three chemicals were also used for the cleaning procedure, were purchased from Lactan Chemikalien und Laborgeraete Vertriebsgesellschaft m.b.H + Co. KG, Graz/Austria. Tungsten carbide was provided by Wolfram Bergbau und Huerten AG, St. Martin i.S./Austria and quartz was obtained from Quarzwerke Austria GmbH, Melk/Austria.

2.2. Sample preparation

Prior to use, the glass beads were cleaned with Piranha Solution (3:7 $\text{H}_2\text{O}:\text{H}_2\text{SO}_4$) followed by a standard clean (1:1:5 $\text{H}_2\text{O}_2:\text{NH}_4\text{OH}:\text{H}_2\text{O}$) and stored in a desiccator over silica gel.

Physical surface modification of glass beads was carried out by friction and impactation in a ball mill (Ball Mill S2, Retsch, Haan/Germany). To get surfaces with different shades of roughness, grinding materials with different Mohs hardness were chosen and glass beads were processed for 8 h and 4 h at 424 rpm. The grinding materials used were tungsten carbide (TC) and quartz (Q) (Table 1). The soda lime glass beads used have a hardness of about 6 on the Mohs scale, so the both grinding materials are harder than glass. The ratio of grinding material to glass beads in the milling chamber was 1:1 (V/V). After grinding the grinding material was separated from the glass beads by sieving on a 250 μm sieve. Then the glass beads were washed with purified water until the supernatant was clean and free of residue of the grinding material (at least 5 times). Finally, the physically treated glass beads were washed again with piranha solution to make sure that all adherent impurities of the grinding procedure had been removed.

2.3. Particle surface investigation

Untreated and physically modified glass beads were examined using a scanning electron microscope (SEM) (Zeiss Ultra 55, Zeiss, Oberkochen/Germany) operating at 5 kV. The glass beads had been sputtered with gold–palladium prior to analysis.

2.4. Particle size distribution

Due to the large size of the glass beads, the number of glass beads seen by the laser beam would have been too low to get a sufficient intensity of the diffraction patterns with the equipment

Table 1
Specifications of the grinding materials used.

Material	Mohs hardness	X_{50} (μm)
Quartz	7	32.17
Tungsten carbide	9.5	23.58

available. Consequently it was not possible to determine the particle size distribution of the glass beads with laser diffraction. That is why the particle size of the untreated as well as physically modified glass beads was investigated using a QUICPIC (Sympatec GmbH, Clausthal-Zellerfeld/Germany) image analysis instrument. For sample dispersion a dry dispersing system (Rodas/L, Sympatec GmbH) and a vibrating chute (Vibri, Sympatec GmbH) were used. The dispersion pressure applied was 0.2 bar. The measuring time was 6 s and 450 pictures/s were taken, so the total number of analyzed particles per measurement was 400–7000. The data were evaluated using the software Windox 5 (Sympatec GmbH). The mean particle size was described by the Feret mean diameter. The Feret diameter is derived from the distance of two tangents to the contour of the particle in a well defined orientation. The method corresponds to the slide gauge principle. The Feret mean diameter is the mean value of the Feret diameters over all orientations (0–180°) according to the principle described above (Sympatec GmbH, 2012).

2.5. Particle sphericity

Sphericity, S , is the ratio of the perimeter of the equivalent circle, P_{EQPC} , to the real perimeter, P_{REAL} (Sympatec GmbH, 2012). The sphericity of untreated and physically modified glass beads was investigated also using the QUICPIC image analysis instrument. A dry dispersing system and a vibrating chute were used for sample dispersion. The dispersion pressure applied was 0.2 bar. The measuring time was 6 s and 450 pictures/s were taken, so the total number of analyzed particles per measurement was 400–7000. Particle sphericity was calculated according to Eq. (1) also using the software Windox 5 (Sympatec GmbH). As a result values between 0 and 1 can be obtained. A value of 1 is given by a perfectly spherical particle. The smaller the value, the more irregular is the shape of the particle (Figs. 2 and 3).

$$S = \frac{P_{EQPC}}{P_{REAL}} = \frac{2\sqrt{\pi \times A}}{P_{REAL}} \quad (1)$$

2.6. Surface roughness

Atomic force microscopy (VEECO, Dimension, Nanoscope IIIa, Bruker AXS GmbH, Karlsruhe/Germany) was used to determine the surface roughness. The untreated and modified glass beads were glued on commercially available glass slides with a two component epoxy resin adhesive (UHU GmbH & Co. KG, Buehl/Baden/Germany). The surface roughness was measured on a square of $10 \mu\text{m} \times 10 \mu\text{m}$ on the top of single particles with tapping-mode imaging in air using standard silicon tips OMCLAC160TS-WZ (Olympus, Tokyo/Japan). The root mean square roughness (R_{rms}) was calculated using the data analysis program Gwyddion 2.25 (Klapetek et al., 2012). The R_{rms} value is an amplitude parameter and gives the root mean square of the measured height deviations from the mean height value of each scan line. To separate local surface roughness from the overall curvature of the beads, bead curvature was subtracted for each AFM image before roughness calculation. For each type of modified glass beads at least 4 different beads were analyzed and on each glass bead three to four $10 \mu\text{m} \times 10 \mu\text{m}$ squares were analyzed. For each square a roughness value was calculated based on Eq. (2)

$$R_{rms} = \sqrt{\frac{1}{N} \sum_{j=1}^N r_j^2} \quad (2)$$

where N is the number of equally spaced image points along all scan lines and r_j is the vertical distance of j th data point from the mean of each scan line (Klapetek et al., 2012).

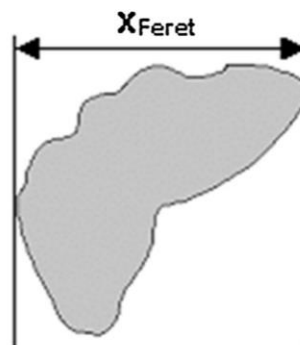


Fig. 2. Feret diameter determination, here: horizontal orientation (0°). Source: Sympatec GmbH (2012).

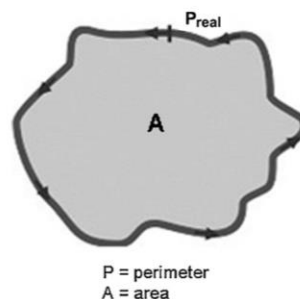


Fig. 3. Sphericity determination. Source: Sympatec GmbH (2012).

2.7. Surface area

The surface area was determined via physical adsorption of krypton with a Tristar II3020 surface area and porosity analyzer (Micromeritics Instrument Company, Norcross/USA). Samples were degassed at least 2 h at 150 °C prior to analysis. A seven point analysis was made between 0.7 and 0.25 relative pressure and the surface area was calculated according to the Brunauer–Emmet–Teller equation. Sample weight was at the minimum 6 g. Samples were analyzed in triplicate.

3. Experimental results and discussion

3.1. Particle size distribution and particle sphericity

When modifying the surface of lactose or mannitol carrier particles, for example by spray drying, besides surface topography, particle size and shape are influenced as well. As already mentioned, one advantage of glass beads as potential carrier particles in DPIs is that by modifying the surface topography particle size and shape are not necessarily changed. To confirm this, the particle size and the sphericity of the untreated and the physically treated glass beads were analyzed. Fig. 4 shows that the physical surface modification does not significantly decrease the particle size of the glass beads that might have been occurred due to attrition or breakage. Fig. 5 shows that the physical surface modification of glass beads does not change the particle shape either. The sphericity values of untreated as well as physically modified glass beads are between 0.92 and 0.97, indicating that all particles are spherical. Large surface irregularities would lead to non spherical particles and would

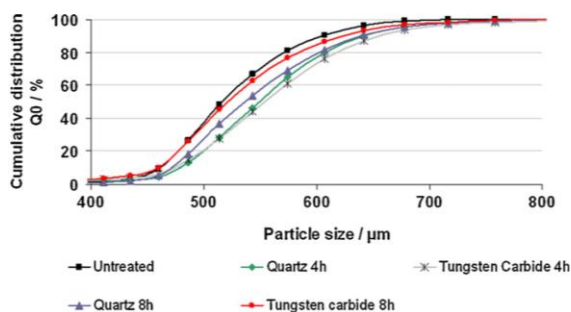


Fig. 4. Particle size distribution of untreated and physically modified glass beads determined by image analysis (mean of $n=3$ PSD curves).

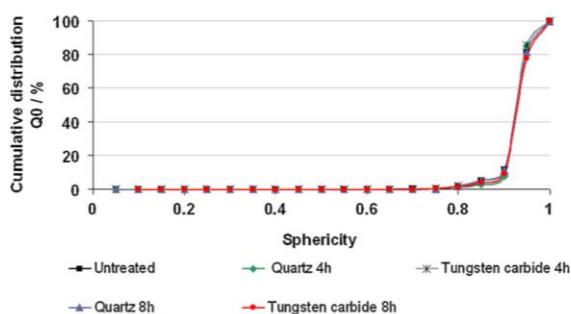


Fig. 5. Particle sphericity of untreated and physically modified glass beads determined by image analysis (mean of $n=3$).

result in lower sphericity values. The sphericity values are rather the same throughout all samples, indicating that glass bead surface processing in a ball mill under the set conditions does not lead to glass bead damage or breakage.

3.2. SEM pictures of glass beads

Fig. 6 shows SEM pictures of untreated (Fig. 6a) glass beads and physically modified (Fig. 6b–e) glass beads. As shown in Fig. 6a, the untreated glass beads have a smooth surface. With an image width of $882.2\ \mu\text{m}$, the untreated as well as physically treated glass

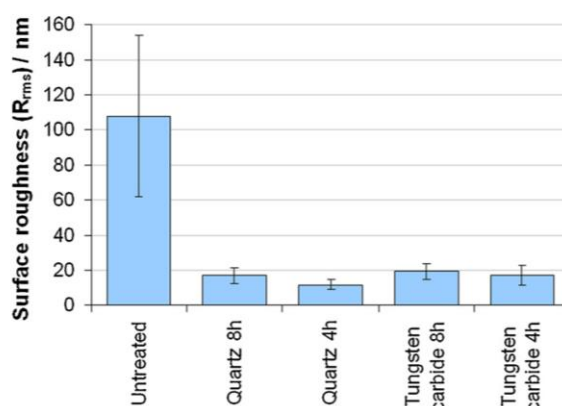


Fig. 7. Surface roughness (R_{rms}) of untreated and physically modified glass beads determined by AFM (mean of $n=12-16 \pm \text{SD}$).

beads look the same. No changes of the surface topography can be observed. SEM images taken at higher magnifications (image width $11.43\ \mu\text{m}$) show that physical surface processing of glass beads in a ball mill leads to changes of the surface topography compared to untreated glass beads. Grinding with materials that are harder and smaller (Table 1) than the glass beads leads to roughnesses only visible at large magnifications. It seems that the surface of the tungsten carbide treated glass beads shows larger surface irregularities than the surface of quartz treated glass beads. This was expected and is well in accordance with the Mohs hardness (quartz 7 and tungsten carbide 9.5) of the grinding materials. From the SEM images it can also be assumed that an 8 h grinding time leads to more pronounced surface changes than a 4 h grinding time. This is applicable to quartz as well as tungsten carbide treatment.

3.3. Surface roughness

In order to quantify the surface topography changes that had been visualized by SEM images at high magnifications, the glass bead surface was analyzed via AFM and the R_{rms} surface roughness value was calculated. In Fig. 7, it can be seen that the R_{rms} value of the untreated glass beads is higher than the R_{rms} values of the physically modified glass beads. This is surprising and was not expected from the SEM images. One explanation for the high R_{rms} value of

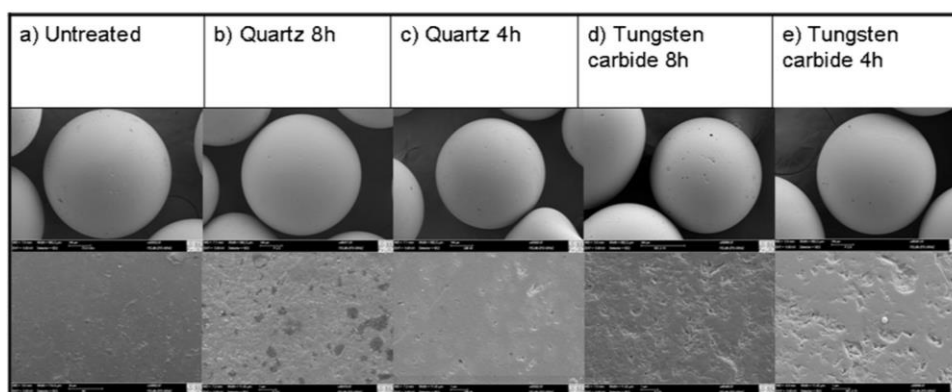


Fig. 6. SEM pictures of (a) untreated and (b–e) physically modified glass beads.

untreated glass beads might be the presence of very few, but deep clefts and/or voids present on the untreated glass beads surface due to the manufacturing process or transport. These surface irregularities, of about $1\ \mu\text{m}$ amplitude can be seen at the surface AFM images of the untreated glass beads displayed in Fig. 8a. However, the magnification used with the SEM was not sufficient in order to make the irregularities visible. As the R_{rms} value determined with AFM is a measure of the roughness amplitude, such occasionally appearing irregularities result in high R_{rms} values and also a relatively high standard deviation if present in the area measured. As the cracks and clefts on the untreated glass bead surface had diminished after grinding (please note the scale of the y-axis), grinding seems to rip off the surface of the glass beads to some extent. However, it is hard to estimate the exact amount of glass that has been ripped off. From the AFM images displayed in Fig. 8a it can be concluded, that a layer of at least $1\ \mu\text{m}$ in thickness must have been removed. However, as the particle size has not been significantly reduced (Fig. 4), the extent of removal is assumed not to exceed several microns. Thus grinding leads to uniform surface roughnesses (Fig. 8b–e). This is illustrated by smaller R_{rms} values and lower standard deviations compared to the untreated glass beads. Moreover, the R_{rms} values of the physically modified glass beads are well in accordance with the SEM images of the modified particles. As SEM images already indicated, glass bead processing with tungsten carbide for 8 h leads to the highest R_{rms} value and thus to the roughest surface. By comparison, grinding with quartz for 4 h leads to the smallest R_{rms} value and so to the least rough surface. The tapping mode images presented in Fig. 8 also show that depending on the grinding material the surface roughness looks different. Processing with quartz (Fig. 8b and c) leads to a finer roughness than processing with tungsten carbide (Fig. 8d and e). Looking at the scale it can also be seen that especially the depth of the roughness is higher when processing with tungsten carbide (Fig. 8c and d). The roughness visible on the images is also well in accordance with the hardness of the grinding materials and the processing time.

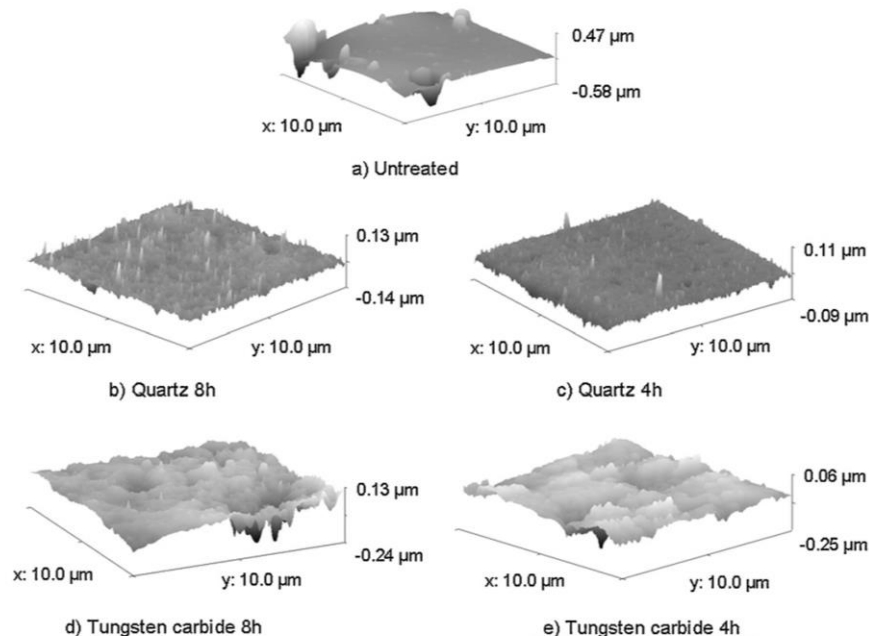


Fig. 8. Tapping mode AFM surface images of (a) untreated glass beads, (b), (c) physically modified glass beads with quartz and (d), (e) physically modified glass beads with tungsten carbide.

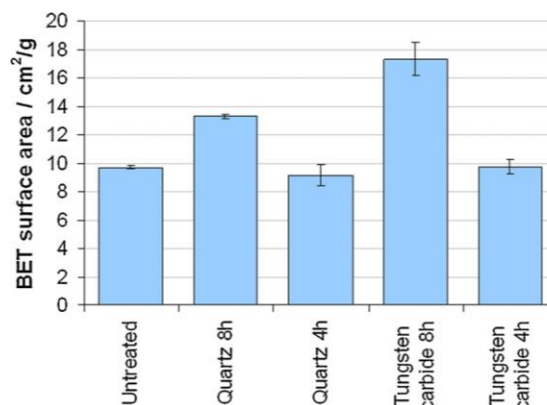


Fig. 9. Specific surface area of untreated and physically modified glass beads determined by nitrogen adsorption and calculated via the Brunauer–Emmett–Teller approach (mean of $n = 3 \pm \text{SD}$).

3.4. Surface area

Another option to quantify the surface topography changes is determining the BET surface area. In Fig. 9 it is evident, that glass beads grinded with tungsten carbide for 8 h exhibit the largest surface area among the physically modified glass beads and glass beads grinded with quartz for 4 h the lowest. Grinding with quartz for 8 h and grinding with tungsten carbide for 4 h lead to specific surface areas in between. Actually, the glass particles grinded for 8 h have higher specific surface area than the glass particles grinded for 4 h. This applies to both grinding materials. These findings match with the results of the AFM roughness analysis and the expectations with regard to the hardness of the grinding materials

and the processing time. In contrast to the R_{rms} values determined by AFM, the untreated glass beads exhibit a surface area of about $9.67 \pm 0.12 \text{ cm}^2/\text{g}$, which does not significantly differ from the surface area of the glass beads treated with quartz and with tungsten carbide for 4 h. Obviously, the few deep clefts on the surface of the untreated glass beads result in a similar surface area as the slightly roughened surface of the 4 h quartz treated glass beads. So for the untreated glass beads the specific surface areas cannot be correlated with the R_{rms} values obtained from AFM measurements.

4. Conclusion

As previously discussed, to improve the performance of DPIs, carrier particles with increased surface roughness had to be engineered. This study shows that the surface roughness of glass beads, intended for the use as carrier in dry powder inhalers, can be successfully modified. Mechanical treatment in a ball mill leads to surfaces with roughnesses in the nanometer scale. Depending on the hardness of the grinding material and the grinding time the surface roughness is more or less pronounced. According to the Mohs hardness of the grinding material, grinding with tungsten carbide leads to rougher surfaces than grinding with quartz. However, surface modification does not change the mean particle size and shape of the glass beads. For measuring the surface roughness that first had been visualized via SEM, two different analytical techniques were applied. As introduced, the surface roughnesses should lead to increased surface areas. The specific surface area of the glass beads was measured via BET gas adsorption. Beside this indirect measurement, the glass beads surface roughness was studied via AFM. Using this technique, on the one hand surface images that visualize the surface roughness qualitatively may be obtained. On the other hand, R_{rms} values may be calculated in order to quantify the surface roughness. The results of the SEM analysis are consistent with the results of the AFM images. Mechanically treated glass beads exhibit rougher surfaces than untreated glass beads. Although cracks and voids on the untreated glass beads cannot be visualized via SEM, they can clearly be seen on AFM surface images. This is due to the larger magnification of AFM. Also the AFM surface images and the calculated R_{rms} values are consistent. The more pronounced the roughnesses on the AFM surface images the higher the calculated R_{rms} values. However, it is interesting that the few but deep clefts on the surface of untreated glass beads are responsible for high R_{rms} values, higher than the R_{rms} values of all the mechanically treated glass beads. An explanation for this is that via AFM the surface amplitude is measured. Although the voids and clefts on the glass beads surface are rare, they are deeper than the roughnesses on the mechanically treated glass beads as by grinding the glass beads surface is ripped off to some extent. By comparison, the BET surface values of untreated glass beads are rather small. They are comparable with the surface values of the 4 h mechanically treated glass beads. It can be concluded that only the combination of several analytical techniques leads to an accurate characterization of the glass beads and allows the comparison of the results among each other.

Beyond these findings generally it has to be considered that differences that may occur might also be caused by the sample size, which is different depending on the analytical technique applied. The BET surface area is measured using the whole glass bead surface and per measurement hundreds of glass beads are measured. Contrary, the mean roughness of the glass beads determined with AFM is measured on small areas on the glass bead surface. Additionally, only a few beads are used for the R_{rms} determination. The glass bead curvature is the limiting factor for the area that can be scanned. In order to avoid that the glass bead curvature influences the results

of the AFM scans, scans have to be carried out on the highest spot of the glass bead and the scanning area has to be restricted to a limited size, so that the spot of the glass bead surface measured is as flat as possible. Due to the limited sample size, special attention has to be paid to the representativity of the sample.

The aim of further work is the determination of interparticle interactions between the glass beads and a model drug, and furthermore checking the correlation of surface characteristics and interparticle interactions. Finally, the respirable fraction of the model drug will be determined and the correlation with the surface roughness of the carrier will be checked in order to show the overall effect of the surface roughness on the performance of the dry powder inhalate.

Acknowledgment

The authors would like to thank the German Research Foundation (DFG) for financial support within the priority program SPP 1486 "Particles in Contact".

References

- Adi, H., Larson, I., Chiou, H., Young, P., Traini, D., Stewart, P., 2006. Agglomerate strength and dispersion of salmeterol xinafoate from powder mixtures for inhalation. *Pharm. Res.* 23, 2556–2565.
- Adi, H., Larson, I., Stewart, P.J., 2007. Adhesion and redistribution of salmeterol xinafoate particles in sugar-based mixtures for inhalation. *Int. J. Pharm.* 337, 229–238.
- Chan, L.W., Lim, L.T., Heng, P.W.S., 2003. Immobilization of fine particles on lactose carrier by precision coating and its effect on the performance of dry powder formulations. *J. Pharm. Sci.* 92, 975–984.
- Daniher, D.I., Zhu, J., 2008. Dry powder platform for pulmonary drug delivery. *Particulateology* 6, 225–238.
- Dickhoff, B.H.J., De Boer, aH., Lambregts, D., Frijlink, H.W., 2006. The effect of carrier surface treatment on drug particle detachment from crystalline carriers in adhesive mixtures for inhalation. *Int. J. Pharm.* 327, 17–25.
- El-Sabawi, D., Price, R., Edge, S., Young, P.M., 2006. Novel temperature controlled surface dissolution of excipient particles for carrier based dry powder inhaler formulations. *Drug Dev. Ind. Pharm.* 32, 243–251.
- Ferrari, F., Cocconi, D., Bettini, R., Giordano, F., Santi, P., Tobyn, M., Price, R., Young, P., Caramella, C., Colombo, P., 2004. The surface roughness of lactose particles can be modulated by wet-smoothing using a high-shear mixer. *AAPS PharmSciTech.* 5, 1–6.
- Guchardi, R., Frei, M., John, E., Kaerger, J.S., 2008. Influence of fine lactose and magnesium stearate on low dose dry powder inhaler formulations. *Int. J. Pharm.* 348, 10–17.
- Iida, K., Hayakawa, Y., Okamoto, H., Danjo, K., Leuenberger, H., 2001. Evaluation of flow properties of dry powder inhalation of salbutamol sulfate with lactose carrier. *Chem. Pharm. Bull.* 49, 1326–1330.
- Iida, K., Hayakawa, Y., Okamoto, H., Danjo, K., Leuenberger, H., 2003. Preparation of dry powder inhalation by surface treatment of lactose carrier particles. *Chem. Pharm. Bull.* 51, 1–5.
- Iida, K., Hayakawa, Y., Okamoto, H., Danjo, K., Luenberger, H., 2004a. Influence of storage humidity on the in vitro inhalation properties of salbutamol sulfate dry powder with surface covered lactose carrier. *Chem. Pharm. Bull.* 52, 444–446.
- Iida, K., Hayakawa, Y., Okamoto, H., Danjo, K., Luenberger, H., 2004b. Effect of surface layering time of lactose carrier particles on dry powder inhalation properties of salbutamol sulfate. *Chem. Pharm. Bull.* 52, 350–353.
- Iida, K., Inagaki, Y., Todo, H., Okamoto, H., Danjo, K., Luenberger, H., 2004c. Effects of surface processing of lactose carrier particles on dry powder inhalation properties of salbutamol sulfate. *Chem. Pharm. Bull.* 52, 938–942.
- Iida, K., Todo, H., Okamoto, H., Danjo, K., Leuenberger, H., 2005. Preparation of dry powder inhalation with lactose carrier particles surface-coated using a Wurster fluidized bed. *Chem. Pharm. Bull.* 53, 431–434.
- Islam, N., Stewart, P., Larson, I., Hartley, P., 2004a. Effect of carrier size on the dispersion of salmeterol xinafoate from interactive mixtures. *J. Pharm. Sci.* 93, 1030–1038.
- Islam, N., Stewart, P., Larson, I., Hartley, P., 2004b. Lactose surface modification by decantation: are drug-fine lactose ratios the key to better dispersion of salmeterol xinafoate from lactose-interactive mixtures? *Pharm. Res.* 21, 492–499.
- Kawashima, Y., Serigano, T., Hino, T., Yamamoto, H., Takeuchi, H., 1998. Effect of surface morphology of carrier lactose on dry powder inhalation property of pranlukast hydrate. *Int. J. Pharm.* 172, 179–188.
- Klapetek, P., Necas, D., Anderson, C., 2012. Gwyddion User Guide, <<http://gwyddion.net/download/user-guide/gwyddion-user-guide-en.pdf>> (accessed 04.02.13).

- Larhrib, H., Martin, G.P., Marriott, C., Prime, D., 2003. The influence of carrier and drug morphology on drug delivery from dry powder formulations. *Int. J. Pharm.* 257, 283–296.
- Littringer, E.M., Mescher, A., Schroettner, H., Achelis, L., Walzel, P., Urbanetz, N.A., 2012. Spray dried mannitol carrier particles with tailored surface properties – the influence of carrier surface roughness and shape. *Eur. J. Pharm. Biopharm.* 82, 194–204.
- Louey, M.D., Razia, S., Stewart, P.J., 2003. Influence of physico-chemical carrier properties on the in vitro aerosol deposition from interactive mixtures. *Int. J. Pharm.* 252, 87–98.
- Louey, M.D., Stewart, P.J., 2002. Particle interactions involved in aerosol dispersion of ternary interactive mixtures. *Pharm. Res.* 19, 1524–1531.
- Maas, S.G., 2009. Optimierung trägerbasierter Pulverinhalate durch Modifikation der Trägeroberfläche mittels Sprühtrocknung, PhD thesis, Heinrich Heine University Duesseldorf.
- Maas, S.G., Schaldach, G., Littringer, E.M., Mescher, A., Griesser, U.J., Braun, D.E., Walzel, P.E., Urbanetz, N.A., 2011. The impact of spray drying outlet temperature on the particle morphology of mannitol. *Powder Technol.* 213, 27–35.
- Podczek, F., 1999. The influence of particle size distribution and surface roughness of carrier particles on the in vitro properties of dry powder inhalations. *Aerosol Sci. Technol.* 31, 301–321.
- Steckel, H., Markefka, P., TeWierik, H., Kammelar, R., 2006. Effect of milling and sieving on functionality of dry powder inhalation products. *Int. J. Pharm.* 309, 51–59.
- Sympatec GmbH, 2012. Fundamentals – Particle Size and Shape Calculation by Image Analysis <<http://www.sympatec.com/EN/ImageAnalysis/Fundamentals.html>> (accessed 04.02.13).
- Tee, S.K., Marriott, C., Zeng, X.M., Martin, G.P., 2000. The use of different sugars as fine and coarse carriers for aerosolised salbutamol sulphate. *Int. J. Pharm.* 208, 111–123.
- Young, P.M., Cocconi, D., Colombo, P., Bettini, R., Price, R., Steele, D.F., Tobyn, M., 2002. Characterization of a surface modified dry powder inhalation carrier prepared by particle smoothing. *J. Pharm. Pharmacol.* 1339–1344.
- Young, P.M., Roberts, D., Chiou, H., Rae, W., Chan, H.-K., Traini, D., 2008. Composite carriers improve the aerosolisation efficiency of drugs for respiratory delivery. *J. Aerosol Sci.* 39, 82–93.
- Zeng, X.M., Martin, G.P., Marriott, C., Pritchard, J., 2000a. The influence of crystallization conditions on the morphology of lactose intended for use as a carrier for dry powder aerosols. *J. Pharm. Pharmacol.* 52, 633–643.
- Zeng, X.M., Martin, G.P., Marriott, C., Pritchard, J., 2000b. Crystallization of lactose from carbopol gels. *Pharm. Res.* 17, 879–886.
- Zeng, X.M., Martin, G.P., Marriott, C., Pritchard, J., 2001a. The use of lactose recrystallised from carbopol gels as a carrier for aerosolised salbutamol sulphate. *Eur. J. Pharm. Biopharm.* 51, 55–62.
- Zeng, X.M., Martin, G.P., Marriott, C., Pritchard, J., 2001b. Lactose as a carrier in dry powder formulations: the influence of surface characteristics on drug delivery. *J. Pharm. Sci.* 90, 1424–1434.

5

Influence of surface coverage on the fine particle fraction: investigating surface modified glass beads as model carriers in dry powder inhalers

Sarah Zellnitz , Hartmuth Schroettner, Nora Anne Urbanetz

Powder Technology, submitted for publication

Influence of surface coverage on the fine particle fraction: investigating surface modified glass beads as model carriers in dry powder inhalers

Sarah Zellnitz^{a*}, Hartmuth Schroettner^b, Nora Anne Urbanetz^a

**Corresponding author. Tel.: +43 316 873 30422; Fax: +43 316 873 1030422;*

E-mail address: sarah.zellnitz@rcpe.at

^aResearch Center Pharmaceutical Engineering GmbH, Inffeldgasse 13, Graz, Austria,

^bAustrian Centre for Electron Microscopy and Nanoanalysis, TU Graz, Steyrergasse 17/III, Graz, Austria,

Keywords: surface coverage, dry powder inhaler, glass beads, surface modification, fine particle fraction

Abstract

The relationship between surface coverage and in vitro respirable fraction – often referred as to fine particle fraction (FPF) – of dry powder inhaler (DPI) formulations for the therapy of asthma were investigated using an artificial lung, the next generation impactor (NGI). Therefore mixtures with 100%, 50% and 25% calculated surface coverage of physically and chemically modified glass beads as model carrier and spray dried salbutamol sulphate as active

pharmaceutical ingredient (API) have been prepared. In any of these cases the actual surface coverage was lower than the calculated surface coverage as a certain amount of API particles adheres to the mixing container wall instead of the glass beads surface. Moreover, API particles detach from the glass beads surface during capsule filling and transport resulting in even lower true surface coverage at the moment when the NGI experiments are performed. When investigating the FPF this true surface coverage has to be taken into account. The FPF increased more or less linearly with increasing surface coverage of the surface modified glass beads but the slopes of the lines are different depending of the carriers used. This can be attributed to the distribution of active sites on the glass beads surface that is individual depending on the surface modification applied and the processing time. However the influence of surface coverage on FPF is also influenced by the choice of the carrier particles. Compared to untreated glass beads physically modified glass beads show increased FPFs whereas chemically modified glass beads show lower FPFs.

5.1 Introduction

Drug detachment of active pharmaceutical ingredient (API) particles from the carrier surface in carrier based dry powder inhaler (DPI) formulations is influenced by various factors like carrier as well as API surface properties, shape and size, inhalation device used and drug to carrier ratio [1]. A lot of research has been done on some of these influencing factors, especially on carrier surface properties and carrier surface modification [2–7]. But also the drug load is an important influencing factor and must not be neglected.

Young et al. [8] studied the influence of micronized salbutamol sulphate concentration on the performance of a model DPI system with lactose as carrier particles. Results showed that an increase in API concentration leads to an increased fine particle dose ((FPD), amount of particles < 5 μ m) first, but to an increased fine particle fraction FPF (% of API particles < 5 μ m that reach the deep lung related to the total amount of particles that leaves the inhaler) only when a certain salbutamol sulphate concentration is used. These findings were attributed to the occupation of active carrier sites by drug particles at low drug

concentrations, since the quantity of drug particles released from the carrier during inhalation remains constant at lower dosing regimes. These active sites in combination with the drug load in formulations have been investigated by Young et al. [9] in another study. Results imply that API particles first adhere to active (high energy) sites on the carrier surface and until these active sites on the carrier are saturated the FPF is low as API particles adhere strongly to the active sites and are not detached easily. When increasing the amount of API also less energetic sites on the carrier surface are occupied and covered. As a consequence API particles adhered to these less energetic sites detach more likely and easily and the FPF increases. Also, El-Sabawi et al. [10] found that due to active sites on the carrier surface drug detachment is lower at lower drug loads, when using salbutamol sulphate in different concentrations as API and lactose as model carriers. Moreover El-Sabawi et al. found that by particle smoothing of lactose carriers active sites on the surface can be reduced and so drug detachment enhanced. The active sites are a result of variations in morphology and surface free energy and as the surface of commonly used lactose carriers is normally inhomogeneous this hypothesis might be true for most of the formulations used in DPIs. Le et al. [11] also investigated DPI systems with lactose carrier particles but formoterol and fluticasone as API particles. Results showed that drug detachment from the lactose carrier and so the fine particle fraction increased linearly with the formoterol concentration in the adhesive mixtures. This can also be explained by the active sites theory but in this case the active sites must have been initially saturated so that an increase in the formoterol concentration immediately led to an increased FPF. However, Le et al. found out that this linear relation is not true when using fluticasone as API. Fluticasone behaves rather different from formoterol and tends to agglomerate and to form clusters. These agglomerates and or clusters cannot be redispersed during inhalation. That is why the FPF first increased when increasing the fluticasone concentration and then decreased with a further increase of the fluticasone concentration. Steckel and Mueller [12] investigated the influence of device, lactose sieve fraction and drug to carrier ratio on the in vitro deposition and found that the FPF decreases when increasing the amount of API (budesonide) in the mixtures, independent of

what sieve fraction of lactose was used. This effect was attributed to the agglomeration of API particles, at high concentrations too.

In most DPI formulations one of these phenomena (active site and agglomeration) or even a combination might occur depending on the physicochemical properties and the concentration of the API used. First all active sites are saturated until a plateau is reached (the FPF remains constant) then due to a further increase of API less active sites are saturated and drug detachment increases [1,8,10,11]. But when increasing the API content further it is also possible that multilayers are formed and the API tends to form clusters/agglomerates. Depending on the properties (e. g. shape and interparticle porosity) of these multilayers, clusters and agglomerates, API particles might be bound stronger or weaker. However, if clusters/agglomerates are detached, it will be difficult to break them up into primary particles. Generally this will result in a decrease of the FPF [9,12].

Young et al.[9] used polystyrene spheres as model carrier to study the effect of drug load on the aerosolization performance and found that the FPF of salbutamol sulphate is not influenced by the drug load when monolayer formation is not exceeded. Only when monolayer formation is approached or exceeded slightly increased FPFs were observed. But when increasing the drug load further the blend becomes unstable, probably due to API agglomeration and blend segregation the FPF decreases again. By contrast the FPD first increased linearly with drug load, up to a point before a decrease in the FPD was observed. This rapid increase can be explained by the absence of active sites since the polystyrene spheres used were free from surface irregularities and had a low variation in drug-carrier adhesion. Whereas the decrease can also be attributed to API agglomeration and blend segregation [9]. In all the other studies the surface coverage and monolayer formation was not part of the research and so it is difficult to compare the results among each other. But nevertheless it could be observed that agglomeration of salbutamol sulphate at high drug loads occurs and leads to decreased FPFs. As already mentioned before this effect was also observed when lactose as carrier particles were used.

The overall goal of the present work is tailoring drug detachment from carrier particles in DPIs via the surface modification of the carrier particles used. Therefore glass beads were used as model carrier because they allow chemical as well as physical modification of their surface without changing the geometric properties like size and shape. Other advantages of glass beads as potential model carrier have been mentioned in a previous work [13]. As mentioned before and described in the literature, the drug load is one important factor influencing the performance of DPIs. In order to be able to study the impact of the surface properties of the carrier particles on the performance of DPI formulations, the drug load has to be the same for each carrier under investigation. As the adhesion of drug particles onto the carriers surface also is influenced by the carrier surface properties the same amount of API weighed in for the preparation of the adhesive mixture does not necessarily mean that the carrier surface is covered to the same extent with drug particles.

That is why in the present work the actual surface coverage of surface modified and untreated glass beads used as model carriers after mixing and handling has been investigated depending on the amount of API that has been weighed in for the preparation of adhesive mixtures. Furthermore the performance of the adhesive mixtures with different actual surface coverages was assessed by determining the FPF of the API salbutamol sulphate. Therefore adhesive mixtures were prepared of untreated and surface modified glass beads with a calculated surface coverage of 100%, 50% and 25% of spray dried salbutamol sulphate. The surface coverage in the present study was carefully considered and did purposely not exceed 100% as the effect of API agglomeration and blend separation as it was documented by Young et al. [9] should be avoided. As a result it should be possible on the one hand to check whether the active site theory is true and on the other hand when comparing the performance of the inhalation powder using glass beads of different surface modification but equal surface coverage to evaluate the impact of surface modification on the performance of the DPI. Finally for each API it should be possible to choose the appropriately surface modified carrier.

5.2 Materials and methods

5.2.1 Materials

Glass beads in the size range of 400 μm to 600 μm ($x_{50} = 537.3\mu\text{m} \pm 7.1\mu\text{m}$; $n = 3$, mean \pm SD) were kindly provided by SiLibeads® (SiLibeads® Glass Beads Type S, Sigmund Lindner GmbH, Warmensteinach, Germany) and served as model carriers either untreated or physically or chemically surface modified. All glass beads were cleaned with Piranha Solution (3:7 = $\text{H}_2\text{O}:\text{H}_2\text{SO}_4$) followed by a standard clean (1:1:5 = $\text{H}_2\text{O}_2:\text{NH}_4\text{OH}:\text{H}_2\text{O}$) prior to use. Salbutamol sulphate (USP25 quality) was purchased from Selectchemie AG (Zuerich, Switzerland) and used as model API after spray drying. Triphenylchlorosilane and 3,3,3-Trifluoropropyltrimethoxysilane were purchased from Sigma-Aldrich Handels GmbH, Vienna, Austria while acetic acid, ammonium hydroxide, sulphuric acid and hydrogen peroxide were purchased from Lactan Chemikalien und Laborgeraete Vertriebsgesellschaft m.b.H & Co. KG, Graz, Austria.

5.2.2 Preparation of surface modified carrier particles

Physical surface modification of glass beads was performed mechanically by friction and impaction in a ball mill (Ball Mill S2, Retsch, Haan, Germany). By using two different grinding materials (tungsten carbide (TC) and quartz (Q)) with different hardness and two different processing times (4 hours and 8 hours) glass beads with different shades of roughness could be generated [13]. Additionally physical surface modification was performed by plasma etching with a TEGAL901. The gases used were CF_4/O_2 and the ratio was 120sccm/15sccm at 1800mTorr. The plasma power was 200W and the exposure time 1 minute. Chemical surface modification was performed by treating the glass beads with two different silanes (Triphenylchlorosilane (TPCS) and 3,3,3-Trifluoropropyltrimethoxysilane (FPTS). Therefore 40g glass beads were soaked with a mixture of 1ml silane and 70ml toluol anhydrous for 24 hours. After treatment glass beads were washed several times with purified water until the filtrate was neutral and dried in an oven at 150°C for 48 hours.

Therefore glass beads with different surface hydrophobicity could be generated.

5.2.3 Characterization of the carrier particles

5.2.3.1 Surface roughness

Atomic force microscopy (VEECO, Dimension, Nanoscope IIIa, Bruker AXS GmbH, Karlsruhe, Germany) was used to determine the surface roughness. The untreated and modified glass beads were glued on commercially available glass slides with a two component epoxy resin adhesive (UHU GmbH & Co. KG, Baden, Germany). The surface roughness was measured on a square of 10 μ m x 10 μ m on the top of single particles with tapping-mode imaging in air using standard silicon tips OMCLAC160TS-WZ (Olympus, Tokyo, Japan). The root mean square roughness (R_{rms}) was calculated using the data analysis program Gwyddion 2.25 (Gwyddion – Free SPM data analysis software under the terms of the GNU General Public License, Petr Klapetek, David Neřcas, and Christopher Anderson, Czech Metrology Institute, <http://gwyddion.net/>). The R_{rms} value is an amplitude parameter and gives the root mean square of the measured height deviations from the mean height value of each scan line. To separate local surface roughness from the overall curvature of the beads, bead curvature was subtracted for each AFM image before roughness calculation. For each type of modified glass beads at least 4 different beads were analyzed and on each glass bead three to four 10 μ m x 10 μ m squares were analyzed. For each square a roughness value was calculated based on equation 1

$$R_{rms} = \sqrt{\frac{1}{N} \sum_{j=1}^N r_j^2} \quad (1)$$

where N is the number of equally spaced image points along all scan lines and r_j is the vertical distance of j^{th} data point from the mean of each scan line [14].

5.2.3.2 Contact angle

Static contact angle measurements with the sessile drop method were performed to determine surface polarity of chemically modified glass beads. Experiments were conducted at room temperature with an OCA 20 contact angle meter (DataPhysics Instruments GmbH, Filderstadt, Germany) with the SCA 20 software. The instrument was coupled with a USB CCD-camera (maximum imaging rate 123images/second). The water drop applied was $< 1\mu\text{l}$ and generated manually. For each type of chemically modified glass beads the contact angle was determined on 20 glass beads and the mean contact angle was calculated.

5.2.4 Spray drying of the API

Salbutamol sulphate was spray dried using a Nano Spray Dryer B-90 (Buechi Labortechnik AG, Flawil, Switzerland) equipped with the long version of the drying chamber. To obtain particles in the size range of $1\mu\text{m} - 5\mu\text{m}$ (characteristic diameters: $x_{10} = 0.45\mu\text{m}$, $x_{50} = 3.07\mu\text{m}$ and $x_{90} = 6.73\mu\text{m}$) a spray head mesh of $7\mu\text{m}$ was chosen and a feed concentration of 7.5%. The flow rate was set to 100L/min and the spraying intensity was set to 30%. Aqueous salbutamol sulphate solutions used for spray drying were prepared with purified water (TKA Micro Pure UV ultrapure water system (TKA Wasseraufbereitungssysteme GmbH, Niederelbert, Germany) equipped with a capsule filter ($0.2\mu\text{m}$)).

5.2.5 Preparation of adhesive mixtures

Adhesive mixtures were prepared with 3 different calculated surface coverages (100%, 50% and 25%). The surface coverage was calculated with the help of the projected surface area of API particles on the glass beads surface and based on the principle of the densest package of API particles on the glass bead surface shown in figure 1. It was assumed that the projected area of 2 triangles with a side length that equals the diameter (d) of one salbutamol sulphate particle (determined via laser diffraction) gives one salbutamol sulphate particle. The surface area of one glass bead was calculated with

equation 2, and the surface area of one salbutamol sulphate particle based on equation 3:

$$(d_{gb} + d_{ss})^2 * \pi \quad (2)$$

$$\left(d_{ss}^{\frac{2}{3}} * 3^{\frac{1}{3}}\right) * 2 \quad (3)$$

where d_{gb} is the diameter of one glass bead and d_{ss} the diameter of one salbutamol sulphate particle. By dividing the so calculated glass bead surface by the surface of one salbutamol sulphate particle one gets the number of SS particles per glass bead for a 100% surface coverage. This value can now be adapted to the desired % surface coverage. When calculating the true surface coverage from the NGI experiments, this mass ratio is taken into account (section 5.2.7). From the mass of one glass bead ($m = V * \rho_{gb} = \pi * d_{gb}^3 * \frac{\rho_{gb}}{6}$) where ρ_{gb} is the density of the glass beads (2500kg/m³) and the mass of salbutamol sulphate particles per glass bead ($\frac{m_{SS}}{GB} = \pi * d_{ss}^3 * \frac{\rho_{ss}}{6} * x$) where ρ_{ss} is the density of spray dried salbutamol sulphate particles (1281kg/m³, determined with a helium pycnometer) and x the number of SS particles per glass bead for any desired surface coverage that has been calculated before, a mass ratio of salbutamol sulphate and glass beads for any desired surface coverage can be calculated and further the amount of salbutamol sulphate to weigh in for the desired coverage. This mass ratio is also important and used when further calculating the actual surface coverage (section 5.2.6).

10g of glass beads and the calculated amount of salbutamol sulphate depending on the desired coverage were weighed into stainless steel mixing vessels (diameter: 3.2cm, height: 3.4cm; filling volume approximately 40%) using the sandwich method. The vessel was then fixed in a Turbula blender TC2 (Willy A. Bachofen Maschinenfabrik, Muttenz, Switzerland) and mixed for 45min at 22rpm. One mixture was prepared for each glass bead modification. Homogeneity of each blend was determined by taking 10 samples of about 150mg from the powder blends via a spatula. Samples were dissolved in 20ml of water of pH = 3 (adjusted by acetic acid) and subsequently analyzed for salbutamol sulphate concentration by reversed phase high performance liquid

chromatography (HPLC method described in Section 5.2.10). The blend homogeneity is expressed as the coefficient of variation of the drug content of $n = 10$ samples. Only samples with blend homogeneity of $< 5\%$ were used for further experiments. Except for untreated glass beads where blend homogeneity of $< 5\%$ could not be achieved. Nevertheless these blends were used for further experiments.

All prepared adhesive mixtures were stored in a desiccator over silica gel prior to use.

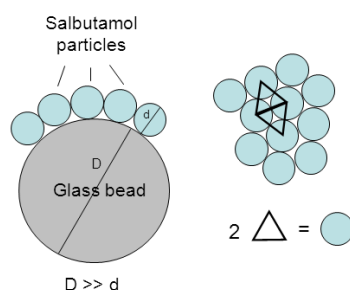


Figure 1: Schematic illustration of the surface coverage calculation.

5.2.6 Determination of the actual surface coverage from the mixing homogeneity

The mass ratio of glass beads and salbutamol sulphate was determined and used for calculating the amount of salbutamol sulphate to weigh in for the desired surface coverage. From the salbutamol content analysis from the 10 samples for the blend homogeneity calculation also a mass ratio of glass beads and salbutamol sulphate could be calculated by knowing the mass of adhesive mixture in each sample and the related mass of salbutamol sulphate obtained from HPLC analysis. By comparing the actual mass ratio and the calculated theoretical mass ratio of glass beads and salbutamol sulphate, the actual surface coverage in % could be calculated.

5.2.7 Determination of the true surface coverage based on the recovered dose from NGI experiments

With the help of the RD determined from the NGI experiments and mass of adhesive mixture that was used per NGI experiment the true surface coverage

for the mixture in the capsule used in the NGI experiment could be calculated. By reducing the mass of adhesive mixture that was used in the experiment by the RD (mass SS per NGI experiment) the mass of glass beads used for each NGI experiment was calculated. By dividing the resulting mass of glass beads by the mass of one glass bead that has been already calculated when calculating the surface coverage (5.2.5) the number of glass beads used in each NGI experiment can be calculated. The same calculation can be done for the number of salbutamol sulphate particles per NGI experiment when by simply dividing the RD by the mass of one salbutamol sulphate particle. This gives the ratio of the number of glass beads and the number of salbutamol sulphate particles per NGI experiments. Comparing this ratio with the ratio of glass beads and salbutamol sulphate from the calculation of the surface coverage (5.2.5) the true coverage for the blends used in the NGI experiment could be calculated.

5.2.8 Scanning electron microscopy

The morphology and structure of each blend was examined using a scanning electron microscope (SEM) (Zeiss Ultra 55, Zeiss, Oberkochen, Germany) operating at 5kV. Samples were gold palladium sputtered

5.2.9 Assessment of fine particles – fine particle fraction (FPF), emitted dose (ED), fine particle dose (FPD)

The aerodynamic assessment of fine particles was performed according to European Pharmacopoeia (preparations for inhalation: aerodynamic assessment of fine particles, Ph. Eur., 7.0) using Apparatus E (Next Generation Impactor (NGI), Copley Scientific, Nottingham, United Kingdom). Prior to each experiment the small cups of the impactor were coated with 2ml, the large cups with 4ml of coating agent (solution of 5% of a mixture of glycerol and polyoxyethylene-20-cetylolether (95:5) in isopropanol) and the preseparator was filled with 10ml of diluted acetic acid (Ph = 3). The inhalation device used for these experiments was the Aerolizer®/Cyclohaler®. As this type of inhaler is a low resistance inhaler and the pressure drop of 4.0kPa could not be achieved a flow rate of 100l/min was adjusted. During the experiments the

solenoid valve of the critical flow controller (TPK, Copley Scientific, Nottingham, United Kingdom) was kept open 2.4 seconds so that 4 liters of air were sucked (SV1040, Busch, Chevenez, Switzerland) through the apparatus. Additionally a leak test was performed prior to each experiment. Within 60s, the pressure of the closed NGI must not increase by more than 2.0kPa. 150mg ($\pm 20\%$) of the adhesive mixtures were filled into hard gelatin capsules of size 4 (G-CAPS®, GoCaps GmbH, Edlingen, Germany) manually. Then a capsule was placed in the compartment in base of the inhaler and by pushing two buttons inwards on base of the inhaler the capsule was pierced so that the powder could be released. For each adhesive mixture two capsules were discharged into the impactor directly after each other. For adhesive mixtures with 25% surface coverage an additional third capsule was discharged to increase the amount of salbutamol sulphate deposited in the impactor and to facilitate the HPLC quantification. The active on the cups was then dissolved in 1ml of diluted acetic acid. The induction port together with the mouthpiece was also rinsed with 10ml of diluted acetic acid and the preseparator with 50ml. Moreover the inhalation device was rinsed with 10ml diluted acetic acid too. The amount of drug in each compartment, the preseparator, the introduction port plus the mouthpiece and the inhaler was subsequently determined via HPLC. According to the European Pharmacopoeia (preparations for inhalation, Ph. Eur., 7.0) the fine particle dose (FPD), the emitted dose (ED) and the fine particle fraction (FPF) were calculated. FPD gives the amount of API exhibiting an aerodynamic diameter of $<5\mu\text{m}$ and the ED the amount of active found in the whole impactor (mouthpiece adaptor, introduction port, preseparator, impaction stages). FPD divided by ED gives the FPF. Additionally the recovered dose (RD) where the amount of salbutamol sulphate recovered in all the stages, the preseparator, the mouthpiece and induction port and the inhaler were summed up, was determined

For each carrier modification the blend with 100% surface coverage was tested in triplicate. To limit the amount of work and number of experiments all the other samples were tested once as previous experiments have shown that the NGI experiments show good reproducibility.

5.2.10 HPLC analysis

Salbutamol sulfate samples were analyzed by HPLC on a Waters 2695 (Waters Corporation, Milford, USA) HPLC system equipped with an autosampler and a Waters 2996 photodiode array detector. UV-detection was performed at 276nm. Mobile phase consisted of 60% A: 5 mM hexanesulfonic acid sodium salt in water + 1% acetic acid and 40% B: methanol. Analysis has been carried out under isocratic elution conditions with a flow rate of 1ml/min. A Phenomenex Luna C18 5 μ m 100A column (150mm x 4.6mm, 5micrin), was used as stationary phase. Column temperature was set to 30°C and an aliquot of 50 μ L of sample solution was injected into the HPLC system. Each sample was analyzed two times. Linearity of the method was confirmed between 2.6 μ g/ml and 70.5 μ g/ml. Every twenty samples a calibration curve, consisting of seven solutions of known concentration, was recorded.

5.3 Results and discussion

5.3.1 Characterization of the carrier particles

Table 1: Surface roughness (R_{rms}) of physically modified glass beads determined by AFM (mean of $n = 12-16 \pm SD$).

	R_{rms} / nm
Q4h	11.86 \pm 2.50
TC 4h	17.23 \pm 5.49
TC 8h	19.30 \pm 4.70
Plasma 1 min	42.52 \pm 12.45

Chemical as well as physical surface processing was applied to get glass beads with different surface properties. The purpose of physical surface treatment was to prepare glass beads with different shades of roughness. By chemical surface processing the glass bead surface should be made hydrophobic. Table 1 gives the surface roughness values for physically modified glass beads. By processing the glass beads in a ball mill and using different grinding materials and processing times glass beads with increasing shades of roughness could be generated. The discussion and more detailed characterization have already been published [13] and are not part of the present work. Additionally, to further increase the surface roughness, glass beads were etched with plasma for 1 minute. As a measure for the surface

polarity/hydrophobicity of chemically modified glass beads the contact angle of water was chosen. The contact angle of water on TPCS modified glass beads is 81.17 ± 3.88 and on FPTS modified glass beads 79.93 ± 3.79 (mean of $n = 20 \pm SD$). By contrast the contact angle of water on untreated glass beads is 16.08 ± 5.37 (mean of $n = 20 \pm SD$). So, due to silanization (chemical surface modification) the glass bead surface became hydrophobic. However, there is no significant difference between the contact angles of TPCS and FPTS treated glass beads.

5.3.2 SEM images of adhesive mixtures

Adhesive mixtures of untreated and the differently modified glass beads with different amounts of salbutamol sulphate were prepared in a tumble blender. The amount of salbutamol sulphate for each mixture was calculated based on the desired surface coverage. The equations used for the calculation are shown in section 5.2.5. Figure 2 shows the SEM images of adhesive mixtures of different carrier particles with different calculated surface coverages (100%, 50% and 25%). It is evident that an actual surface coverage of 100% could not be achieved although weighing in an amount of salbutamol sulphate that according to the calculations should have resulted in 100% coverage. However, the lower the calculated surface coverages the less API particles are present on the glass bead surface (figure 2). Moreover it has to be mentioned that the salbutamol sulphate particles do not adhere very strongly onto the glass beads surface. When transferring or working with the sample, salbutamol sulphate is found to stick on the container walls and the spatula.

In contrast to physically modified glass beads high drug loads of chemically modified glass beads are not distributed homogeneously over the glass beads surface, but some parts of the glass beads are covered very densely whereas other parts are more or less uncovered (figure 2f and 2g). This can be explained by the cohesion force between salbutamol sulphate particles, which is stronger than the adhesion force between salbutamol sulphate particles and chemically modified glass beads. Hence, salbutamol sulphate particles tend to adhere more likely to other salbutamol sulphate particles that are already attached to the glass beads surface than to the glass beads surface itself. As a

consequence salbutamol sulphate particles form clusters/agglomerates on the glass beads surface. By comparison, salbutamol sulphate particles are distributed more homogeneously over the surface of untreated and physically modified glass beads indicating stronger adhesion forces between untreated and physically modified glass beads and API particles than cohesion forces between the API particles.

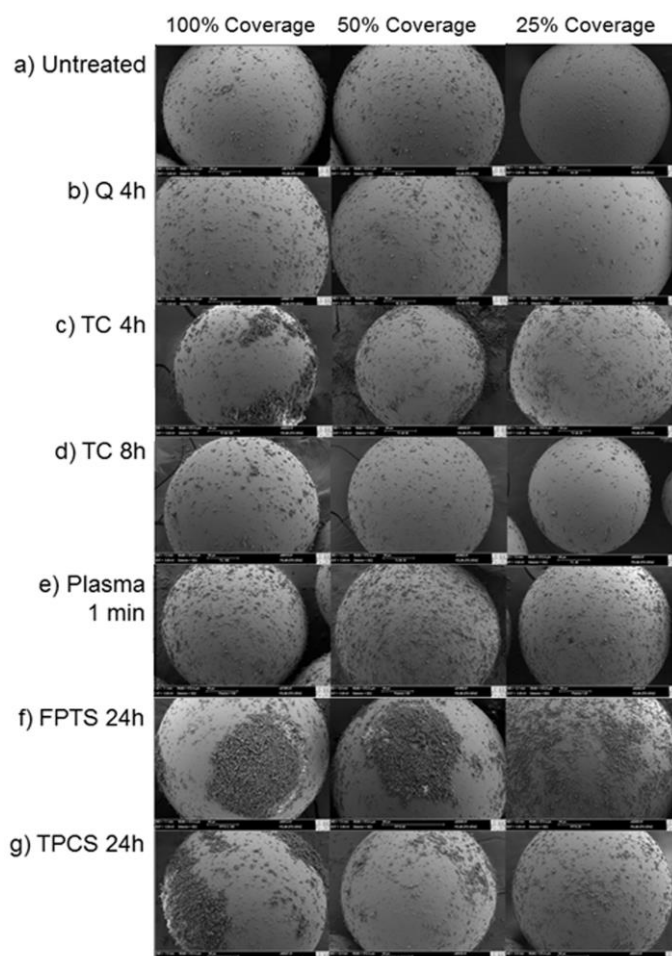


Figure 2: SEM micrographs (image width of 572.4 μ m) of blends with different surface coverage of the glass beads a) untreated, b) physically modified with quartz for 4h, c) physically modified with tungsten carbide for 4h and d) 8h, e) etched with plasma for 1min, f) chemically modified with FPTS for 24h and g) chemically modified with TPCS for 24h as carrier particles.

5.3.3 Actual surface coverage from mixing homogeneity experiments

From SEM images in figure 2 it can be taken that regardless of what glass beads were used a 100% surface coverage could not be achieved although the amount of API weighed in was calculated for a 100% surface coverage. Hence, the actual surface coverage was determined for each blend out of the mixing

homogeneity results described in section 5.2.6. (figure 3). Results show that when weighing in for a 100% calculated surface coverage the actual surface coverage was between 57.22% for untreated glass beads and 76.93% for glass beads modified with FPTS for 24h. The actual surface coverage for mixtures with a 50% calculated surface coverage was between 23.14% for untreated glass beads and 42.65% for glass beads modified with FPTS for 24h. For mixtures with 25% calculated surface coverage, the actual surface coverage was between 10.87% for untreated glass beads and with 22.25% also highest for glass beads modified with FPTS for 24h. Thus, results in figure 3 confirm that the actual surface coverage was consistently lower than the calculated surface coverage. This is true for untreated and all the modified glass beads. An explanation might be the fact that not all API particles that have been weighed in adhere to the glass beads surface during mixing. Besides adhesion onto the glass beads surface it was observed that a certain amount of API particles also adheres to the mixing vessel wall. This is the reason why the actual surface coverage is lower than the calculated surface coverage for all the glass beads used.

However, it is evident that there is a more or less linear relationship between the calculated surface coverage and the actual surface coverage for each glass bead type. The more API was weighed in and available for the mixture, the more API adhered to the glass beads surface. Furthermore, compared to untreated glass beads, the actual surface coverage that can be reached is higher when using modified glass beads. For physically modified glass beads this can be explained by the surface modifying procedures. It might be assumed that by physical treatment high energetic or also called active sites have been introduced on the glass beads surface so that more salbutamol sulphate particles can adhere to the glass beads surface. However, there is no correlation between the height of the actual surface coverage and the surface roughness. For chemically modified glass beads this can be explained by the agglomeration of API particles on the surface of chemically modified glass beads that has been visualized via SEM (figure 2f and 2g). These agglomerates lead to relatively high surface coverages, when quantifying the amount of salbutamol sulphate on the glass beads surface via HPLC.

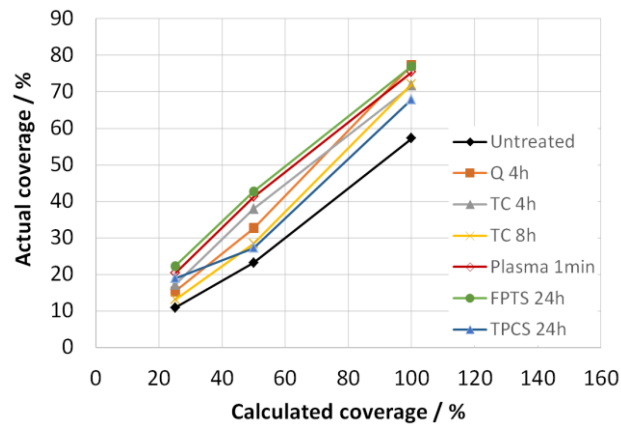


Figure 3: Actual surface coverage for the distinct blends of untreated and surface modified glass beads with 100%, 50% and 25% calculated surface coverage plotted against the calculated surface coverage.

5.3.4 True surface coverage from NGI experiments

With the help of the recovered dose (RD), the true surface coverage for each blend at the moment of the NGI experiment could be calculated (section 5.2.7). Results in figure 4 show that the true surface coverage is lower compared to the actual surface coverage. This is true for untreated and modified glass beads and can be explained by the detachment of salbutamol sulphate particles from the carrier beforehand during handling (e.g. transport and/or capsule filling) of the adhesive mixtures. However, tendencies are still the same; glass beads modified with FPTS for 24h show the highest surface coverage, whereas untreated glass beads show the lowest. Nevertheless, the differences between untreated glass beads and glass beads that have been physically modified seem to diminish. This may refer to the fact that the surface energy of the active sites introduced by physical treatment may gradually decrease as time goes by. When later discussing the influence of surface coverage on the aerosolization performance of the blends, it will always be referred to the true surface coverage.

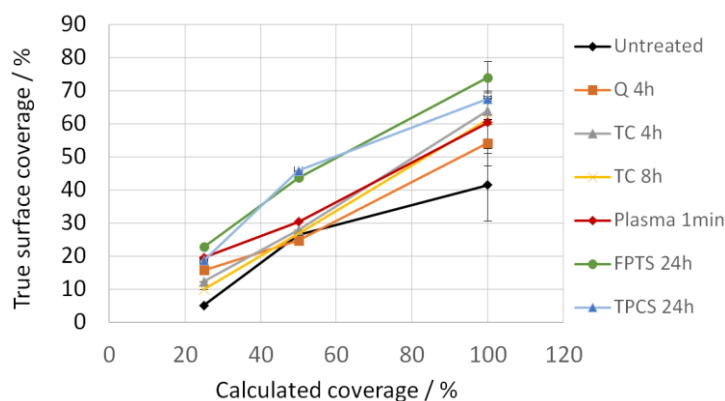


Figure 4: True surface coverage determined from the NGI experiments for the distinct blends of untreated and modified glass beads with 100%, 50% and 25% calculated surface coverage plotted against the calculated surface coverage.

5.3.5 Assessment of fine particles – Influence of surface coverage on aerodynamic behavior

The aerodynamic behavior of glass beads/salbutamol sulphate blends was estimated with the Next Generation Impactor (NGI) making it possible to study the in vitro deposition profile of the lung (table 2).

Table 2: Aerodynamic characteristics of the adhesive mixtures of spray dried salbutamol sulphate and untreated as well as differently modified carrier particles (ED = emitted dose; FPD = fine particle dose; RD = recovered dose and FPF = fine particle fraction; mean \pm SD, n = 3).

	RD per 150mg mixture (μ g)	ED per 150 mg mixture (μ g)	ED / RD (%)	FPD per 150 mg mixture (μ g)	FPF (%)
Untreated 100	549.26 \pm 86.76	411.07 \pm 45.14	75.26 \pm 3.70	167.47 \pm 44.87	32.54 \pm 4.51
Untreated 50	456.94	365.3	79.94	105.04	23.5
Untreated 25	93.39	61.88	66.26	16.35	18.82
Q4h 100	933.97 \pm 119.93	674.28 \pm 148.29	71.86 \pm 8.69	242.64 \pm 44.82	36.17 \pm 2.07
Q4h 50	428.35	339.05	79.15	94.29	27.12
Q4h 25	273.19	209.38	76.64	49.91	23.84
TC4h 100	619.04 \pm 102.34	420.78 \pm 28.54	81.02 \pm 0.88	148.08 \pm 14.19	35.16 \pm 0.99
TC4h 50	443.77	370.59	83.51	116.49	31.43
TC4h 25	197.16	150.5	76.33	40.09	26.64
TC8h 100	1055.42 \pm 108.54	922.97 \pm 141.93	87.30 \pm 7.76	266.35 \pm 36.12	41.23 \pm 0.43
TC8h 50	482.46	385.55	79.91	124.36	32.26
TC8h 25	179.94	143.96	80.01	39.67	27.56
Plasma 1 min 100	991.76 \pm 153.6	820.81 \pm 150.86	82.58 \pm 2.42	340.64 \pm 49.36	41.67 \pm 1.63
Plasma 1 min 50	501.07	400.435	79.92	121.4	30.32
Plasma 1 mn 25	322.70	247.1	76.57	52.59	21.28
FPTS 24h 100	1213.06 \pm 76.44	1138.21 \pm 156.37	93.61 \pm 5.99	107.34 \pm 12.06	9.45 \pm 0.24
FPTS 24h 50	719.37	593.1	82.45	45.99	7.75
FPTS 24h 25	375.82	331.09	88.10	15.95	4.82
TPCS 24h 100	1210.98 \pm 110.97	1049.36 \pm 76.25	86.75 \pm 1.58	337.17 \pm 20.71	32.07 \pm 0.46
TPCS 24h 50	1134.79	618.14	78.23	148.25	15.28
TPCS 24h 25	790.14	263.24	81.15	33.77	9.66

As blends were filled into capsules manually and thus the mass in the capsules varies and further either 2 or 3 capsules were used for the NGI experiment, recovered dose (RD), emitted dose (ED) and fine particle dose (FPD) were calculated per 150mg mass mixture (target weight per capsule) so that the values can be compared among each other for the different blends.

When considering the RD (μg) shown in table 2, the observations that have been made when discussing the true surface coverage are reflected again as the true surface coverage has been calculated from the RD. Within each type of glass beads, the RD increases with increasing calculated surface coverage simply because at higher surface coverage more API particles are present on the glass bead surface and thus must be recovered in either, the inhaler, the mouth and throat, the preseparator or one of the NGI trays. Comparing the RDs among the differently modified glass beads, untreated glass beads exhibit the lowest true surface coverage and also the lowest RD. Compared to untreated glass beads physically modified glass beads show mostly higher true surface coverage and also higher RDs, whereas chemically modified glass beads especially glass beads treated with FPTs for 24h exhibit highest true surface coverage and also highest RDs.

Table 2 also shows the ED (μg) and FPD (μg) for untreated and modified glass beads. Like the true surface coverage and the RD, within each type of glass beads the ED increases with increasing calculated surface coverage, as more salbutamol sulphate particles are present on the glass beads surfaces and thus emitted from the inhaler. Comparing the EDs among the differently modified glass beads, the untreated glass beads, which exhibit the lowest true surface coverage also, show the lowest ED. Due to the surface modifications the true surface coverage, that can be achieved, increases and also the EDs for the modified glass beads increase. Highest EDs could be reached for chemically modified glass beads with FPTs as those have the highest true surface coverage among all carrier particles tested. Therefore it seems that the height of the true surface coverage and the RD correlates with the height of the ED (μg). Although within each type of glass beads the FPD increases with increasing ED a correlation between FPD and ED cannot be found when comparing the differently modified glass beads. The most prominent example

are the chemically modified glass beads as they show lower FPDs with respect to untreated glass beads although their EDs are much higher.

As there is always a risk of API particles to stick to the inhaler wall especially when the adhesion of the API particles to the carrier surface is low, the ED was compared to the RD. The more API particles are present on the glass beads surface, the less strong the API particle will stick to the carrier surface and may remain in the inhaler sticking to the inhaler wall. The reason for the less strong adhesion with increasing surface coverage is that besides high energetic sites also low energetic sites on the glass beads surface might be saturated with API particles. Consequently, API particles adhering to these low energetic sites would be detached more easily, so that more API particles would be prone to stick to the inhaler wall rather than to the carrier surface and thus would remain in the inhaler. Therefore, the ratio between recovered dose (RD) and emitted dose (ED) was determined to find out whether this hypothesis is true and more API particles remain in the inhaler at higher surface coverage. Moreover, it was checked whether certain surface modifications have led to less adhesive bonds between API particles and the glass bead surface, so that consequently API particles might detach more easily and result in more API particles remaining in the inhaler. However, this was not observed as the ED (%) is more or less constant. Figure 4 shows that regardless of the surface coverage and the surface modification of the carrier, about 80% of the API available for each NGI experiment were emitted from the inhaler. As the percentage of API particles emitted during the NGI experiments is nearly the same for each coverage and every type of glass beads, the FPF of the different glass beads and for the different surface coverages can be well compared among each other.

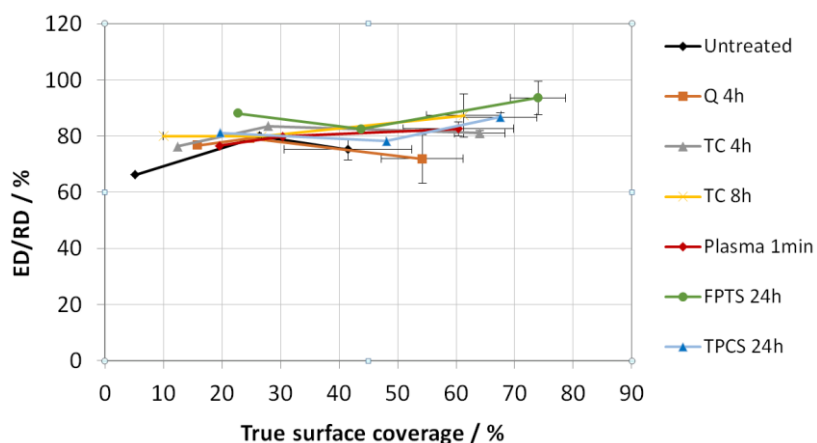


Figure 5: Influence of the surface coverage on the emitted dose (%), expressed in relation to the RD, for all the different blends investigated.

The FPF may be defined as the main parameter describing the performance of a DPI carrier system. It suits for checking the influence of surface coverage as well as the influence of carrier surface modification on the performance of DPIs. The exact values for the FPF of salbutamol sulphate released from the different blends are given in table 2. Results show that by reducing the calculated surface coverage by half also the FPF is reduced. The FPF for blends with physically modified glass beads and 25% calculated surface coverage is between 21.28% and 27.12%. When increasing the calculated surface coverage to 50% the FPF increases up to 32.26% and when further increasing the calculated surface coverage to 100% the FPF reaches 41.67%. In addition one can say that for all the physically modified glass beads the FPFs of blends with the same calculated surface coverage are in the same range. By contrast the FPFs for chemically modified glass beads, especially for the FPTS modified glass beads are significantly lower at same calculated surface coverage. The values range from about 9.45% to 32.07% for 100% calculated surface coverage and 4.82% to 9.66% for a calculated surface coverage of 25%.

For better understanding the influence of surface coverage of surface modified glass beads on the performance of DPIs and thus FPF of salbutamol sulphate, the true surface coverage has to be taken into account. Figure 6 shows the relationship between true surface coverage and FPF. As expected the FPF increases with increasing true surface coverage. This is true for untreated and all the modified glass beads, but the slopes of the resulting lines are different.

An explanation lays in the number and energy level of active sites on the glass beads surface that have been occupied by the drug particles. As the active sites are not monoenergetic [8] but exhibit an energy distribution the slopes of a graph, where the FPF is plotted versus the true surface coverage, may vary depending on the distribution of active sites on the glass beads surface and thus on the modification of the glass beads.

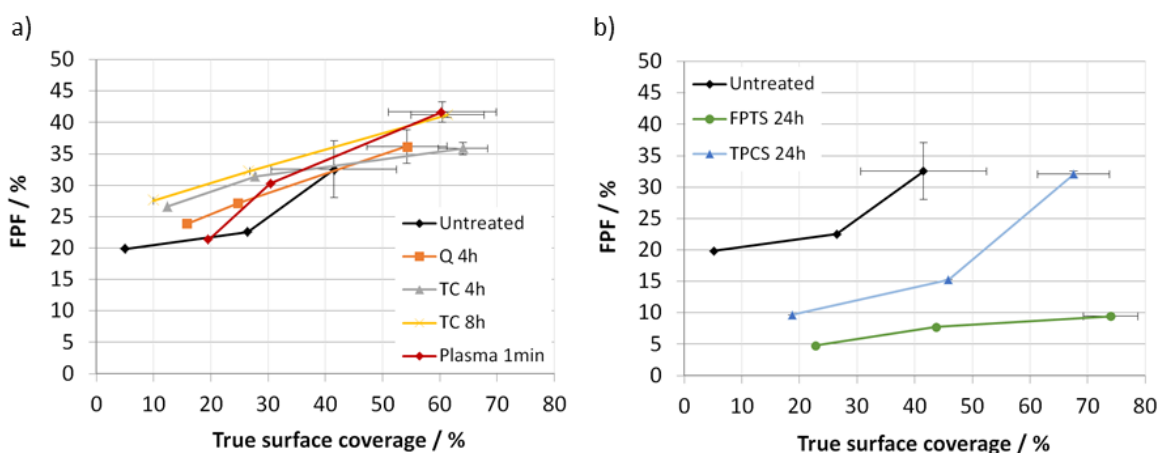


Figure 6: Influence of surface coverage on the fine particle fraction for a) untreated and physically modified glass beads and b) untreated and chemically modified glass beads.

Compared to untreated glass beads it was expected that the FPF of physically modified glass beads increases with increasing surface roughness (Q4h, TC 4h, TC 8h and plasma 1min). Due to the surface roughness the contact area between API and glass bead surface should have been reduced and thus interparticle interactions, what consequently would lead to increased drug detachment and FPFs. Results in figure 5a show that physically modified glass beads have slightly higher FPFs than untreated glass beads. So this is as it would have been expected. It seems that by introducing surface roughnesses, the contact area as well as interparticle forces between glass beads and salbutamol sulphate particles are decreased and consequently the FPF increased. This is somehow contradictory to what has been observed for the true surface coverage, because the true surface coverage is lowest for untreated glass beads. According to the hypothesis regarding the impact of surface roughness on the FPF the adhesion force acting between untreated glass beads and salbutamol sulphate particles should be stronger than the adhesion force acting between physically modified glass beads and salbutamol

sulphate particles. The true surface coverage should consequently be relatively high and the FPF accordingly low for untreated glass beads. Instead the true surface coverage of untreated glass beads was unexpectedly low what should have led to higher FPFs. It is proposed that by physical surface treatment not only the surface roughness is altered but also the energy of active sites on the glass beads surface. However, the newly introduced active sites are subject to aging as already mentioned above and diminish as time goes by. This means that the attachment of API particles and thus the actual surface coverage is governed by the temporary influence of the newly introduced active sites and surface roughness, whereas drug detachment and thus the FPF mainly by surface roughness.

Having a closer look at the ball mill modified glass beads it can be seen that the FPF increases with increasing surface roughness. The FPF for glass beads modified with quartz for 4h is higher than the FPF for untreated glass beads, followed by glass beads treated with tungsten carbide for 4h. The highest FPF is shown for glass beads modified with tungsten carbide for 8h. As glass beads treated with plasma for 1min exhibit the roughest surface, we would have expected the highest FPFs. But at low surface coverage the FPF is in the range of the FPF of untreated glass beads and glass beads treated with quartz for 4h. Only at high surface coverage the FPF is in the range of the FPF of glass beads treated with TC for 8h and thus adequately high with respect to surface roughness. Noticeable is that the slope of the line for glass beads modified with plasma for 1min is steeper than all the other lines, indicating a different energy distribution of active sites compared to untreated glass beads and glass beads treated in a ball mill. Therefore, it is difficult to compare the differently modified glass beads among each other as results concerning the value of the FPF can be different at different true surface coverage. For example the FPF of glass beads etched with plasma for 1min at 30% true surface coverage is slightly lower than the FPF of glass beads treated with tungsten carbide for 4h. On the contrary comparing the FPFs of these two samples at 70% true surface coverage, the FPF of glass beads etched with plasma for 1min is significantly higher than the FPF of glass beads treated with tungsten carbide for 4h. According to that, it also might be assumed that for

each carrier modification there is an optimum surface coverage for high drug detachment and thus FPF.

By contrast chemical surface treatment does not alter surface roughness but surface chemistry. As salbutamol sulphate is polar and due to silanization the surface becomes hydrophobic, one might assume that the adhesion between chemically modified glass beads and salbutamol sulphate is not that strong so that drug detachment might be facilitated. However results in figure 6b show that the FPF for chemically modified glass beads is significantly lower compared to untreated glass beads regardless of the surface coverage. The reason for this may lay in the fact that API clusters are formed on the surface of chemically modified glass beads during mixing (figure. 2f and 2g) due to the high cohesion force between salbutamol sulphate particles which exceeds the adhesion force between salbutamol sulphate and the glass beads. So API particles cannot be detached as single particles during inhalation but as whole particle agglomerates. As the ED for chemically modified glass beads is high, it seems that the drag and lift forces, which are generated in the inhaler during inhalation and which are responsible for drug detachment and drug dispersion [15], are not able to break up the detached API agglomerates. Hence, API particles trapped in these agglomerates impact in the upper airways and are not able to reach the deep lung. As a result the FPF for chemically modified glass beads is low. This phenomenon has also been described before by Young et al.[9] and Steckel et al.[12] Although the coverage degrees were chosen carefully to avoid multilayer formation, the cluster formation on the surface of chemically modified glass beads could not be impeded.

5.3.6 Conclusion

This study shows that when using untreated and surface modified carrier particles for blends in DPIs and trying to load the carriers with 25%, 50% and 100% of salbutamol sulphate (calculated surface coverage) the resulting actual surface coverage is always lower as a part of the API sticks to the mixing vessel and is lost for surface coverage. Even more, API can be lost during capsule filling, handling and transport, so the true surface coverage of glass beads used to test the performance of the formulations in NGI experiments can

even be lower. So when studying the performance of DPIs the true surface coverage has to be taken into account as dependent on the carrier material used, the actual and true surface coverage can differ notably from the targeted or calculated surface coverage. Compared to untreated glass beads the actual and the true surface coverage that can be reached is higher for modified glass beads, especially for the chemically modified glass beads. However, the difference between differently physically and differently chemically modified glass beads is not pronounced.

Moreover it is shown that the performance of DPIs, equivalent to the FPF, increases with increasing surface coverage. However when plotting the FPF versus the true surface coverage the slope of the resulting lines differ from each other depending on the carrier material used. This indicates that the energy distribution of the sites of contact between the drug and the carrier differs depending on the carrier used.

Summing up, the results show that increased surface coverage leads to increased FPF. However the influence of surface coverage on FPF is less pronounced than the choice of the carrier particles. Compared to untreated and chemically modified glass beads physically modified glass beads show a higher FPF which increases with increasing surface roughness.

The aim of future work will be the preparation of mixtures with more than 100% calculated surface coverage to see whether saturation of the surface coverage takes place and whether the FPF also reaches a point of saturation where an increase in surface coverage does not lead to an increase in FPF.

Acknowledgements

The authors would like to thank the German Research Foundation (DFG) for financial support within the priority program SPP 1486 "Particles in Contact". The authors also would like to thank Zinaida Kutelova from the research group of Prof Tomas, Otto von Guericke University Magdeburg, for the preparation of chemically modified glass beads used in this study. Moreover the authors acknowledge the research groups of Prof. Butt and Dr. Kappl, Max Plank Institute for Polymer Research Mainz, for the provision of the AFM equipment and assisting with the AFM measurements.

References

- [1] A.H. de Boer, B.H.J. Dickhoff, P. Hagedoorn, D. Gjaltema, J. Goede, D. Lambregts, et al., A critical evaluation of the relevant parameters for drug redispersion from adhesive mixtures during inhalation., *Int. J. Pharm.* 294 (2005) 173–84.
- [2] X.M. Zeng, G.P. Martin, C. Marriott, J. Pritchard, Lactose as a carrier in dry powder formulations: the influence of surface characteristics on drug delivery., *J. Pharm. Sci.* 90 (2001) 1424–1434.
- [3] X.M. Zeng, G.P. Martin, C. Marriott, J. Pritchard, The influence of crystallization conditions on the morphology of lactose intended for use as a carrier for dry powder aerosols., *J. Pharm. Pharmacol.* 52 (2000) 633–643.
- [4] P.M. Young, H. Chan, H. Chiou, S. Edge, T.H.S. Tee, D. Traini, The Influence of Mechanical Processing of Dry Powder Inhaler Carriers on Drug Aerosolization Performance, *Wiley Inter Sci.* 96 (2007) 1331–1341.
- [5] K. Iida, Y. Inagaki, H. Todo, H. Okamoto, K. Danjo, H. Luenberger, Effects of surface processing of lactose carrier particles on dry powder inhalation properties of salbutamol sulfate., *Chem. Pharm. Bull. (Tokyo)*. 52 (2004) 938–942.
- [6] H. Steckel, P. Markefka, H. TeWierik, R. Kammelar, Effect of milling and sieving on functionality of dry powder inhalation products., *Int. J. Pharm.* 309 (2006) 51–59.
- [7] E.M. Littringer, A. Mescher, H. Schroettner, L. Achelis, P. Walzel, N. A. Urbanetz, Spray dried mannitol carrier particles with tailored surface properties - The influence of carrier surface roughness and shape., *Eur. J. Pharm. Biopharm.* 82 (2012) 194 –204.
- [8] P.M. Young, S. Edge, D. Traini, M.D. Jones, R. Price, D. El-Sabawi, et al., The influence of dose on the performance of dry powder inhalation systems., *Int. J. Pharm.* 296 (2005) 26–33.

- [9] P.M. Young, O. Wood, J. Ooi, D. Traini, The influence of drug loading on formulation structure and aerosol performance in carrier based dry powder inhalers., *Int. J. Pharm.* 416 (2011) 129–35.
- [10] D. El-Sabawi, S. Edge, R. Price, P.M. Young, Continued investigation into the influence of loaded dose on the performance of dry powder inhalers: surface smoothing effects., *Drug Dev. Ind. Pharm.* 32 (2008) 1135–1138.
- [11] V.N.P. Le, T.H. Hoang Thi, E. Robins, M.P. Flament, In vitro evaluation of powders for inhalation: the effect of drug concentration on particle detachment., *Int. J. Pharm.* 424 (2012) 44–9.
- [12] H. Steckel, B.W. Mu, In vitro evaluation of dry powder inhalers II: influence of carrier particle size and concentration on in vitro deposition, *Int. J. Pharm.* 154 (1997) 31–37.
- [13] S. Zellnitz, J.D. Redlinger-Pohn, M. Kappl, H. Schroettner, N.A. Urbanetz, Preparation and characterization of physically modified glass beads used as model carriers in dry powder inhalers., *Int. J. Pharm.* 447 (2013) 132–8.
- [14] P. Klapetek, D. Necas, C. Anderson, Gwyddion user guide, (2012) 1–126. <http://gwyddion.net/download/user-guide/gwyddion-user-guide-en.pdf>
- [15] A. Voss, W.H. Finlay, Deagglomeration of dry powder pharmaceutical aerosols., *Int. J. Pharm.* 248 (2002) 39–50.

6

Influence of surface characteristics of modified glass beads as model carriers in dry powder inhalers (DPIs) on the aerosolization performance

Sarah Zellnitz , Hartmuth Schroettner, Nora Anne Urbanetz

Drug Development and Industrial Pharmacy, submitted for publication

Influence of surface characteristics of modified glass beads as model carriers in dry powder inhalers (DPIs) on the aerosolization performance

Sarah Zellnitz^{a*}, Hartmuth Schroettner^b, Nora Anne Urbanetz^a

**Corresponding author. Tel.: +43 316 873 30422; Fax: +43 316 873 1030422;*

E-mail address: sarah.zellnitz@rcpe.at

^aResearch Center Pharmaceutical Engineering GmbH, Inffeldgasse 13, Graz, Austria,

^bAustrian Centre for Electron Microscopy and Nanoanalysis, TU Graz, Steyrergasse 17/III, Graz, Austria,

Keywords: surface roughness, surface area, glass beads, inhalation, fine particle fraction

Abstract

The aim of the present work is to investigate the effect of surface characteristics (surface roughness and specific surface area) of surface modified glass beads as model carriers in dry powder inhalers (DPIs) on the aerosolization and thus the in vitro respirable fraction often referred to as fine particle fraction (FPF). By processing glass beads in a ball mill with different grinding materials (quartz and tungsten carbide) and varying grinding time (4h

and 8h) and by plasma etching for 1min, glass beads with different shades of surface roughness and increased surface area were prepared. Compared to untreated glass beads surface modified rough glass beads show increased FPFs. Drug detachment from modified glass beads is also more reproducible than from untreated glass beads indicated by lower standard deviations for the FPFs of the modified glass beads. Moreover the FPF of the modified glass beads correlates with the surface characteristics of the modified glass beads. The higher the surface roughness and the higher the specific surface area of the glass beads the higher is the FPF. Thus surface modified glass beads make an ideal carrier for tailoring the performance of DPIs in the therapy of asthma and chronically obstructive pulmonary diseases.

6.1 Introduction

Formulations administered via dry powder inhalers (DPIs) typically consist of a coarse carrier (diameter: 50 μ m – 200 μ m) and the active pharmaceutical ingredient (API) with an aerodynamic particle diameter of 1 μ m – 5 μ m [1]. By mixing the coarse carrier and the API, a so called adhesive mixture where the API particles adhere on the carrier surface is formed. Dosing in DPIs is carried out volumetrically and these adhesive mixtures enhance the flowability of the drug and thus the dosing accuracy as the micron sized API particles alone are cohesive and poor flowing. For a high deposition of API particles in the deep lung however, it is necessary that the drug particles are detached from the carrier again during inhalation. Drug particles which are not detached during inhalation will impact together with the coarse carrier in the mouth, throat or upper airways and consequently be swallowed. Considering this fact, play interparticle interactions an important role in such kind of formulations. Interparticle interactions between drug and carrier have to be high enough that the formulation is stable during handling, transport and dosing, but at the same time low enough that the drug particles are detached during inhalation.

The main goal in the inhalation field is to achieve a high and reproducible deposition in the deep lung, which is often also referred to as high fine particle fraction (FPF), high aerosolization efficiency or simply high performance of DPIs. Insufficient drug detachment from the carrier surface is often the cause

of poor aerosolization efficiency often reported with DPIs [2,3]. Therefore, carrier particles play an important role in development of DPIs as any changes in the physicochemical properties and especially the surface topography of the carrier particles have the potential to alter the drug aerosolization profile [4]. In particular, the modification of the surface topography/roughness of the carrier particles has a major influence on interparticle interactions and further drug detachment. Thus, a lot of research has been done on the modification of the surface topography of commonly used carrier particles, like lactose and mannitol with the objective of improving the performance of DPIs and increasing the fine particle fraction (FPF). In this context, spray drying of mannitol was presented to form mannitol particles with altered surface roughness [5,6], milling of lactose was reported to make carrier particle surface more homogenous [7], further the crystallization of lactose particles from different media and under different crystallization conditions [8–12] and surface processing with a high speed elliptical-rotor type powder mixer [13] were described as methods to successfully alter the surface topography of carrier particles. Nevertheless, although all these attempts were suitable to modify the surface topography of the carrier particles, other factors like particle shape or particle size were altered as well in most of these studies. Particle size and particle shape also influence interparticle interactions, what makes studying the influence of surface characteristic on the aerosolization performance, which is also comparable to interparticle interactions difficult. For that reason surface modified glass beads with increased surface area and different shades of roughness are used as model carriers in the present work. The preparation and characterization of these glass beads has been described in a previous work [14]. Glass beads were chosen because various prospects of surface modification can be applied, without changing particle size and particle shape. Hence, the changes of drug aerosolization from the distinct modified glass beads can be solely attributed to the surface topography of the carrier particles. Although glass beads are physiologically indifferent, the inhalation of glass beads is not appropriate from a medical point of view. Therefore, a grid retaining the glass beads in the inhaler must be implemented in the inhalation device.

The findings reported in literature dealing with the influence of surface topography/roughness on the performance of DPI formulations and thus the FPF are inconsistent. This can be explained by the different shades of surface roughness that are introduced depending on the surface modifying procedures applied. Also, the relation of surface roughness to the size and shape of the API particle largely impacts interparticle interactions and thus drug detachment and FPF [15]. The shade of surface roughness governs the contact area between carrier and API. Larger roughness valleys lead to increased (figure 1b) contact areas and smaller roughness valleys to decreased (figure 1c) contact areas and thus interparticle interactions. From this perspective, it is important that an appropriate shade of surface roughness (figure 1c) is introduced in order to increase drug detachment from the carrier and consequently the aerosolization efficiency of DPIs [16].

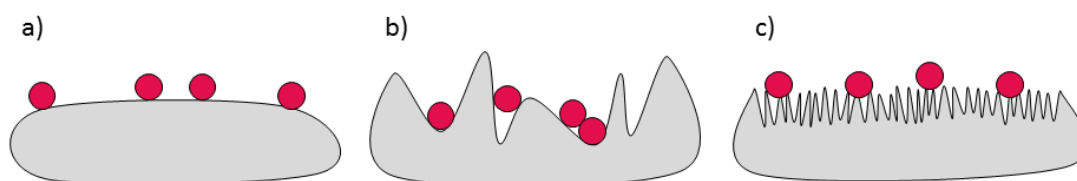


Figure 1: Impact of surface roughness on interparticle interactions.

The aim of the present work therefore was to investigate the effect of surface roughness of modified carrier particles on the aerosolization performance of DPIs. The characterization of some of the modified carrier particles that is dealt with in the present paper has been described in a previous paper [14]. To describe the performance of DPIs the fine particle fraction was chosen. The correlation of the FPF with the surface roughness of the carrier was also checked in order to show the overall effect of the surface roughness on the performance of the dry powder inhalates.

6.2 Materials and methods

6.2.1 Materials

Glass Beads in the size range of 400 μm to 600 μm ($x_{50} = 537.3\mu\text{m} \pm 7.1\mu\text{m}$) were kindly provided by SiLibeads® (SiLibeads® Glass Beads Type S, Sigmund Lindner GmbH, Warmensteinach, Germany). Prior to use glass beads were cleaned with Piranha Solution (3:7 H₂O:H₂SO₄) followed by a standard clean (1:1:5 H₂O₂:NH₄OH:H₂O). Acetic acid, ammonium hydroxide, methanol, sulphuric acid and hydrogen peroxide were purchased from Lactan Chemikalien und Laborgeraete Vertriebsgesellschaft m.b.H & Co. KG, Graz, Austria. Tungsten carbide was provided from Wolfram Bergbau und Huetten AG, St. Martin i.S., Austria and quartz was obtained from Quarzwerke Austria GmbH, Melk, Austria.

Salbutamol sulphate (USP25 quality) was purchased from Selectchemie (Zuerich, Switzerland) and used as model API after spray drying. Size 4 gelatine capsules (G-CAPS®) were obtained courtesy of GoCaps GmbH (Edlingen, Germany).

6.2.2 Sample preparation

Surface modification of glass beads was performed physically by friction and impaction in a ball mill (Ball Mill S2, Retsch, Haan, Germany). Glass beads were processed for 4h and 8h at 424rpm with two different grinding materials (quartz (Q) and tungsten carbide (TC)) with varying hardness. Thereby, glass beads with different shades of roughness could be prepared [14]. Additionally physical surface modification was performed by plasma etching with a TEGAL901. The gases used were CF₄/O₂ and the ratio was 120sccm/15sccm at 1800mTorr. The plasma power was 200W and the exposure time 1min.

6.2.3 Characterization of the modified glass beads

6.2.3.1 Surface roughness

The surface roughness of untreated and modified glass beads was determined via atomic force microscopy (VEECO, Dimension, Nanoscope IIIa, Bruker AXS

GmbH, Karlsruhe, Germany). A two component epoxy resin adhesive (UHU GmbH & Co. KG, Baden, Germany) was used to fix the glass beads on commercially available glass slides prior to analysis. The surface roughness was measured with tapping-mode imaging in air using standard silicon tips OMCLAC160TS-WZ (Olympus, Tokyo, Japan). The data analysis program Gwyddion 2.25 (Gwyddion – Free SPM data analysis software under the terms of the GNU General Public License, Petr Klapetek, David Neřcas, and Christopher Anderson, Czech Metrology Institute, <http://gwyddion.net/>) was used to calculate the root mean square roughness (R_{rms}). The R_{rms} value is an amplitude parameter and gives the root mean square of the measured height deviations from the mean height value of each scan line [17]. To separate local surface roughness from the overall curvature of the beads, bead curvature was subtracted for each AFM image before roughness calculation. For each type of modified glass beads at least 4 different beads were analyzed and on each glass bead three to four $10\mu\text{m} \times 10\mu\text{m}$ squares were analyzed. For each square a roughness value was calculated.

6.2.3.2 Specific surface area

A Tristar II3020 surface area and porosity analyzer (Micromeritics Instrument Company, Norcross, U.S.A) was used to determine the specific surface area of untreated and modified glass beads via gas adsorption. Samples were degassed at least 2h at 150°C prior to analysis and Krypton was used as adsorber gas. A seven point analysis was made between 0.7 and 0.25 relative pressure and the surface area was calculated according to the Brunauer-Emmet-Teller equation. Sample weight was at the minimum 6g. Samples were analyzed in triplicate.

6.2.4 Spray drying of the API

Salbutamol sulphate was spray dried using a Nano Spray Dryer B-90 (Buechi Labortechnik AG, Flawil, Switzerland) equipped with the long version of the drying chamber. To form particles in the size range of $1\mu\text{m} - 5\mu\text{m}$ (characteristic diameters: $x10 = 0.45\mu\text{m}$, $x50 = 3.07\mu\text{m}$ and $x90 = 6.73\mu\text{m}$) a sprayhead mesh of $7\mu\text{m}$ was chosen and a feed concentration of 7.5% [18].

The flow rate was set to 110L/min and the spraying intensity was set to 30%. Aqueous salbutamol sulphate solutions used for spray drying were prepared with purified water (TKA Micro Pure UV ultrapure water system, TKA Wasseraufbereitungssysteme GmbH, Niederelbert, Germany) equipped with a capsule filter (0.2µm).

6.2.5 Preparation of adhesive mixtures

Adhesive mixtures were prepared with 3 different calculated surface coverages (100%, 50% and 25%). The surface coverage was calculated with the help of the projected surface area of API particles on the glass beads surface and based on the principle of the densest package of API particles on the glass bead surface shown in figure 2. It was assumed that the projected area of 2 triangles with a side length that equals the diameter (d) of one salbutamol sulphate particle (determined via laser diffraction) gives one salbutamol sulphate particle. The surface area of one glass bead was calculated with equation 2, and the surface area of one salbutamol sulphate particle based on equation 3:

$$(d_{gb} + d_{ss})^2 * \pi \quad (2)$$

$$\left(d_{ss}^{\frac{2}{4}} * 3^{\frac{1}{2}}\right) * 2 \quad (3)$$

where d_{gb} is the diameter of one glass bead and d_{ss} the diameter of one salbutamol sulphate particle. By dividing the so calculated glass bead surface by the surface of one salbutamol sulphate particle one get the number of SS particles per glass bead for a 100% surface coverage. This value can now be adapted to the desired % surface coverage. From the mass of one glass bead ($m = V * \rho_{gb} = \pi * d_{gb}^3 * \frac{\rho_{gb}}{6}$) where ρ_{gb} is the density of the glass beads (2500kg/m²) and the mass of salbutamol sulphate particles per glass bead ($\frac{m_{SS}}{GB} = \pi * d_{ss}^3 * \frac{\rho_{ss}}{6} * x$) where ρ_{ss} is the density of spray dried salbutamol sulphate particles (1281kg/m², determined with a helium pycnometer) and x the number of SS particles per glass bead for any desired surface coverage that has been calculated before a mass ratio of salbutamol sulphate and glass beads for any desired surface coverage can be calculated and further the

amount of salbutamol sulphate to weigh in for the desired coverage. This mass ratio is also important and used when further calculating the actual surface coverage from the mixing homogeneity experiments (section 6.2.6). 10g of glass beads and the calculated amount of salbutamol sulphate depending on the desired coverage were weighed into stainless steel mixing vessels (diameter: 3.2cm, height: 3.4cm; filling volume approximately 40%) using the sandwich method. Then the blends were mixed in a Turbula blender TC2 (Willy A. Bachofen Maschinenfabrik, Muttenz, Switzerland) for 45min at 22rpm. One mixture as prepared for each glass bead modification. Homogeneity of each blend was determined by taking 10 samples of about 150mg from the powder blends via a spatula. Samples were dissolved in 20ml of buffer (water adjusted to pH = 3 by acetic acid) and subsequently analyzed for salbutamol sulphate concentration by reversed phase high performance liquid chromatography (HPLC method described in Section 6.2.10). The blend homogeneity is expressed as the coefficient of variation of the drug content of $n = 10$ samples. Only samples with blend homogeneity of $< 5\%$ were used for further experiments. Except for untreated glass beads where blend homogeneity of $< 5\%$ could not be achieved. Nevertheless these blends were used for further experiments.

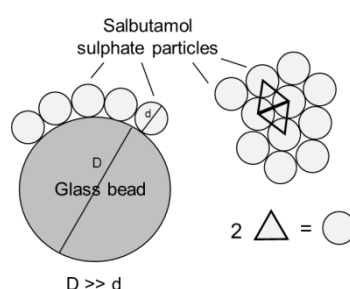


Figure 2: Schematic illustration of the surface coverage calculation.

All prepared adhesive mixtures were stored in a desiccator over silica gel prior to use.

6.2.6 Actual surface coverage

By knowing the mass of adhesive mixture in each sample and the related mass of salbutamol sulphate obtained from HPLC analysis, a mass ratio of

glass beads and salbutamol sulphate could be calculated from the salbutamol content analysis for the blend homogeneity calculation. For calculating the amount of salbutamol sulphate to weigh in for the desired surface coverage also a mass ratio of glass beads and salbutamol sulphate was determined. By comparing the actual mass ratio and the calculated theoretical mass ratio of glass beads and salbutamol sulphate, the actual surface coverage in % could be calculated.

6.2.7 True surface coverage

With the help of the RD determined from the NGI experiments and mass of adhesive mixture that was used per NGI experiment the true surface coverage for the mixture in the capsule used in the NGI experiment could be calculated. By reducing the mass of adhesive mixture that was used in the experiment by the RD (mass SS per NGI experiment) the mass of glass beads used for each NGI experiment was calculated. By dividing the resulting mass of glass beads by the mass of one glass bead that has been already calculated when calculating the surface coverage (6.2.5) the number of glass beads used in each NGI experiment can be calculated. The same calculation can be done for the number of salbutamol sulphate particles per NGI experiment when by simply dividing the RD by the mass of one salbutamol sulphate particle. This gives the ratio of the number of glass beads and the number of salbutamol sulphate particles per NGI experiments. Comparing this ratio with the ratio of glass beads and salbutamol sulphate from the calculation of the surface coverage (6.2.5) the true coverage for the blends used in the NGI experiment could be calculated.

6.2.8 Scanning electron microscopy

The surface of the modified glass beads and the quality of the adhesive mixtures was examined using a scanning electron microscope (SEM) (Zeiss Ultra 55, Zeiss, Oberkochen, Germany) operating at 5kV. Samples were gold palladium sputtered.

6.2.9 Aerodynamic assessment of fine particles

The aerodynamic assessment of fine particles was carried out using Apparatus E (Next Generation Impactor (NGI), Copley Scientific, Nottingham, United Kingdom). Prior to each experiment the small cups of the impactor were coated with 2ml, the large cups with 4ml of coating agent (solution of 5% of a mixture of glycerol and polyoxyethylene-20-cetylolether (95:5) in isopropanol) and the preseparator was filled with 10ml of buffer (water adjusted to pH = 3 with acetic acid). The inhalation device used for these experiments was the Aerolizer®/Cyclohaler®. As this type of inhaler is a low resistance inhaler and the pressure drop of 4.0kPa could not be achieved a flow rate of 100l/min was adjusted. During the experiments the solenoid valve of the critical flow controller (TPK, Copley Scientific, Nottingham, United Kingdom) was kept open 2.4s so that 4l of air were sucked (SV1040, Busch, Chevenez, Switzerland) through the apparatus. Additionally a leak test was performed prior to each experiment. Within 60s, the pressure of the closed NGI must not increase by more than 2.0kPa. 150mg ($\pm 20\%$) of the adhesive mixtures were filled into hard gelatine capsules of size 4. Then a capsule was placed in the compartment in base of the inhaler and by squeezing two buttons inwards on base of the inhaler the capsule was pierced so that the powder could be released. For each adhesive mixture two capsules were discharged into the impactor directly after each other. Then the impactor was dismantled and the active on the cups was dissolved in 10ml of buffer. The introduction port together with the mouthpiece was also rinsed with 10ml of buffer and the preseparator with 50ml. The amount of drug in each compartment, the preseparator, the introduction port plus the mouthpiece and the inhaler was subsequently determined via HPLC. According to the European Pharmacopoeia (preparations for inhalation, Ph. Eur., 7.0) the fine particle dose (FPD), the emitted dose (ED) and the fine particle fraction (FPF) were calculated. FPD gives the amount of API exhibiting an aerodynamic diameter of $<5\mu\text{m}$ and the ED the amount of active found in the whole impactor (mouthpiece adaptor, introduction port, preseparator, impaction stages). FPD divided by ED gives the FPF. Each blend/formulation was tested three times.

6.2.10 HPLC analysis

Salbutamol sulfate samples were analyzed by HPLC on a Waters 2695 (Milford, USA) HPLC system equipped with an autosampler and a Waters 2996 photodiode array detector. UV-detection was performed at 276nm. Mobile phase consisted of 60% A: 5mM hexanesulfonic acid sodium salt in water + 1% acetic acid and 40% B: methanol. Analysis has been carried out under isocratic elution conditions with a flow rate of 1ml/min. A Phenomenex Luna C18 5 μ m 100A column (150mm x 4.6mm, 5micrin), was used as stationary phase. Column temperature was set to 30°C and an aliquot of 50 μ L of sample solution was injected into the HPLC system. Each sample was analyzed two times. Linearity of the method was confirmed between 2.6 μ g/ml and 70.5 μ g/ml. Every twenty samples a calibration curve, consisting of seven solutions of known concentration, was recorded.

6.3 Results and discussion

6.3.1 Characterization of the modified glass beads

In order to be able to discuss the impact of surface roughness of modified carrier particles on the aerosolization performance of DPIs SEM pictures as well as the surface roughness parameter R_{rms} and the surface area will be discussed in this paper. SEM pictures in figure 3 show that the surface topography of glass beads processed in a ball mill (figure 3a, 3b, 3c and 3d) as well as glass beads etched with plasma (figure 3e) has changed compared to untreated glass beads (figure. 3a). Comparing quartz and tungsten carbide as grinding materials, it seems that processing with tungsten carbide leads to rougher surfaces than processing with quartz. SEM images also reveal that the surface changes are more pronounced after 8h grinding time compared to 4h grinding time. This can be observed for both quartz and tungsten carbide. Accordingly, the results correspond with the processing times (4h and 8h) and the Mohs hardness (quartz 7, tungsten carbide 9.5 and by comparison soda lime glass 6) of the grinding materials. The surface of glass beads etched with plasma for 1min appears differently, compared to the entire ball mill treated glass beads. By processing the glass beads in a ball mill, parts of the surface

seem to be abraded and valleys on the glass beads surface introduced. By contrast, it seems that the changes in surface topography of plasma etched glass beads result from elevations on the glass beads surface. It is opposed that these elevations are small pieces of the glass beads that have been first removed from the glass beads surface and directly afterwards attached again onto the glass beads surface during the plasma etching procedure. Due to the high energy input during plasma etching, the reattached glass pieces are melted to the surface, what leads to the characteristic structure shown in figure 3f.

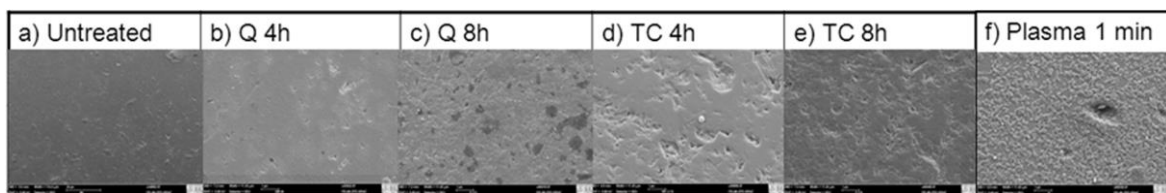


Figure 3: SEM pictures of a) untreated and b), c), d), e) f) physically modified glass beads.

As a measure of surface roughness, the R_{rms} values were determined via AFM and the specific surface area was determined via gas adsorption. Results in table 1 show that, the harder the grinding materials used and the longer the processing time the higher is the resulting surface roughness and also the specific surface area. However, the surface roughness of untreated glass beads is higher than the roughness of all the modified glass beads. This can be explained by few but rather deep surface irregularities or valleys present on the surface of untreated glass beads that result from the manufacturing process and/or transport. As the R_{rms} is a vertical roughness parameter, indicating the depths of the valleys on the surface, the resulting surface roughness is consequently high. Processing in a ball mill seems to abrade parts of the surface of the glass beads and thereby leads to homogenous rough surfaces. Consequently, the surface roughness measured via AFM is smaller. By comparison the specific surface area of untreated glass beads is lower and in the range of the specific surface area of glass beads treated with Q for 4h and TC for 4h. Therefore, it seems that the uniformly rough surface of glass beads treated with Q for 4h and TC for 4h leads to a comparable surface area as the few deep valleys on the surface of untreated glass beads.

However, this issue has been discussed in more detail in a previous work [14]. In conclusion, the combination of several analytical techniques leads to an accurate characterization of the glass beads and allows the comparison of the results among each other. Glass beads etched with plasma for 1min exhibit the highest surface roughness and also the highest specific surface area.

Table 1: Surface roughness (R_{rms}) and specific surface area values for untreated and modified glass beads.

	Untreated	Q4h	Q8h	TC4h	TC8h	Plasma 1 min
Surface roughness / nm	107.75 ± 46.24	11.86 ± 2.52	16.87 ± 4.47	17.12 ± 5.49	19.28 ± 4.70	42.52 ± 12.45
Specific surface area / cm ² /g	9.67 ± 0.12	9.13 ± 0.76	13.27 ± 1.52	9.73 ± 0.55	17.30 ± 1.17	19.00 ± 0.20

6.3.2 Correlation of actual and calculated surface coverage

As preliminary studies showed that the amount of API particles attached to the glass beads in fact is always lower than the amount of API calculated and weighed in. In addition the amount of API particles sticking on the carrier surface is dependent on the carrier surface topography. In order to obtain adhesive mixtures with similar surface coverage a way has to be found taking these phenomena into consideration. This could be achieved by determining the actual surface coverage, which represents the amount of API particles sticking on the carrier surface after the mixing procedure (section 6.2.6). By preparing mixtures with three different amounts of API corresponding to calculated surface coverages of 100%, 50% and 25%, and by correlating the three calculated surface coverages and the corresponding actual coverages, it was possible to determine the amount of API particles that has to be weighed in for any desired actual surface coverage.

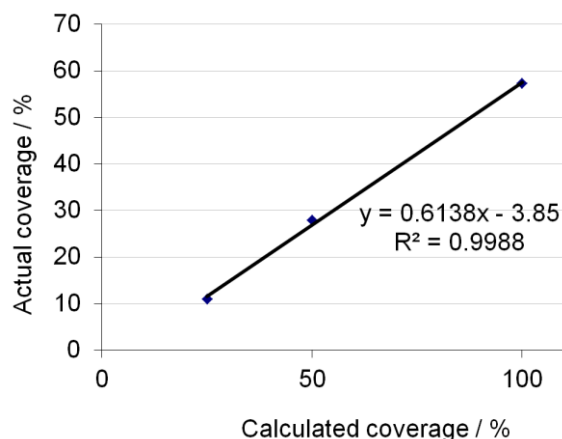


Figure 4: Correlation of calculated surface coverage and actual surface coverage for untreated glass beads.

Figure 4 shows that there is a quite good correlation between the actual and the calculated surface coverage of untreated glass beads. This is also true for all the other modified glass beads ($R^2 < 0.988$). However, the slopes of the straight line are distinct depending on the glass beads used as carrier (table 2). This can be explained by the energetic distribution of so called “active sites” on the glass beads surface whereon the API particles adhere more or less likely.

To avoid multilayer formation and cluster formation of the salbutamol particles, the desired actual surface coverage was set to 30% in this study.

Table 2: Linear equations for untreated glass beads and mechanically modified glass beads obtained from the plot of actual surface coverage versus calculated surface coverage.

Sample	Linear equation
Untreated	$y = 0.614x - 3.850$
Q 4h	$y = 0.8242 - 6.57$
Q 8h	$y = 0.6288x + 5.345$
TC 4h	$y = 0.7294x - 0.025$
TC 8h	$y = 0.7983x - 8.705$
Plasma 1min	$y = 0.726x + 3.305$

6.3.3 SEM micrographs of adhesive mixtures with untreated and modified glass beads

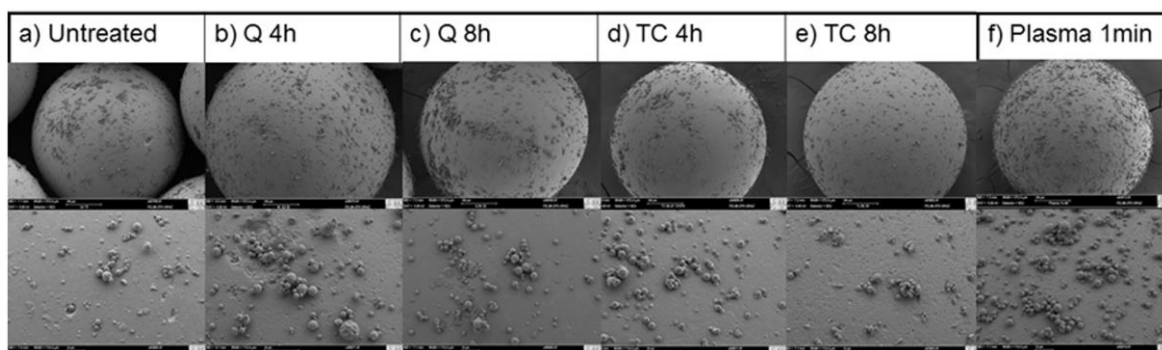


Figure 5: SEM images of comparable mixtures ($30\% \pm 5\%$ surface coverage) of a) untreated and b), c), d), e) modified glass beads and spray dried salbutamol sulphate.

Figure 5 shows SEM images of mixtures with $30\% \pm 5\%$ actual surface coverage for untreated and all the modified glass beads. It seems that the salbutamol sulphate particles are distributed homogeneously over the glass beads surface and no multilayer and hardly any cluster formation occurs at an actual surface coverage of $30\% \pm 5\%$. Although, the surface coverage of glass beads etched with plasma for 1min seems to be higher than the surface coverage of untreated and ball mill modified glass beads. SEM images were only taken for a few number of glass beads, which might result in images that do not exactly represent the surface coverage of the whole mixture. Nevertheless, by determining the actual surface coverage it was proven that all the prepared mixtures have same actual surface coverages ($30\% \pm 5\%$).

6.3.4 True surface coverage

Preliminary studies showed that salbutamol sulphate particles are detached from the carrier during handling (e.g. transport and/or capsule filling) of the adhesive mixtures. That is why besides the actual surface coverage also the true surface coverage at the moment of the NGI experiment was calculated for each blend (section 6.2.7) in order to know if the different mixtures are still comparable from a coverage point of view. Results showed that the true surface coverage is always lower than the actual surface coverage obtained from the mixing homogeneity. Nevertheless, the resulting true surface

coverage is consistently lower, so that instead of $30 \pm 5\%$ intended actual surface coverage the resulting true surface coverage is $24.5 \pm 5.5\%$. Thus, it is still possible to compare the different mixtures among each other.

6.3.5 Assessment of aerodynamic behavior

The FPF may be defined as the main parameter describing the performance of a DPI system. Especially in this study, where capsules for the NGI experiments are filled by hand and the mass of mixture used for each experiment varies by about $\pm 20\%$, the FPF suits best for checking the influence of carrier surface modification on the performance of DPIs.

Figure 6 displays the FPFs of mixtures containing untreated and surface modified glass beads with a true surface coverage of $23.5 \pm 5.5\%$. Results show that the FPF obtained from mixtures containing modified glass beads is more reproducible than the FPF obtained from mixtures containing untreated glass beads. This is indicated by lower standard deviations for the FPFs of the modified glass beads. This can be attributed to the occasional appearing valleys present on the surface of untreated glass beads that result from the manufacturing process and/or transport and lead to quite inhomogeneous surfaces [14]. API particles might hide in these deep clefts and voids on the glass beads surface and thus might not be detached during inhalation. Depending on the number of clefts and voids present on the glass beads used for the inhalation experiments, more or less API particles are hidden and thus not available for detachment. Physical surface treatment either in a ball mill or by plasma etching results in homogenous rough surfaces that allow a more constant drug detachment and thus more reproducible FPFs.

Compared to untreated glass beads surface most of the modified glass beads show slightly increased FPFs. Upon closer investigation, the FPFs of mixtures with glass beads treated with Q for 4h and TC for 4h are in the range of the FPF of untreated glass beads but more constant. Nonetheless, the FPFs of mixtures containing glass beads treated with TC for 8h and Plasma for 1min are significantly higher. The homogenous rough surfaces that have resulted from ball mill treatment with Q for 4h and TC for 4h seem to be as effective as the inhomogeneous surfaces of untreated glass beads, with their occasional

appearing deep voids and clefts, when considering the amount of API particles that can be detached during inhalation. A big advantage of the modified glass beads is however that drug detachment from the surface is more constant as there are no clefts and voids anymore, where the API particles can hide.

Moreover, when comparing the surface modified carriers among each other, figure 6 indicates that the FPF increases with increasing surface roughness and surface area of the glass beads. To better understand this relationship between surface characteristics and FPF, the correlation of surface characteristics and aerodynamic behavior will be discussed in the following section.

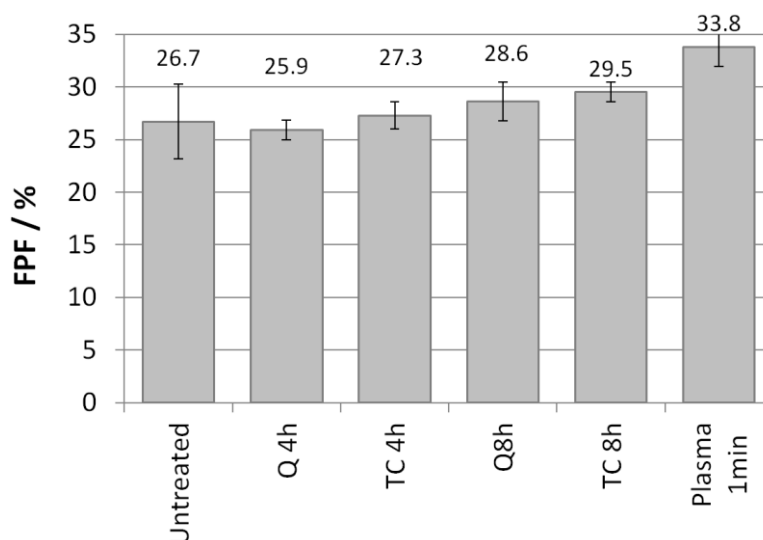


Figure 6: FPF of adhesive mixtures containing untreated glass beads, glass beads modified with Q for 4h and 8h, TC for 4h and 8h and plasma for 1min with a true surface coverage of $24.5\% \pm 5.5\%$ ($n = 3 \pm SD$).

6.3.6 Correlation of surface characteristics and aerodynamic behavior

To better understand the relationship between surface characteristics and FPF, an attempt was made to correlate the surface characteristics (surface roughness R_{rms} and specific surface area) of the modified glass beads with the FPF. Untreated glass beads were excluded from the correlation as their surface is quite inhomogeneous due to the presence of few, but deep valleys on their surface. This already caused problems when characterizing the glass beads, as an appropriate characterization of the glass beads was only

possible when applying several analytical techniques [14]. Consequently surface characteristic as well as FPF results of untreated glass beads have to be treated cautiously.

6.3.6.1 Surface roughness

SEM images already indicated and AFM analysis confirmed that glass bead etching with plasma for 1min leads to the highest R_{rms} value and thus to the roughest surface. By comparison, grinding with quartz for 4h leads to the smallest R_{rms} value and so to the least rough surface. Grinding with Q for 8h and TC for 4h and for 8h whereas leads to surface roughnesses in between. This trend can also be observed when considering the FPF. Figure 7 shows that the FPF tends to increase more or less linearly with the surface roughness, with a coefficient of determination R^2 of approximately 0.83. The correlation coefficient resulting from the correlation of the FPF and the surface roughness is 0.909 and indicates a positive correlation. The FPF increases with increasing surface roughness of the carrier particles. This is well in accordance with our expectations and findings from Kawashima et al. that found that carrier particles with increased surface roughness and surface area lead to higher FPFs [16]. By introducing surface roughness to the glass bead surface, the contact area between the glass beads and the API particles is reduced and further also interparticle interactions. Therefore, with increasing surface roughness and the accompanying reduced contact area, drug detachment is facilitated and as a consequence the FPF is increased.

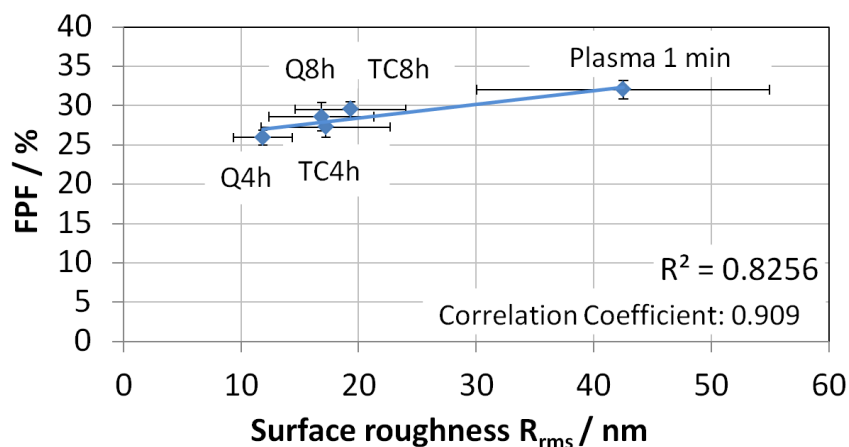


Figure 7 Correlation of surface roughness R_{rms} ($n = 12-16 \pm SD$) and FPF ($n = 3 \pm SD$) for surface modified glass beads.

6.3.6.2 Surface area

Besides the surface roughness, the specific surface area was determined to additionally quantify the changes in surface topography caused by mechanical surface processing. Therefore, also the correlation of the specific surface areas of the differently modified glass beads and the associated fine particle fractions was investigated.

The lowest specific surface area is shown for glass beads processed with quartz for 4h, followed by glass beads processed with tungsten carbide for 4h and glass beads processed with quartz for 8h. The highest surface area among the ball mill modified glass beads is shown for the glass particles grinded with tungsten carbide for 8h. So, these findings match with the expectations about the hardness of the grinding materials and the processing times: harder grinding materials and longer processing times result in higher specific surface areas. The highest specific surface area however is shown for glass beads etched with plasma for 1min. These findings about the height of the specific surface area also correlate with the results of the AFM roughness analysis. Looking at the FPF, the same trend can be observed. Glass beads etched with plasma for 1min exhibit the highest FPF, followed by glass beads grinded with TC for 8h. The lowest FPF is shown for glass beads, grinded with Q for 4h and grinding with Q for 8h and grinding with TC for 4h lead to specific surface areas in between.

Figure 8 shows that the FPF correlates almost linearly with the height of the specific surface area of the modified carriers, with a coefficient of determination, R^2 of approximately 0.91. The FPF correlates even better with the specific surface area (Correlation Coefficient 0.954) than with the surface roughness (Correlation Coefficient 0.909). However the trend is the same, with an increasing specific surface area also the FPF increases.

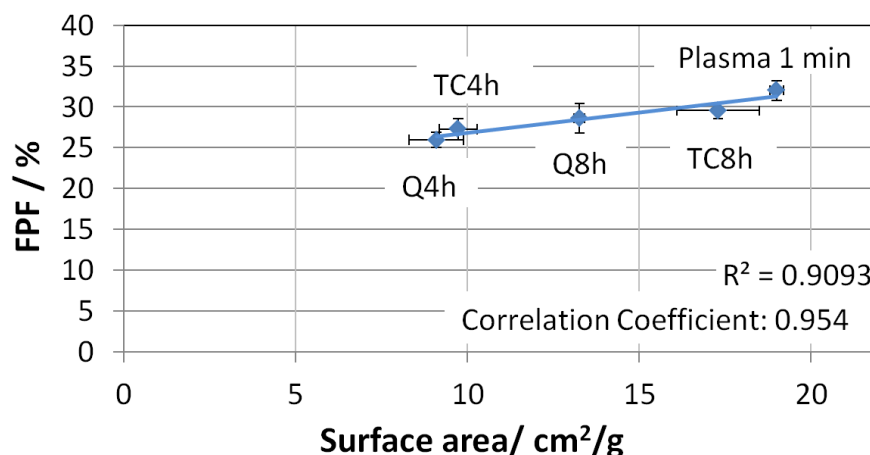


Figure 8 Correlation of specific surface area ($n = 3 \pm \text{SD}$) and FPF ($n = 3 \pm \text{SD}$) for surface modified glass beads.

6.4 Conclusion

This study shows that by the correlation of calculated and actual surface coverage and the resulting equations, the amount of API to weigh in (calculated surface coverage) for any desired actual surface can be calculated. Thus, comparable mixtures with same actual surface coverage can be prepared.

FPFs of adhesive mixtures, exhibiting the same actual and true surface coverage and containing surface modified carriers correlate with the surface roughness either expressed as R_{rms} value or specific surface area of the carriers. The FPF increases with increasing surface roughness. Results show that compared to untreated glass beads, surface modified glass beads show slightly increased FPFs. The FPF delivered from modified glass beads is also more constant what is indicated by lower standard deviations for the FPFs of the modified glass beads.

Concluding, the FPF can be tailored by the use of surface modified rough glass beads as carrier particles. Moreover drug detachment and thus the FPF from the surface modified carrier particles varies less compared to untreated glass beads.

Acknowledgements

The authors acknowledge the financial support of this research project by the German Research Foundation (DFG) for financial support within the priority

program SPP 1486 “Particles in Contact”. The authors also would like to thank the research groups of Prof. Butt and Dr. Kappl, Max Plank Institute for Polymer Research Mainz, for the provision of the AFM equipment and assisting with the AFM measurements.

References

- [1] G. Pilcer, N. Wauthoz, K. Amighi, Lactose characteristics and the generation of the aerosol., *Adv. Drug Deliv. Rev.* 64 (2012) 233–56.
- [2] X.M. Zeng, a P. Martin, C. Marriott, J. Pritchard, The influence of carrier morphology on drug delivery by dry powder inhalers., *Int. J. Pharm.* 200 (2000) 93–106.
- [3] Y. Rahimpour, M. Kouhsoltani, H. Hamishehkar, Alternative carriers in dry powder inhaler formulations., *Drug Discov. Today.* 00 (2013) 1–9.
- [4] X.M. Zeng, K.H. Pandhal, G.P. Martin, The influence of lactose carrier on the content homogeneity and dispersibility of beclomethasone dipropionate from dry powder aerosols., *Int. J. Pharm.* 197 (2000) 41–52.
- [5] H. Larhrib, G.P. Martin, C. Marriott, D. Prime, The influence of carrier and drug morphology on drug delivery from dry powder formulations, *Int. J. Pharm.* 257 (2003) 283–296.
- [6] X.M. Zeng, G.P. Martin, C. Marriott, J. Pritchard, The influence of crystallization conditions on the morphology of lactose intended for use as a carrier for dry powder aerosols., *J. Pharm. Pharmacol.* 52 (2000) 633–643.
- [7] X.M. Zeng, G.P. Martin, C. Marriott, J. Pritchard, Crystallization of lactose from carbopol gels., *Pharm. Res.* 17 (2000) 879–886.
- [8] X.M. Zeng, G.P. Martin, C. Marriott, J. Pritchard, The use of lactose recrystallised from carbopol gels as a carrier for aerosolised salbutamol sulphate., *Eur. J. Pharm. Biopharm.* 51 (2001) 55–62.

- [9] X.M. Zeng, G.P. Martin, C. Marriott, J. Pritchard, Lactose as a carrier in dry powder formulations: the influence of surface characteristics on drug delivery., *J. Pharm. Sci.* 90 (2001) 1424–1434.
- [10] S.G. Maas, G. Schaldach, E.M. Littringer, A. Mescher, U.J. Griesser, D.E. Braun, et al., The impact of spray drying outlet temperature on the particle morphology of mannitol, *Powder Technol.* 213 (2011) 27–35.
- [11] E.M. Littringer, A. Mescher, H. Schroettner, L. Achelis, P. Walzel, N. A. Urbanetz, Spray dried mannitol carrier particles with tailored surface properties - The influence of carrier surface roughness and shape., *Eur. J. Pharm. Biopharm.* 82 (2012) 194 –204.
- [12] F. Ferrari, D. Cocconi, R. Bettini, F. Giordano, P. Santi, M. Tobyn, et al., The surface roughness of lactose particles can be modulated by wet-smoothing using a high-shear mixer., *AAPS PharmSciTech.* 5 (2004) 1–6.
- [13] K. Iida, Y. Inagaki, H. Todo, H. Okamoto, K. Danjo, H. Luenberger, Effects of surface processing of lactose carrier particles on dry powder inhalation properties of salbutamol sulfate., *Chem. Pharm. Bull. (Tokyo).* 52 (2004) 938–942.
- [14] H. Steckel, P. Markefka, H. TeWierik, R. Kammelar, Effect of milling and sieving on functionality of dry powder inhalation products., *Int. J. Pharm.* 309 (2006) 51–59.
- [15] S. Zellnitz, J.D. Redlinger-Pohn, M. Kappl, H. Schroettner, N.A. Urbanetz, Preparation and characterization of physically modified glass beads used as model carriers in dry powder inhalers., *Int. J. Pharm.* 447 (2013) 132–8.
- [16] P.M. Young, D. Roberts, H. Chiou, W. Rae, H.-K. Chan, D. Traini, Composite carriers improve the aerosolization efficiency of drugs for respiratory delivery, *J. Aerosol Sci.* 39 (2008) 82–93.

[17] Y. Kawashima, T. Serigano, T. Hino, H. Yamamoto, H. Takeuchi, Effect of surface morphology of carrier lactose on dry powder inhalation property of pranlukast hydrate, *Int. J. Pharm.* 172 (1998) 179–188.

[18] E.M. Littringer, S. Zellnitz, K. Hammernik, V. Adamer, H. Friedl, N. a. Urbanetz, Spray Drying of Aqueous Salbutamol Sulfate Solutions Using the Nano Spray Dryer B-90—The Impact of Process Parameters on Particle Size, *Dry. Technol.* 31 (2013) 1346–1353

.

7

Towards the optimisation and adaptation of dry powder inhalers

Yan Cui, Silvio Schmalfuß, Sarah Zellnitz, Nora Anne Urbanetz, Martin Sommerfeld

International Journal of Pharmaceutics, in press



ELSEVIER

Contents lists available at ScienceDirect

International Journal of Pharmaceutics

journal homepage: www.elsevier.com/locate/ijpharm

Towards the optimisation and adaptation of dry powder inhalers

Y. Cui^a, S. Schmalfuß^a, S. Zellnitz^b, M. Sommerfeld^{a,*}, N. Urbanetz^b^a Martin-Luther-Universität Halle-Wittenberg, Zentrum für Ingenieurwissenschaften, Halle/Saale D-06099, Germany^b Research Center Pharmaceutical Engineering GmbH, Inffeldgasse 13, Graz A-8010, Austria

ARTICLE INFO

Article history:

Received 28 February 2014

Received in revised form 25 April 2014

Accepted 29 April 2014

Available online xxx

Keywords:

Dry powder inhaler

Carrier glass beads

Surface modification

Computational fluid dynamics

Fluid stresses on carrier

Prediction of drug detachment

ABSTRACT

Pulmonary drug delivery by dry powder inhalers is becoming more and more popular. Such an inhalation device must insure that during the inhalation process the drug powder is detached from the carrier due to fluid flow stresses. The goal of the project is the development of a drug powder detachment model to be used in numerical computations (CFD, computational fluid dynamics) of fluid flow and carrier particle motion through the inhaler and the resulting efficiency of drug delivery. This programme will be the basis for the optimisation of inhaler geometry and dry powder inhaler formulation. For this purpose a multi-scale approach is adopted. First the flow field through the inhaler is numerically calculated with OpenFOAM[®] and the flow stresses experienced by the carrier particles are recorded. This information is used for micro-scale simulations using the Lattice-Boltzmann method where only one carrier particle covered with drug powder is placed in cubic flow domain and exposed to the relevant flow situations, e.g. plug and shear flow with different Reynolds numbers. Therefrom the fluid forces on the drug particles are obtained. In order to allow the determination of the drug particle detachment possibility by lift-off, sliding or rolling, also measurements by AFM (atomic force microscope) were conducted for different carrier particle surface structures. The contact properties, such as van der Waals force, friction coefficient and adhesion surface energy were used to determine, from a force or moment balance (fluid forces versus contact forces), the detachment probability by the three mechanisms as a function of carrier particle Reynolds number. These results will be used for deriving the drug powder detachment model.

© 2014 Elsevier B.V. All rights reserved.

1. Introduction

Due to the lack of propellants, high patient compliance and high dose carrying capacity pulmonary drug delivery by dry powder inhalers (DPIs) are increasingly being used in the therapy of asthma and other chronic pulmonary diseases. Therefore, numerous designs of inhalers are on the market (Smith and Parry-Billings, 2003; Islam and Gladki, 2008). Active pharmaceutical ingredient (API) particles that can be administered via dry powder inhalers have to exhibit aerodynamic diameters in the size range of 1 μm –5 μm as only particles of this size can reach the tiny airways of the deep lung. Particles of such small size are very cohesive and show poor flow properties which leads to difficulties concerning volumetric dosing. To overcome this problem the fine drug powder is mostly blended with larger carrier particles (in the size range of 50 μm –100 μm). During blending the small API

particles will stick to the surface of the larger carrier particles so that they will be partially covered. Such large particles exhibit adequate flowability and can be easily handled.

For achieving high drug delivery efficiency during inhalation, the fine drug particles need to be detached from the carrier within the inhaler device through the stresses in the air flow or collisions with device walls. If detachment does not take place, the drug particles sticking on the carrier surface will impact in the mouth and the throat. The fluid dynamic detachment of the drug powder in the complex airflow of an inhaler is realised by acceleration/deceleration of the carrier particles (i.e. inertial force), flow shear gradients and turbulent stresses (Telko and Hickey, 2005). In order to deliver a high amount of detached drug particles a proper balancing between the adhesive forces between carrier and drug and the removal forces during the inhalation process is necessary. Thus inter-particle interactions between API and carrier play a key role in this kind of formulations. On one hand they have to be high enough that the API sticks to the carrier surface, thus ensuring proper handling as well as uniform dosing, and on the other hand low enough that drug detachment from the carrier surface during inhalation is guaranteed. One approach to tailor inter-particle-interactions between drug and carrier is the surface modification

* Corresponding author. Tel.: +49 345 5523681; fax: +49 345 5527586.

E-mail addresses: yan.cui@iw.uni-halle.de (Y. Cui),silvio.schmalfluss@hs-merseburg.de (S. Schmalfuß), sarah.zellnitz@tugraz.at (S. Zellnitz), martin.sommerfeld@iw.uni-halle.de (M. Sommerfeld).<http://dx.doi.org/10.1016/j.ijpharm.2014.04.065>

of the carrier particles (Zellnitz et al., 2011). Besides the balancing of inter-particle interactions the inhaler design needs to ensure sufficiently high flow stresses on the carrier particles for yielding high detachment rates. So the detachment of drug particles from the carrier is a prerequisite for a high respirable fraction in vivo that is equivalent to a high fine particle fraction (FPF) in vitro. The FPF is determined by a standardised procedure using cascade impactors and represents the ratio of the fine particle dose (FPD) and the mass of API leaving the inhaler (emitted dose (ED)) in %. The FPD is the mass of drug particles below 5 μm . The FPF is a common parameter to compare the performance of different inhaler types and different formulations among each other.

The impactors used and the procedure of determining the FPF are described in the monograph "Aerodynamic assessment of fine particles for preparations for inhalation" of the European Pharmacopoeia. Impactor data are an important and principal part of marketing authorization applications for new dry powder inhaler formulations. Consequently, so far the design and optimisation of inhalers is mainly based on experimental analysis. Essential for the performance of an inhaler is a high amount of drug powder (i.e. fine particle fraction) that is able to leave the inhaler and reach the deep lung. As already has been mentioned the determination of the FPF is mainly done using different types of cascade impactors (Steckel and Müller, 1997; de Koning, 2001). Numerous such experimental studies have been conducted for analysing the influence of inhaler devices on the FPF (Srichana et al., 1998; Telko and Hickey, 2005; Chew et al., 2002; Newman and Busse, 2002). However, these experimental approaches are rather cumbersome and time-consuming. In the development of new inhaler formulations or new inhalers it would be beneficial to employ techniques where data acquisition is more rapid. Therefore, it would be advantageous developing a drug detachment model which could be used in connection with the application of computational fluid dynamics (CFD) for analysing inhaler performance and overcome the time consuming impactor experiments.

In the past CFD has been already applied by a number of research groups for studying the performance of inhalers. These studies are related to an analysis of flow structure and particle motion inside an inhaler mostly. Objectives were for example the study of the particle motion in different inhaler designs (Donovan et al., 2011), the influence of a grid inserted into the outflow tube (Coates et al., 2004) or the effect of mouthpiece shape (Coates et al., 2007). In all of these

numerical calculations only the motion of the carrier particles was tracked for visualisation purposes (see Donovan et al., 2011). Describing the detachment of drug particles from the carrier would require additional modelling and was not considered in numerical studies performed so far.

The aim of the present contribution is the development of Lagrangian detachment models which eventually should allow the numerical prediction of inhaler performance and efficiency. For this purpose a multi-scale analysis is adopted here (Fig. 1). First the flow field through the entire inhaler device (here the Cyclohaler[®]) is calculated numerically using OpenFOAM[®] and the fluid dynamic stresses acting on the carrier particles are recorded and statistically analysed (Cui et al., 2013). With these flow conditions micro-scale numerical simulations based on the Lattice-Boltzmann method (LBM) are conducted for a fixed carrier particle covered with hundreds of drug particles. From the simulated fluid forces acting on the drug particles the possibility of detachment is determined based on measured van der Waals forces and friction coefficients as well as other contact properties. The van der Waals forces acting between carrier particles and drug particles were determined via atomic force microscopy (AFM). The friction coefficients were determined via a FT4 Powder Rheometer. Moreover, the adhesion surface energy of untreated and physically modified glass beads was determined from the static contact angles of water and α -bromonaphthalene.

In the future the results from the LBM simulations (i.e. drug detachment rate) and the experiments (interaction parameters between carrier particles and drug particles) will be used to develop a drug detachment model for Lagrangian calculation of the entire device using OpenFOAM[®] (macro-scale simulations). Moreover, the calculations need to be validated based on measured fine particle fraction leaving the inhaler by using cascade impactors (Fig. 1).

2. Macro scale calculations

For the numerical calculations of stationary flow through an inhaler the open source code OpenFOAM[®] is applied. Herewith the Reynolds-averaged conservation equations (RANS) in connection with the k - ω -SST turbulence model are solved. The considered inhaler (i.e. the Cyclohaler[®]) is discretised by a tetrahedral mesh consisting of about 300,000 cells (Fig. 2). The inner diameter of the mouthpiece is 10.5 mm and that of the swirl chamber is 19 mm.

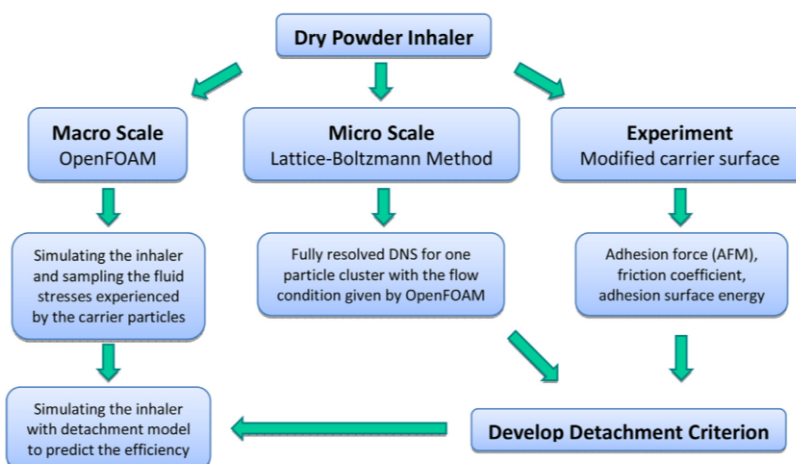


Fig. 1. Sketch of the multi scale approach adopted for analysing drug powder detachment in an inhaler and connection between simulation and experiment.

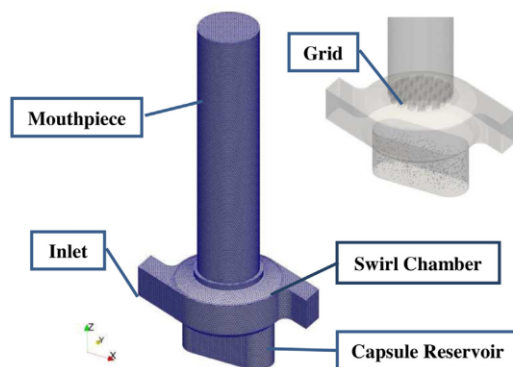


Fig. 2. Numerical grid for the inhaler simulations and zoom of the grid at the entrance to the mouthpiece with initial particle positions in the capsule reservoir.

The origin for the coordinate along the inhaler is the upper edge of the swirl chamber. The distance to the mouth piece exit is 48.1 mm and to the bottom of the reservoir is 14.3 mm (negative coordinate). The depth of the reservoir is 7.8 mm. The flow condition considered here corresponds to 70 l/min which is a typical inspiratory maximum flow rate (Newman and Busse, 2002). In order to obtain an appropriate outflow velocity profile at the exit of the mouthpiece, first a pipe flow (diameter identical to the mouthpiece of the inhaler) was calculated with the present flow rate (i.e. 70 l/min, bulk flow velocity 13.5 m/s). The developed velocity profile and the associated turbulence properties were then used as outlet condition for the inhaler calculation. At the two tangential inlets only the ambient total pressure needs to be prescribed. At the walls standard wall functions were applied. Numerical calculations of the inhaler were conducted without and with grid mounted at the exit of the swirl chamber (Fig. 2). The purpose of the grid is twofold. First it acts like a kind of flow straightener whereby the swirl in the exit pipe (mouthpiece) is reduced to a large extent and second carrier particles may hit the grid, inducing a detachment of the drug powder.

The particles were tracked in the calculated stationary flow field by neglecting their influence on the flow field. In total 1000 particles with a diameter of 110 μm (particle density 2500 kg/m^3) were considered which initially were randomly distributed in the capsule reservoir (Fig. 2). The initial particle velocity was set to zero. At the beginning of the Lagrangian calculation the particles were released and moved by the fluid dynamic forces. At the moment only drag and gravity forces were considered. The generation of the instantaneous fluid velocity along the particle trajectory is based on the simple discrete eddy approach (see for example Sommerfeld et al., 2008). Particle-wall collisions are treated as inelastic with $e = 0.96$ and $\mu = 0.01$.

3. Inhaler results

The flow field obtained for the two inhaler geometries (i.e. without and with grid) is illustrated in Fig. 3 where the colour level corresponds to the magnitude of the fluid velocity. The geometry without grid yields a fluctuating flow during the course of convergence which is often observed for swirling flows. The swirling flow extends from the swirl chamber (lower part) into the mouthpiece (straight pipe) yielding rather high velocity magnitudes in the near wall region (i.e. about 30 m/s). The insertion of a grid (standard geometry of a Cyclohaler[®]) removes the swirl in the mouthpiece to a large extent, whereby the highest velocities are

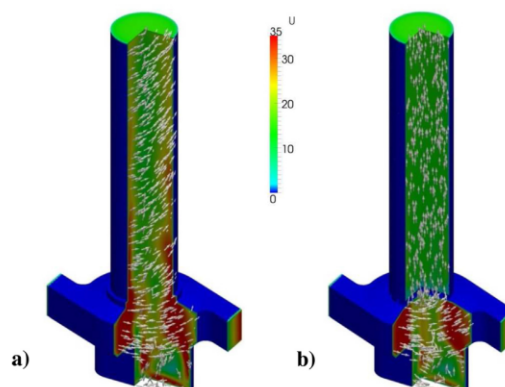


Fig. 3. Visualisation of calculated stationary velocity fields (i.e. colour scale: magnitude of velocity in m/s) in both inhaler geometries and velocity vectors near the inhaler wall; (a) without grid, (b) with grid (Cyclohaler[®], 70 l/min).

only obtained in the swirl chamber (Fig. 3b). The overlaid velocity vectors in the near wall region illustrate the swirl intensity in both cases. Due to the presence of the grid the pressure drop across the entire inhaler is about twice as large then for the configuration without grid (i.e. without grid: $\Delta p = 1.56$ kPa; with grid 2.98 kPa), although without grid the high swirl being present at the mouthpiece outlet results in additional losses.

Also responsible for drug particle detachment from the carrier particles is the turbulence intensity. In Fig. 4 the colour levels for the turbulent kinetic energy are compared for both geometries. Without grid extremely high turbulence levels are found in the swirl chamber and the initial part of the straight pipe (i.e. $k > 50$ m^2/s^2 ; fluctuating velocity $\sigma > 5.8$ m/s). The geometry with grid yields smaller regions of high turbulence in the swirl chamber and, additionally, a region of high turbulence just downstream of the grid (Fig. 4).

Particle trajectories in both configurations are shown in Fig. 5. Due to the sustained swirl in the mouthpiece for the grid-free configuration the particles are performing a spiral motion through the mouthpiece and are centrifuged out of the core region towards the wall. Moreover, particles are circulating in the swirl chamber. With grid, the particles reside for a longer period in the swirl chamber performing a circulating motion (Fig. 5b). Those particles moving through the mouthpiece are showing more or less straight paths. For the case without grid all released carrier particles leave the inhaler after 0.2 s, while with grid it takes 0.6 s as the particles reside for a longer time in the swirl chamber. In both configurations the particle motion is strongly affected by wall collisions. The relatively straight particle paths between successive wall collisions are an indication of a rather weak response of the particles to turbulence.

In the following, the fluid stresses along the particle trajectories are analysed. Therefore, at each time step of the Lagrangian tracking of the particles, the local values of the instantaneous relative velocity, the mean flow gradient and the turbulent kinetic energy at the particle position are stored and then processed to obtain the relative frequencies (probability distribution functions, PDF). The PDF of the particle Reynolds number ($\text{Re} = \rho \cdot D_p \cdot U_{\text{rel,inst}} / \mu$) calculated with the instantaneous relative velocity (also shown as an abscissa) and the particle diameter of 110 μm show for the case without grid a distribution with a relatively wide plateau between 15 and 30 m/s (Fig. 6). A bimodal distribution with a maximum of Re at about 70 and 200 is found for the case with grid. These values correspond to instantaneous relative velocities of about 10 m/s and 30 m/s. The averaged instantaneous relative velocity is however identical for both cases (i.e. about 24 m/s). High values in the range of 30 m/s are

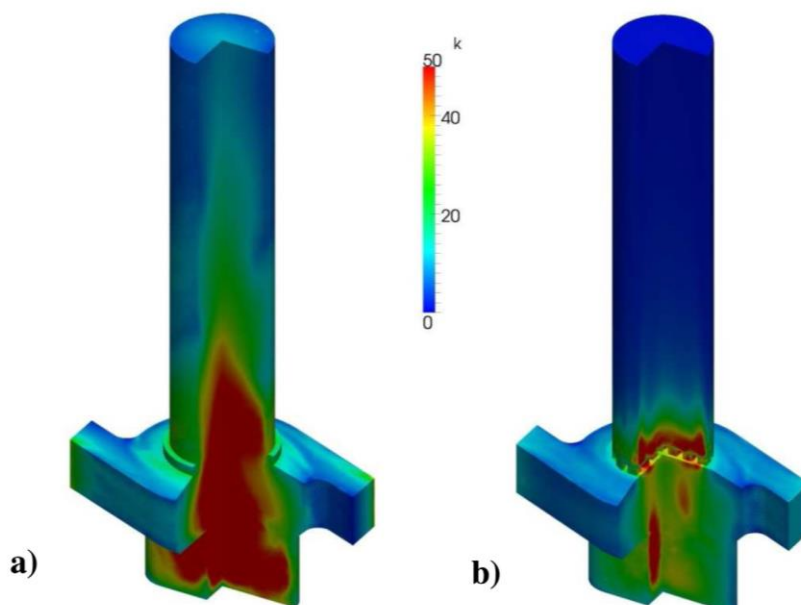


Fig. 4. Visualisation of calculated turbulent kinetic energy (colour scale in m^2/s^2) inside the inhaler; (a) without grid, (b) with grid (Cyclohaler[®], 70 l/min).

experienced only by the particles in the swirl chamber with a low velocity core and a high velocity annular flow. Hence, particles being released in the reservoir are captured by the high velocity tangential inlet flow (average inlet velocity of about 25 m/s) and thus see a high relative velocity. Also the particle momentum loss due to frequent wall collisions gives rise to such high slip velocities. The PDFs become more obvious by looking at the instantaneous relative velocity with respect to the location within the inhaler for both cases (Fig. 7). Note that $z=0$ m corresponds to the upper edge of the swirl chamber, just underneath the grid location. Without grid, quite a number of particles are found in the mouthpiece with slip velocities of around 15 m/s, coming from the high gas velocity in the near wall region (see Fig. 3a). In the swirl chamber slip velocities of around 30 m/s are most frequent. This yields the wide velocity plateau (Fig. 6). When the grid is considered in the simulations many particles are trapped in the swirl chamber for a long time

seeing also a slip velocity of around 30 m/s and fewer particles are detected in the mouthpiece with slip velocities of around 10 m/s. Hence, the high relative velocities experience by the particles in the swirl chamber support drug powder detachment.

The PDFs of the mean shear rate experienced by the particles show a maximum for low shear rates of about 9000 l/s without and with grid (Fig. 8). These shear rates are mainly found in the swirl chamber for both cases. The higher shear rates up to 80,000 l/s are experienced by the particles in the boundary layers of swirl chamber and mouthpiece. As both PDFs are almost identical also the averaged shear rate is roughly the same, i.e. 35,000 l/s. Eventually also turbulence will have an impact on drug powder detachment since turbulent eddies will hit the carrier and locally introduce high velocities. Therefore, the PDFs of the turbulence intensity Tu are also evaluated, which are determined from the turbulent kinetic energy assuming isotropic turbulence and the

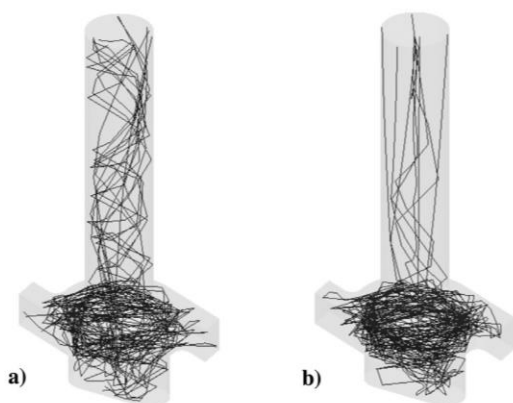


Fig. 5. Calculated representative particle trajectories through the inhaler; (a) without grid, (b) with grid (Cyclohaler[®], 70 l/min).

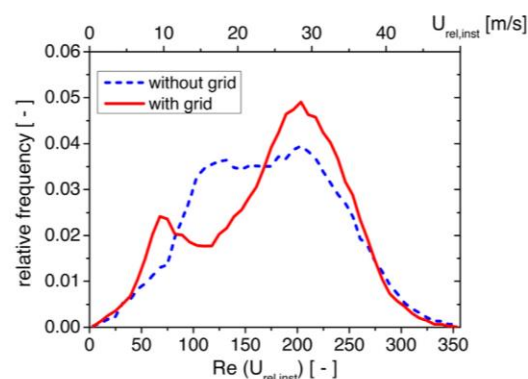


Fig. 6. Relative frequency (PDF) of the instantaneous Reynolds number experienced by the particles moving through the inhaler (Cyclohaler[®], 70 l/min).

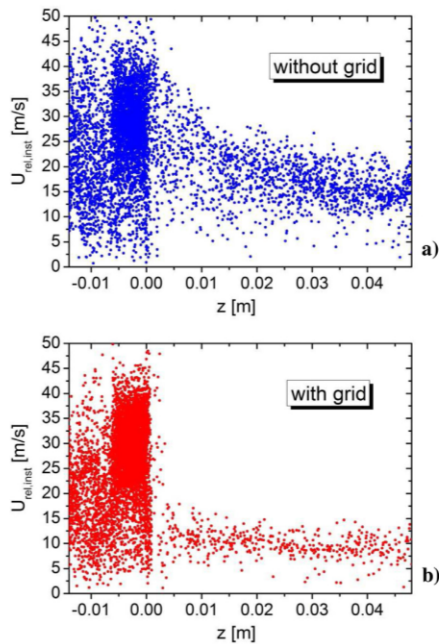


Fig. 7. Scatter plot of the instantaneous relative velocity experienced by the carrier particles with respect to the location within the inhaler; (a) without grid, (b) with grid (Cyclohaler[®], 70 l/min).

mean relative velocity between particle and air (Fig. 9).

$$Tu = \frac{\sigma_{rms}}{U_{rel}} = \frac{1}{U_{rel}} \sqrt{\frac{2}{3}k} \quad (1)$$

Highest frequencies of occurrence are found for about $Tu < 10\%$ for both geometries. However, without grid the probability of higher Tu values is slightly larger than with grid. Consequently the mean value is 9.5% without grid and 7.4% with grid, respectively.

As mentioned in the introduction, also collisions of the carrier particles with the walls or the grid (if present) may induce a detachment of the drug powder. Hence, the number of wall collisions along the inhaler normalised by the total wall collision number is shown in Fig. 10. The highest probability of wall collisions is, as expected, found in the swirl chamber where the particles reside longest (see also Fig. 5). For both cases the

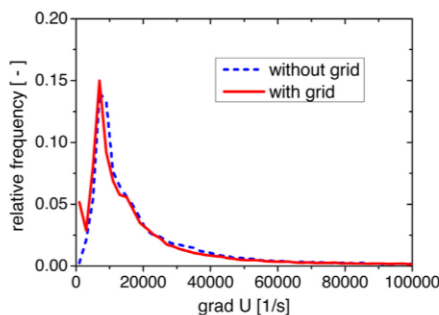


Fig. 8. Relative frequency of the mean fluid shear rate experienced by the particles when moving in the inhaler for both geometries (Cyclohaler[®], 70 l/min).

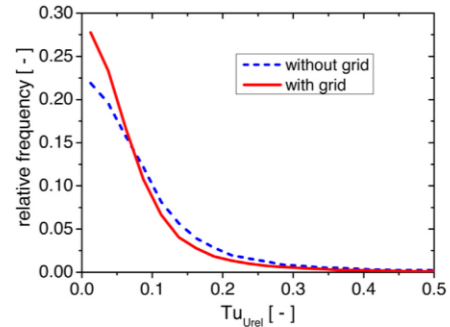


Fig. 9. PDF of turbulence intensity ($Tu = \sigma/U_{rel}$; $\sigma = \sqrt{2/3k}$) sampled by the particles along their trajectory through the inhaler, without and with grid (Cyclohaler[®], 70 l/min).

distributions are very similar and the relative wall collision frequency shows a bimodal shape, indicating the highest wall collision rates in the edges of the swirl chamber. With grid the wall collision rate in the swirl chamber is higher. In the case without grid also some wall collisions are occurring in the straight pipe, since the particles perform a spiral motion close to the wall (see also Fig. 5). As a result, the wall collision rate along the mouthpiece is almost constant. Overall, the wall collision rate is highest for the case without grid (i.e. 2402 collisions/s). With grid about 2114 collisions/s with the wall are registered, mainly occurring in the swirl chamber.

The fluid stresses obtained from the calculation of the particle motion in the inhaler are now used to analyse the probability of detachment based on micro-scale simulations by the Lattice-Boltzmann method considering only one fixed carrier particle covered with hundreds of drug particles. The detachment due to wall collisions will be analysed at a later stage.

4. Micro scale simulations

For the micro scale simulations of fully resolved particles, the Lattice-Boltzmann method (LBM) is adopted and further developed (Dietzel et al., 2011; Dietzel and Sommerfeld, 2013). Here the change of the probability distribution function, which describes the number of fluid elements having the velocity v at location x and time t , is solved to simulate the flow of a Newtonian fluid. Hence, besides the spatial discretization realized by the numerical grid, the fluid element velocities and the time are discretised as well. As a result, information is allowed to propagate to a neighbouring

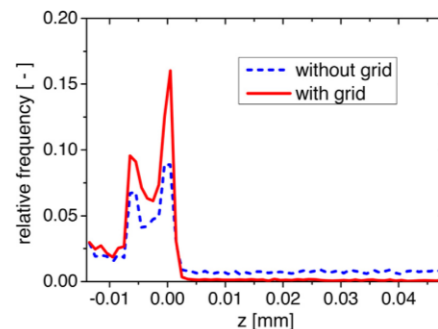


Fig. 10. PDF of relative particle-wall collision frequency with respect to the location in the inhaler, without and with grid (zero is the beginning of the mouthpiece) (Cyclohaler[®], 70 l/min).

lattice node in one of the discrete lattice directions at one time step only, followed by a collision step. In the collision step the distribution functions tend to be brought back to the equilibrium distribution function. The discretised Lattice–Boltzmann equation combined with single relaxation time collision operator approximated by the BGK (Bhatnagar–Gross–Krook) (Bhatnagar et al., 1954) approach is given by:

$$f_{\sigma i}(x + \xi_{\sigma i} \Delta t, t + \Delta t) - f_{\sigma i}(x, t) = -\frac{\Delta t}{\tau} (f_{\sigma i}(x, t) - f_{\sigma i}^{(0)}(x, t)) \quad (2)$$

where $f_{\sigma i}^{(0)}$ is the discrete equilibrium distribution function, $\Delta x = \xi_{\sigma i} \Delta t$ is the width of the spatial discretization, Δt is the length of one time step and τ is the relaxation time. The term on the left hand side corresponds to the propagation and that on the right hand side is the non-equilibrium part, being the difference between calculated and equilibrium distribution functions (collision term). In this work the D3Q19 (3 dimensions and 19 directions) model is used.

In order to adapt the LBM for more accurate, high spatial resolution calculations of the flow around complex shaped particles or agglomerates, the standard LBM approach was upgraded by the following two methods. First, the standard step-like wall boundary conditions (bounce-back boundary condition) was replaced by a curved boundary condition (Bouzidi et al., 2001; Guo et al., 2002) which accurately accounts for the distance between wall and the nodes of the fluid domain. Moreover, for closely capturing the particle contour with a sufficient number of grid nodes a local grid refinement method was applied (Crouse, 2003; Dietzel and Sommerfeld, 2010, 2013). This implies that regions around a complex particle are calculated on a fine mesh whereas regions in the outer flow domain without strong gradients are calculated on a coarse mesh in order to save computational time. Each grid refinement level implies the reduction of the cell face by exactly a factor of two only (Dietzel and Sommerfeld, 2013). The number of grid refinement steps is depending on the considered problem.

In the present simulations the fluid forces acting on hundreds of fine drug particles adhered to a carrier particle shall be determined. However, when two particles are near contact, i.e. separation less than one lattice spacing, there exists a problem to calculate the forces on these particles separately. Normally, the nodes inside the particle are solid nodes and outside of the particle are fluid nodes. The forces over a particle are obtained from a momentum balance at the surface (reflexion of the fluid elements at the particle boundary, see Dietzel and Sommerfeld, 2013). When particles are in close contact (separation less than one lattice), there is a lack of fluid nodes between the particles, and consequently some solid nodes are included to calculate the particle force. However, those solid nodes have no fluid information and therefore the force calculation will be wrong. One way to avoid this problem is to introduce some temporary fluid property

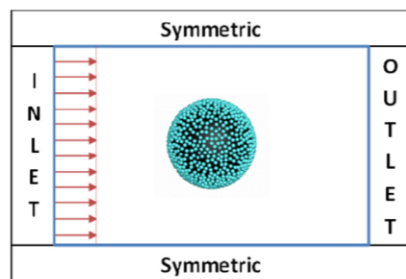


Fig. 11. Computational domain with applied boundary condition and centrally placed particle cluster.

(i.e. distribution functions) to the solid nodes within that particle (Ernst et al., 2013). Due to the no-slip boundary condition at the particle surface, the fluid velocities at these nodes may be set equal to the particle velocity. The missing distribution function is then determined on the basis of the equilibrium distribution function. The method has been validated by Ernst et al. (2013) for several test cases. With the application of this method, it is possible to calculate separately forces on both particles being in close contact.

5. Setup of LBM simulations

The simulations were conducted for a spherical carrier particle (in this case $D_{\text{carrier}} = 100 \mu\text{m}$) randomly covered with a mono-layer of fine spherical powder (i.e. $D_{\text{fine}} = 5$ or $10 \mu\text{m}$). The target value in the random generation of the drug particle distribution is the degree of coverage which is the cross-section area of all fine particles divided by the surface area of a fictitious sphere with the diameter ($D_{\text{fine}} + D_{\text{carrier}}$). This gives the number of fine particles, by assuring that only a mono-layer is produced, i.e. each fine particle must have contact with the carrier surface. As an example, for the size ratio of $5 \mu\text{m}/100 \mu\text{m}$ the coverage degree of 50% yields 882 fine particles.

The particle cluster (carrier with drug powder) is then centrally fixed in the cubic flow domain shown in Fig. 11 and exposed to different kinds of stationary flow situations. The domain size, specified in terms of the carrier particle diameter and the number of grids (i.e. used for the base-grid) depends on the Reynolds number which is defined with the diameter of the carrier particle D_{carrier} and the inflow velocity U_0 (see Table 1):

$$\text{Re} = \frac{\rho D_{\text{carrier}} U_0}{\mu} \quad (3)$$

For the higher Reynolds numbers the base grid was halved and the domain size slightly increased in all directions. The number of refinement regions around the particle cluster was 3 or 4 depending on the conditions. For all the simulations the fine particle diameter was resolved by at least 6 grid cells of the finest grid. The selection of the grid dimensions, as well as the domain size, was based on an extensive parameter study for optimizing accuracy and computational effort. The boundary conditions used for the simulations are shown in Fig. 11. At the inlet a pre-defined velocity profile (i.e. plug or shear flow) was specified and the outlet condition is based on the gradient free assumption for all fluid properties. At all side faces symmetry boundary conditions are used (Fig. 11).

The numerical simulations are performed by exposing the fixed particle cluster to different laminar plug and shear flow situations with typical Reynolds numbers resulting from the RANS calculations. Based on that, the fluid dynamic forces on the drug particles are analysed and the probability of detachment is determined in connection with the measured adhesion properties.

The drug particles attached to the surface of the bigger carrier particle experience fluid dynamic and particle–particle interaction forces (Fig. 12). From the LBM simulations, the total fluid dynamic force F_{total} acting on all drug particles is obtained which can be separated in normal (F_n) and tangential (F_t) components. The normal force is defined to be positive if it points away from the

Table 1
Domain size specified in terms of the carrier particle diameter and the number of cells for the base grid.

	Stream-wise direction	Lateral directions
Re < 100	$7.8 \cdot D_{\text{carrier}}$ $60 \cdot \Delta x_{\text{coarse}}$	$6.5 \cdot D_{\text{carrier}}$ $50 \cdot \Delta x_{\text{coarse}}$
Re > 100	$10.4 \cdot D_{\text{carrier}}$ $160 \cdot \Delta x_{\text{coarse}}$	$9.1 \cdot D_{\text{carrier}}$ $140 \cdot \Delta x_{\text{coarse}}$

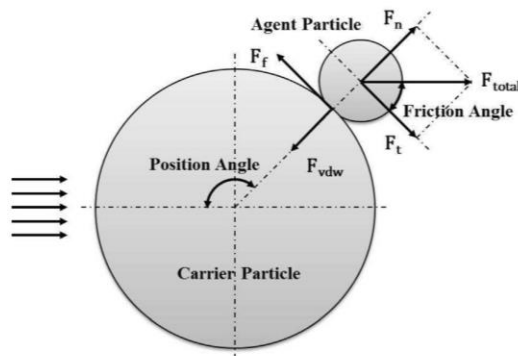


Fig. 12. Illustration of forces acting on the fine drug particles.

carrier and otherwise it is negative. The van der Waals force (F_{vdw}) is the only adhesion force between agent and carrier particle considered here. The fluid dynamic tangential force (F_t) acts against the friction force F_f resulting from Coulombs law of friction. The gravity force on the drug particles is negligible, since it is very small compared to the other forces.

The position angle (see Fig. 12) indicates the location of the drug particle on the surface of the carrier particle with respect to the stream-wise direction. This angle ranges from 0° to 180° and is symmetric with regard to the axis through the carrier particle in stream-wise direction. In the next section, forces will be evaluated depending on the position angle (i.e. location of agent particles).

6. Forces on drug particles

The objective of the numerical studies is the evaluation of the normal and tangential fluid forces on the fine particles as a function of their position on the carrier and the flow condition. Exemplarily all total force vectors for the fine particles are shown in Fig. 13 for three Reynolds numbers together with the flow field about the cluster. It is obvious that the direction and magnitude of the forces are strongly correlated with the flow structure about the cluster. For higher Reynolds numbers there develops backward flow behind the cluster which completely changes the force vector field. As a result, just in front of the separation line (i.e. indicating the wake region) the fluid dynamic forces are directed away from the cluster.

As a consequence of the random variation of fine particle distribution on the surface of the carrier and the involved fluid dynamic interaction between the fines also the forces for a given position angle will vary. Therefore, at least four simulation runs were conducted for all the conditions, each with a different random fine particle distribution on the carrier. Moreover, the fluid dynamic force on each fine particle shows oscillations in time which are due to the time-dependent nature of the flow, especially at higher Reynolds numbers. Consequently, the forces on the fine particles were recorded in the course of time. A steady-state value of the force was obtained for each fine particle by averaging over a certain time period towards the end of the simulation. This averaging period depends on the considered flow condition and was typically between 2500 and 5000 time steps for a laminar flow.

Since the flow about the particle cluster is axi-symmetric for a plug flow, the forces on all the fine particles may be plotted in

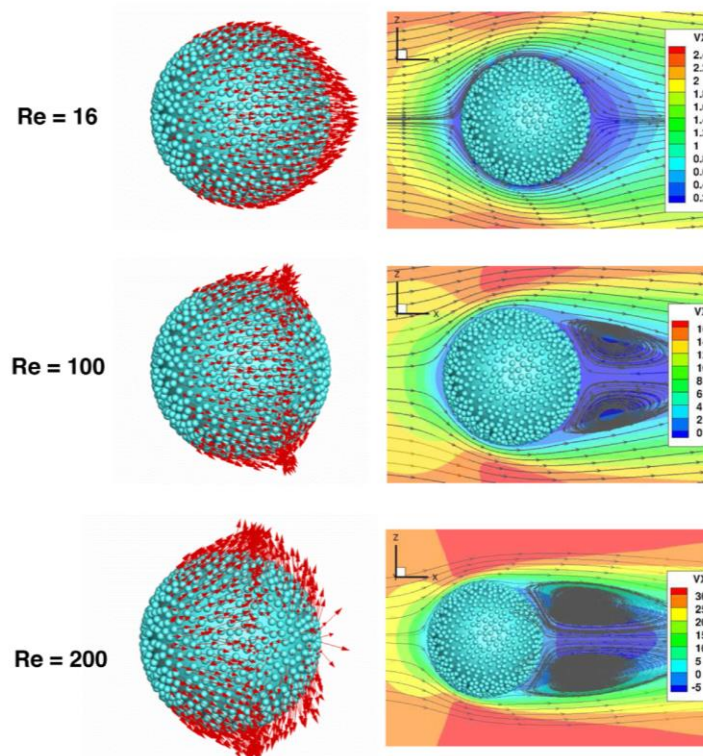


Fig. 13. Flow field about the particle cluster and resulting total forces on the fine particles for three Reynolds numbers (degree of coverage 50%, $D_{fine}/D_{carrier} = 5/100$).

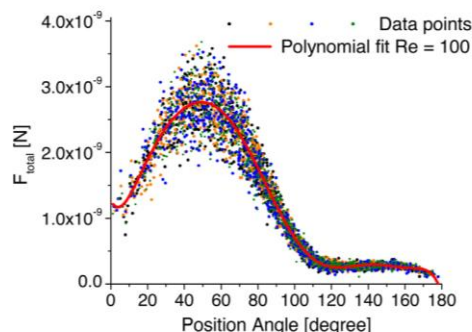


Fig. 14. Total force on all the fine particles in dependence of position angle for four different random distributions (coloured dots) and resulting polynomial fitting curve ($Re = 100$, coverage degree 50%, $D_{\text{fine}}/D_{\text{carrier}} = 5/100$). (For interpretation of the references to colour in this figure legend, the reader is referred to the web version of this article.)

dependence of the position angle (Fig. 14). Each point in Fig. 14 is the temporal average of the total force on one fine particle and the different colours correspond to the result obtained for one of the four runs with different drug particle distributions. Due to the large scatter of the forces it is more convenient to consider a polynomial fitting curve through all the data points in the following (Fig. 14). The maximum of the total force is found at an angle of about 50° from the front stagnation point. This is also the region with the largest scatter of the forces. In the wake region, i.e. beyond an angle of about 110° , the total force on the fine particles is considerably smaller (see also Fig. 13).

The magnitude of the forces and the characteristic angles (e.g. location of maximum) of course largely depend on the Reynolds number. This is obvious from Fig. 15 showing the fitting curves for the normal force on the fine particles. As to be expected, the magnitude of the force is increasing with the Reynolds number. In the front section of the cluster (i.e. position angles smaller than $40\text{--}50^\circ$) the normal force is of course negative implying that these fine particles cannot be detached by lift-off as they are pushed towards the carrier. Beyond this stagnation region the normal force on the fine particles becomes positive allowing a lift-off when it becomes larger than the van der Waals force. The position angle of the maximum normal force decreases with increasing Reynolds number as a consequence of wake development (Figs. 13 and 15).

Moreover, the influence of the degree of coverage on the normal force distribution was studied, representative for a Reynolds number of 100 (Fig. 16). The simulation results reveal that with decreasing coverage the normal force is increasing. This is an

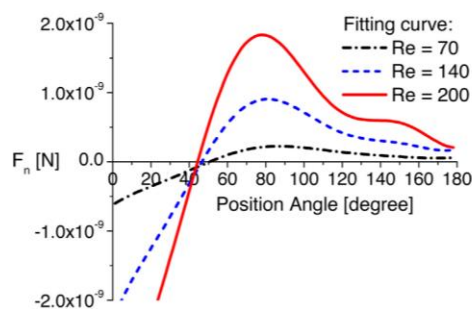


Fig. 15. Fitting curves for the normal force on the fine particles as a function of position angle for different Reynolds numbers (coverage degree 50%, $D_{\text{fine}}/D_{\text{carrier}} = 5/100$).

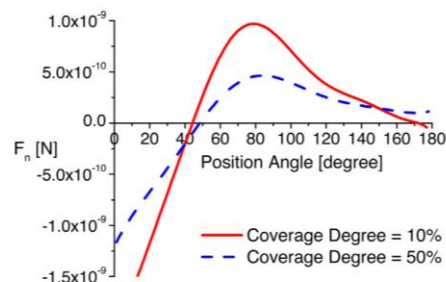


Fig. 16. Fitting curves for the normal force on the fine particles as a function of position angle for different degree of coverage ($Re = 100$, $D_{\text{fine}}/D_{\text{carrier}} = 5/100$).

obvious result since in the case of large coverage the flow is going more or less across the fine particles so that each small particle is located in the wind shadow of a front particle. For low degree of coverage the flow about the fine particles becomes again attached to the surface of the carrier behind them. Hence, the next fine particle is exposed to a stronger flow. With increasing Reynolds number the difference in the normal force for different coverage degrees is increasing. As a consequence, in producing the blend, it should be tried to achieve a low coverage in order to have a better prerequisite for drug powder detachment in an inhaler.

The particle size ratio ($D_{\text{fine}}/D_{\text{carrier}}$) also plays an important role for the forces on the fines and eventually the detachment probability. When increasing the fine particle size from $5\ \mu\text{m}$ to $10\ \mu\text{m}$, the absolute values of the normal force increase remarkably (Fig. 17). The reason is that the fluid dynamic force is related to the cross section area of the particle. When the diameter of fine particle doubles, then the value of fluid dynamic force increases four times. However, in practice drug particle of $10\ \mu\text{m}$ are not suitable, since they will not reach the alveoli of the lung as they deposit before due to inertia.

Finally, also simulations with a shear flow were realized. For that purpose the upper and lower boundaries of the flow domain were considered as a solid wall with no-slip conditions (see Fig. 11). In order to obtain relatively high shear rates and a certain stream-wise (i.e. to the right) gas velocity on the carrier centre the upper wall was moved to the right with a higher velocity than the lower wall being moved to the left. The conditions considered yielded a Reynolds number of 70 and a shear rate of $100,962\ \text{s}^{-1}$. This was actually the highest shear rate which could be realized in the simulations. The comparison of the normal force on the drug particles in dependence of the position angle for the case with plug and shear flow is shown in Fig. 18 together with the resulting flow structure about the particle cluster. It should be noted that the

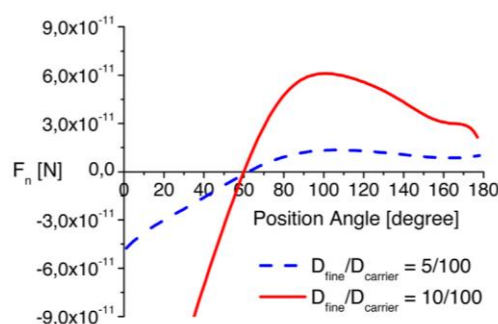


Fig. 17. Fitting curves for the normal force on the fine particles as a function of position angle for different size ratios ($Re = 16$, coverage degree 50%).

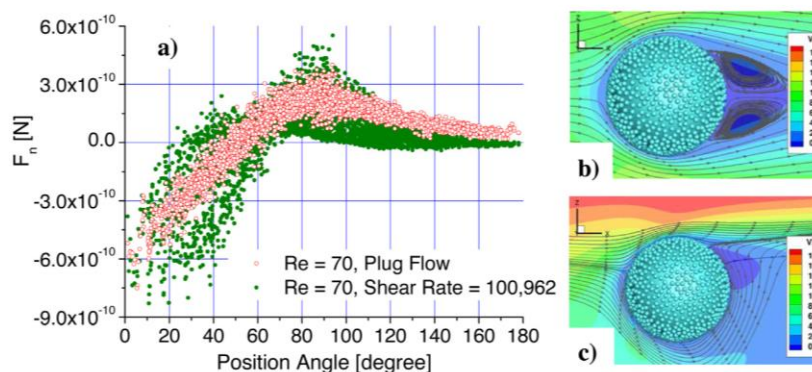


Fig. 18. Comparison of plug and shear flow about the particle cluster at identical Reynolds number ($Re = 70$); (a) normal forces in dependence of the position angle; (b) flow structure for the plug flow; (c) flow structure for the shear flow (coverage degree 50%, $D_{fine}/D_{carrier} = 5/100$).

shear flow across the cluster is not axi-symmetric. Therefore, the normal forces on the drug particles on the front side of the carrier (i.e. up to an angle of about 50°) show a large scatter. The maximum forces appearing at a position angle of about $80\text{--}90^\circ$ are almost identical with those obtained for the plug flow. The wake region behind the cluster has almost disappeared under shear flow conditions and the flow is mainly going upward around the cluster. This yields a normal force which is even smaller than in the plug flow case. Consequently a shear flow is not more effective for the detachment of the drug particles from the carrier.

7. AFM adhesion force measurements

For allowing the calculation of the detachment possibility from the simulated fluid dynamic forces, it is necessary to know adhesion forces and particle–particle interaction parameters, which were determined experimentally. To overcome the experimental complexities glass bead carrier particles with a diameter of around $500\ \mu\text{m}$ were used instead of the $100\ \mu\text{m}$ particles considered in the simulations with LBM. Since the adhesion force is mainly governed by the API particle diameter and the surface structure the difference for the two particle sizes is not very large. An estimate of the adhesion force based on Hamaker for the $100\ \mu\text{m}$ particles yielded a value of $151.7\ \text{nN}$ and for the $500\ \mu\text{m}$

particles an adhesion force of $155.2\ \text{nN}$ was obtained for an API diameter of $3\ \mu\text{m}$.

Consequently, glass beads (SiLibeads[®] Glass Beads Type S) in the size range between $400\ \mu\text{m}$ and $600\ \mu\text{m}$ (median diameters: $x_{50} = 537.3\ \mu\text{m} \pm 7.1\ \mu\text{m}$), kindly provided by Sigmund Linder GmbH, Germany, were used as model carrier either untreated (Fig. 19a) or physically modified (Fig. 19b and c). Physical modification has been performed by treating the glass beads in a ball mill (Ball Mill S2, Retsch, Haan, Germany) using different grinding materials (quartz (Q), Mohs hardness 7, $x_{50} = 32.17\ \mu\text{m}$ and tungsten carbide (TC) Mohs hardness 9.5, $x_{50} = 23.58\ \mu\text{m}$) and treatment durations (4 h for quartz and 8 h for tungsten carbide treatment) as described by Zellnitz et al. (2013).

Salbutamol sulphate (USP25 quality) was provided by Selectchemie (Zuerich, Switzerland) and served as model API. The API was spray-dried using a Nano Spray Dryer B-90 (Buechi Labortechnik AG, Flawil, Switzerland) equipped with the long version of the drying chamber. To form particles in the size range of $1\ \mu\text{m}$ – $5\ \mu\text{m}$ (characteristic diameters: $x_{10} = 0.45\ \mu\text{m}$, $x_{50} = 3.07\ \mu\text{m}$ and $x_{90} = 6.73\ \mu\text{m}$) a spray-head mesh of $7\ \mu\text{m}$ was chosen and a feed concentration of 7.5% (i.e. solids mass over liquid mass). The flow rate was set to $100\ \text{l/min}$ and the spraying intensity was set to 30%. Aqueous salbutamol sulphate solutions used for spray drying were prepared with purified water (TKA

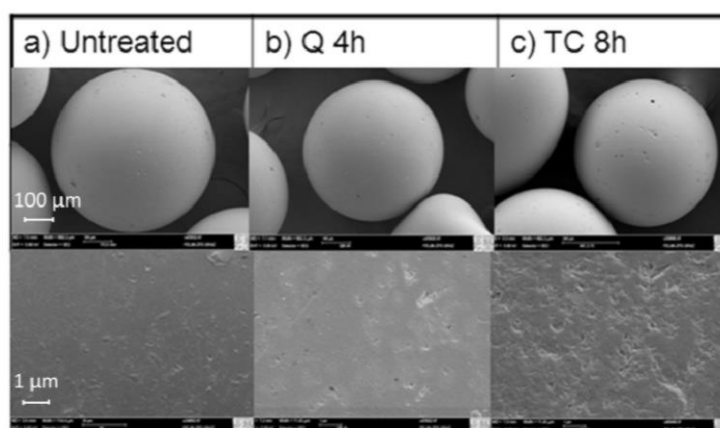


Fig. 19. Scanning electron micrographs of (a) untreated glass beads (b) glass beads treated with quartz for 4 h and (c) treated with tungsten carbide for 8 h (Ultra 55, Zeiss, operating at 5 kV, samples gold palladium sputtered; upper images: image width of $882.2\ \mu\text{m}$, lower images: image width of $11.43\ \mu\text{m}$).

Micro Pure UV ultrapure water system, TKA Wasseraufbereitungs-systeme GmbH, Niederelbert, Germany) equipped with a capsule filter (0.2 μm).

Atomic force microscopy (VEECO, Dimension, Nanoscope IIIa, Bruker AXS GmbH, Karlsruhe/Germany) operated in contact mode was used to determine the adhesion force between glass beads and spray dried salbutamol sulphate particles. The untreated and surface modified rough glass beads were glued on commercially available glass slides with a two component epoxy resin adhesive (UHU GmbH & Co. KG, Buehl/Baden/Germany). The colloidal probes were prepared by attaching the 3 μm sized salbutamol sulphate particles on the tip of a tipless AFM cantilever (NSC 12/tipless/no Al, NT-MDT Anatec Instruments AG, Oelsnitz/Germany) with the help of a micro-manipulator (3D oil-hydraulic manipulator MMO-203, Narishige Group, Tokyo, Japan). Therefore, the particles were spread on a glass slide and attached to the cantilever tip by moving the cantilever towards a particle with the micro-manipulator and collecting it from the glass slide with the help of the adhesive that has been attached to the cantilever tip before.

The imaging scan rate was 1 Hz and the scan size was 5 $\mu\text{m} \times 5 \mu\text{m}$. The scan area was divided into a grid of 25 equidistant points and on each point 50 force curves were taken. Thus 1250 force curves were acquired on each glass bead (25 points in the scan size and 50 force curves on each point). For each glass bead/API combination a mean adhesion force was calculated out of the 1250 force curves. This procedure was repeated three times using a new pair of API and glass bead every time. Finally a mean value was calculated out of the three means obtained for the adhesion force between the three different salbutamol sulphate particles and the corresponding glass beads. Extraction of adhesion force data from the AFM force spectroscopy raw data was carried out with automated routines written in LabView.

Table 2 shows that the adhesion force between surface modified glass beads and salbutamol sulphate is remarkably lower than the adhesion force between untreated glass beads and salbutamol sulphate. This can be explained by the rougher surfaces of the modified glass beads. When introducing surface roughness the contact area between the glass beads and the salbutamol sulphate particle is reduced and hence also the adhesion force between them. Glass beads modified with tungsten carbide for 8 h are rougher than glass beads modified with quartz for 4 h (see Fig. 19), and consequently the adhesion force between glass beads modified with tungsten carbide for 8 h and salbutamol sulphate is also lower (Fig. 20).

8. Measurement of friction coefficients

The wall friction angle (WFA) of untreated and physically modified glass beads was determined using a FT4 Powder Rheometer System (Freeman Technology, Gloucestershire/United Kingdom). From the friction angles the friction coefficients were calculated (friction coefficient = \tan WFA) for untreated and modified glass beads.

Table 2

Measured adhesion forces via AFM (mean of $n = 3 \pm \text{SD}$), wall friction angle (mean of $n = 3 \pm \text{SD}$) and adhesion surface energy for untreated and modified glass beads (mean of $n = 20 \pm \text{SD}$).

	Adhesion force [nN]	Friction angle [°]	Friction coefficient [-]	Surface energy [mJ/m ²]
Untreated	257.48 \pm 59.67	4.49 \pm 0.19	0.079 \pm 0.003	53.36 \pm 7.94
Q 4 h	127.83 \pm 28.23	4.79 \pm 0.34	0.084 \pm 0.006	73.68 \pm 5.61
TC 8 h	62.48 \pm 52.96	6.34 \pm 0.36	0.111 \pm 0.0063	65.76 \pm 2.99

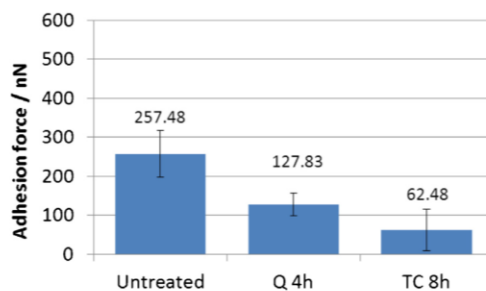


Fig. 20. Bar chart of adhesion forces measured via AFM for untreated and modified glass beads (mean of $n = 3 \pm \text{SD}$).

Results in Table 2 show that untreated glass beads exhibit the lowest friction coefficient and friction angle and glass beads modified with TC for 8 h the highest. The friction coefficient and friction angle for glass beads modified with Q for 4 h are in between. According to these results there is an increase in friction angle and friction coefficient with increasing surface roughness of the glass beads.

9. Surface energy measurements

The surface energy of untreated and physically modified glass beads was calculated from the static contact angles of water and α -bromonaphthalene based on the method of Owens–Wendt–Rabel–Kaelble (OWRK). Experiments were conducted at room temperature on an OCA 20 contact angle meter (DataPhysics Instruments GmbH, Filderstadt/Germany) with SCA 20 software. The instrument was coupled with a USB CCD-camera (maximum imaging rate 123 images/s). The water drop applied was $< 1 \mu\text{l}$ and generated manually. For each glass bead modification the contact angle was determined on 20 glass beads and the mean contact angle was calculated.

Table 2 shows that the surface energy of untreated glass beads is lower compared to the surface energy of physically modified rough glass beads. For physically modified glass beads there is a significant difference between the surface energy of glass beads treated with Q for 4 h and TC for 8 h but no significant trend could be observed. This can be explained by the surface roughness of physically modified glass beads, since surface roughness/irregularities largely affect the contact angle determination of water and thus the results of the surface energy measurement.

10. Particle detachment probability

For the detachment of the drug particles from the carrier through the fluid stresses (normal and tangential force) the adhesion force (van der Waals) and the friction force have to be overcome. There exist three possible ways of detachment (Ibrahim et al., 2003), which are based on the following conditions (see also Fig. 12):

Lift-off:

$$F_n > F_{vdw} \quad (4)$$

Sliding (Coulomb's law of friction):

$$F_t > \mu(F_{vdw} - F_n) \quad (5)$$

Rolling (momentum balance):

$$0.685D_{fine}F_t + aF_n > aF_{vdw} \quad (6)$$

here the factor of 0.685 comes from the effective point of attack of the tangential fluid force (Fig. 21) as shown by O'Neill, (1968).

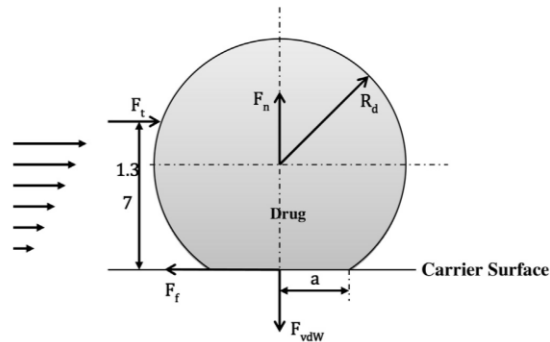


Fig. 21. Spherical particle deposited on a plane wall with contact area and relevant forces.

When two particles or a particle with a plane surface are in contact a finite circular contact area with the radius a develops (i.e. ideally for perfectly smooth objects). The size of this contact area is depending on the effective normal force (i.e. $P = F_{vdW} - F_n$) and the adhesion properties which are material dependent and are summarised in the composite Young's modulus K . Moreover, the contact radius depends for two particles in contact on the effective radius R .

$$a = \left(\frac{R}{K} (P + 3\pi\gamma R + \sqrt{6\pi\gamma RP + (3\pi\gamma R)^2}) \right)^{1/3} \quad (7)$$

$$K = \frac{4}{3} \left[\frac{1 - \sigma_{fine}^2}{E_{fine}} + \frac{1 - \sigma_{carrier}^2}{E_{carrier}} \right]^{-1} \quad (8)$$

$$R = \frac{D_{carrier} D_{fine}}{2(D_{carrier} + D_{fine})} \quad (9)$$

where γ is surface energy of adhesion, E_{fine} and $E_{carrier}$ are the values of Young's modulus and σ_{fine} and $\sigma_{carrier}$ are the values of Poisson's ratio for the drug and carrier particle, respectively.

As the LBM simulations showed, the maximum normal fluid dynamic force (see e.g. Fig. 15) is very small even at the highest Reynolds number, so that lift-off is not likely to occur when comparing it with the measured F_{vdW} for all kinds of considered particles (Table 2), i. e. untreated and surface modified. As a result detachment may only occur through sliding or rolling (see Eqs. (5) and (6)). According to the simulated fluid dynamic forces (i.e. F_n and F_t) for the different conditions the possibility of detachment through sliding or rolling for all the drug particles on the carrier was evaluated. The determination of the detachment probability for the three particle types with different surface structure (see Fig. 19) was based on the measured adhesion force, friction coefficient and adhesion surface energy (see Table 2). The other properties of the drug and carrier particle needed for this calculation are summarised in Table 3. The number of detached particles according to Eqs. (5) or (6) was then divided by the total number of the drug particles attached to the carrier. This

Table 3
Material property for drug and carrier particles used in the simulations.

	Fine drug particle	Carrier particle
Diameter	5 μm	100 μm
Density	1290 kg/m^3	2500 kg/m^3
Young's modulus	2.15 GPa	63 GPa
Poisson ratio	0.3 [–]	0.24 [–]

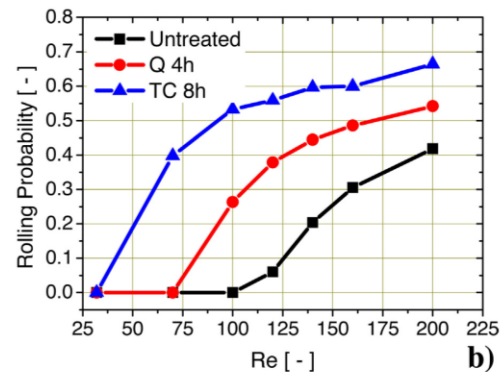
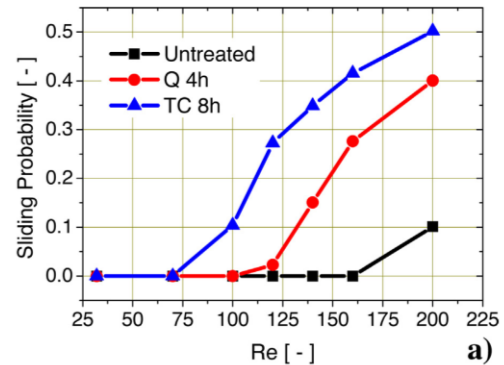


Fig. 22. Fraction of fine drug particles being detached from the carrier by sliding (a) or rolling (b) as a function of Reynolds number for different surface roughness of the carrier particle according to Table 2 (coverage degree 10%, $D_{fine}/D_{carrier} = 5/100$).

calculation was done for the 4 (25 and 50% degree of coverage) or 8 (10% degree of coverage) simulations done for the same flow conditions, but with different random distribution of the drug particles. The final result was plotted versus the Reynolds number (Fig. 22). All the curves have a typical shape, known from the re-suspension rate of small particles from plane walls, when shear rate is increased (Phares et al., 2000; Zhang et al., 2010; Goldasteh et al., 2013). For low Re the detachment probability is zero, then begins to increase at a certain critical Re-number and approaches at higher Re some limiting value. Rolling detachment always occurs at lower critical Reynolds numbers. Of course when increasing the surface roughness the adhesion force is decreasing and the detachment probability rises. For the carrier particles treated for 8 h with tungsten carbide (TC) the detachment probability is larger than 60% for Re=200. For the interpretation of these results it should be kept in mind that the detachment probability was calculated for one fixed orientation of the cluster with respect to the oncoming flow and one fixed flow velocity. In reality the instantaneous relative flow velocity will strongly vary along the trajectory of the cluster through the inhaler and also the cluster might rotate due to shear flow interaction and wall collisions. Finally also the influence of the degree of coverage on the rolling detachment probability was calculated. In accordance with the result in Fig. 16, the detachment probability increases remarkably when decreasing the degree of coverage (Fig. 23). This is the result of the higher fluid dynamic forces on the drug particles for a sparse coverage, since the flow goes more likely around the entire drug particles.

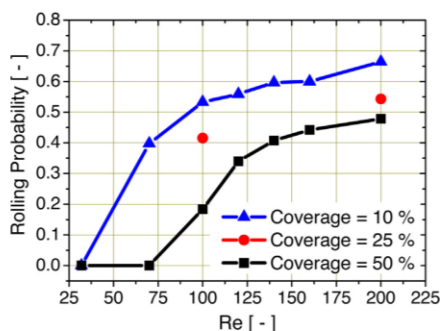


Fig. 23. Fraction of fine drug particles being detached from the carrier by rolling as a function of Reynolds number for different coverage degree (surface treatment: TC 8 h, $D_{\text{fine}}/D_{\text{carrier}} = 5/100$).

11. Summary and Conclusions

The fluid stresses acting on a particle cluster (including carrier particle and drug powder) during its way through an inhaler were statistically analysed based on CFD (computational fluid dynamics) using a RANS approach. This information will be the basis to estimate the drug particle detachment probability. Both an inhaler without and with grid are calculated and compared for a fixed stationary flow rate of 70 l/min. The grid mounted at the entrance to the mouthpiece (geometry used in practice) removed the swirl to a large extent and provoked that the particles reside for a long time in the swirl chamber. Without grid, swirl exists throughout the mouthpiece and quite a number of carrier particles leave the inhaler. The instantaneous relative velocities, the shear rates and the turbulence intensities experienced by the carrier particles are not remarkably different in both geometries. With grid the distribution of the instantaneous relative velocity is bi-modal with maxima at 10 m/s and 30 m/s (i.e. $Re = 70$ and 200) and without grid the distribution shows a flat plateau between 15 and 30 m/s. The turbulence intensity experienced by the particles is somewhat higher in configuration without grid and reaches values up to about 30%. Hence, the grid is very effective in keeping the carrier particles for a long time in the swirl chamber where they experience the largest flow stresses yielding an effective detachment of the drug powder.

The question is now; how large is the detachment rate of the fine drug particles from the surface of the carrier. For estimating this important attribute, fully resolved LBM simulations were performed for a cluster consisting of a carrier particle covered with hundreds of micron-sized drug particles. This cluster was exposed to laminar plug and shear flow and the fluid forces acting on the drug particles were calculated in dependence of their location on the carrier surface. Only a normal force pointing away from the carrier might yield a lift-off of the drug particle. The maximum normal force, which was found at an angle of about 80° from the front stagnation point, was found to be only 2 nN even for a Reynolds number of 200 (slip velocity about 30 m/s).

The detachment of the drug particles might occur through lift-off, sliding and rolling. For calculating these possibilities from the simulated flow forces the opposing particle–particle interaction forces are required together with some material properties. For achieving high detachment rates, the adhesion force (i.e. van de Waals force) may be adapted to the fluid forces by surface treatment of the carrier glass beads. This was the main objective in the present study. Therefore, untreated glass beads and glass beads with two ways of surface treatment, yielding different surface roughness,

were considered. For these carrier particles the adhesion force, wall friction coefficient and adhesion surface energy were measured. It was clearly shown, that the adhesion force may be distinctively reduced by increasing the surface roughness.

Even for the roughest carrier surface the measured adhesion force was about 60 nN which is much larger than the calculated maximum normal fluid force of 2 nN at a typical Reynolds number of 200; wherefore drug particle lift-off never can occur. The sliding and rolling detachment probabilities calculated with the simulated fluid forces and the measured particle–particle interaction properties clearly show that rolling detachment occurs at lower Reynolds numbers than sliding detachment. Consequently, rolling detachment has a higher probability than sliding detachment for all considered types of carrier particles. As to be expected, the highest detachment probabilities are achieved for the treated carrier glass beads TC 8 h having the largest roughness. For Reynolds numbers beyond 125 the rolling detachment probability reaches already 60%. When increasing the degree of drug powder coverage, the detachment probability is reduced as a consequence of the decreasing fluid forces.

With all the information from the LBM simulations and the measurements it is now possible to develop a detachment model which will be used in the frame of Euler/Lagrange calculations for optimising inhaler devices with low pressure drop and high application efficiency.

Acknowledgements

The authors acknowledge the financial support of this research project by the Deutsche Forschungsgemeinschaft (DFG), Germany in the frame of the priority research programme SPP 1486 (PiKo) under contract No. SO 204/38-1 and 2 as well as UR 214/3-2. Furthermore, the generous support of the numerical developments of the LBM code by Mr. M. Ernst and M. Dietzel is gratefully acknowledged. The authors also would like to thank the research groups of Prof. Butt and Dr. Kappel, Max Plank Institute for Polymer Research Mainz, for the provision of the AFM equipment and assisting with the AFM measurements.

References

- Bhatnagar, P.L., Gross, E.P., Krook, M., 1954. A model for collision processes in gases. I. Small amplitude processes in charged and neutral one-component systems. *Phys. Rev.* 94, 511–525.
- Bouzidi, M., Firdaouss, M., Lallemand, P., 2001. Momentum transfer of a Boltzmann–Lattice fluid with boundaries. *Phys. Fluids* 13, 3452–3459.
- Chew, N.Y.K., Chan, H.-K., Bagster, D.F., Mukhraiya, J., 2002. Characterization of pharmaceutical powder inhalers: estimation of energy input for powder dispersion and effect of capsule device configuration. *J. Aerosol Sci.* 33, 999–1008.
- Coates, M.S., Fletcher, D.F., Chan, H.-K., Raper, J.A., 2004. Effect of design on the performance of a dry powder inhaler using computational fluid dynamics. Part 1: grid structure and mouthpiece length. *J. Pharm. Sci.* 93, 2863–2876.
- Coates, M.S., Chan, H.-K., Fletcher, D.F., Chiou, H., 2007. Influence of mouthpiece geometry on the aerosol delivery performance of a dry powder inhaler. *Pharm. Res.* 24, 1450–1456.
- Crouse, B., 2003. Lattice–Boltzmann strömungssimulationen auf baumdatenstrukturen. Dissertation. Technische Universität München.
- Cui, Y., Schmalfuß, S., Sommerfeld, M., 2013. On the detachment of fine drug powder from carrier particles within an inhaler device CD-ROM. Proceedings 8th International Conference on Multiphase Flow/ICMF 2013, Jeju, Korea, May 26–May 31 Paper No. 438.
- de Koning, J.P., 2001. Dry powder inhalation: technical and physiological aspects, prescribing and use. PhD Thesis, University of Groningen.
- Dietzel, M., Sommerfeld, M., 2010. LBM simulations on agglomerate transport and deposition. *AIP Conf. Proc.* 1207, 796–801.
- Dietzel, M., Sommerfeld, M., 2013. Numerical calculation of flow resistance for agglomerates with different morphology by the Lattice–Boltzmann method. *Powder Tech.* Vol. 250, 122–137.
- Dietzel, M., Ernst, M., Sommerfeld, M., 2011. Application of the Lattice–Boltzmann method in two-phase flow studies: from point-particles to fully resolved particles. Proceedings of the ASME-JSME-KSME Joint Fluids Engineering Conference Hamamatsu, Shizuoka, Japan, July 2011 Paper No. AJK 2011-04033.

- Donovan, M.J., Kim, S.H., Raman, V., Smyth, H.D., 2011. Dry powder inhaler device influence on carrier particle performance. *J. Pharm. Sci.* . doi:10.1002/jps.
- Ernst, M., Dietzel, M., Sommerfeld, M., 2013. Simulation of the sedimentation and agglomeration of resolved particles. *Acta Mech.* Vol. 224, 2425–2449.
- Goldasteh, I., Ahmadi, G., Ferro, A.R., 2013. Monte Carlo simulation of micron size spherical particle removal and resuspension from substrate under fluid flows. *J. Aerosol Sci.* Vol. 66, 62–71.
- Guo, Z., Zheng, C., Shi, B., 2002. An extrapolation method for boundary conditions in Lattice-Boltzmann method. *Phys. Fluids* 14, .
- Ibrahim, A.H., Dunn, P.F., Brach, R.M., 2003. Microparticle detachment from surfaces exposed to turbulent air flow: controlled experiments and modeling. *J. Aerosol Sci.* 34, 765–782.
- Islam, N., Gladki, E., 2008. Dry powder inhalers (DPIs) – a review of device reliability and innovation. *Int. J. Pharm.* 360, 1–11.
- Newman, S.P., Busse, W.W., 2002. Evolution of dry powder inhaler design, formulation and performance. *Respir. Med.* 96, 293–304.
- O'Neill, M.E., 1968. A Sphere in contact with a plane wall in a slow linear shear flow. *Chem. Eng. Sci.* Vol. 23, 1293–1298.
- Phares, D.J., Smedley, G.T., Flagan, R.C., 2000. Effect of particle size and material properties on aerodynamic resuspension from surfaces. *J. Aerosol Sci.* Vol. 31, 1335–1353.
- Smith, I.J., Parry-Billings, M., 2003. The inhalers of the future? A review of dry powder devices on the market today. *Pulm. Pharmacol. Therapeut.* 16, 79–95.
- Sommerfeld, M., van Wachem, B., Oliemans, R., 2008. Best Practice Guidelines for Computational Fluid Dynamics of Dispersed Multiphase Flows. ERCOFTAC (European Research Community on Flow, Turbulence and Combustion ISBN 978-91-633-3564-8 978–991.
- Srichana, T., Martin, G.P., Marriott, C., 1998. Dry powder inhalers: the influence of device resistance and powder formulation on drug and lactose deposition in vitro. *Eur. J. Pharm. Sci.* 7, 73–80.
- Steckel, H., Müller, B.W., 1997. In vitro evaluation of dry powder inhalers I: drug deposition of commonly used devices. *Int. J. Pharm.* 154, 19–29.
- Telko, M.J., Hickey, A.J., 2005. Dry powder inhaler formulation. *Respir. Care* 50, 1209–1227.
- Zellnitz, S., Redlinger-Pohn, J.D., Schröttner, H., Urbanetz, N.A., 2011. Improving the performance of dry powder inhalers by tailoring interparticle interactions. *Drug Delivery to the Lung (DDL22)* Edinburgh.
- Zellnitz, S., Redlinger-Pohn, J.D., Schroettner, H., Kappl, M., Urbanetz, N.A., 2013. Preparation and characterization of physically modified glass beads used as model carriers in dry powder inhalers. *Int. J. Pharm.* 447, 132–138.
- Zhang, F., Kissane, M., Reeks, M., 2010. Particle resuspension modelling in turbulent flow. 7th Int. Conf. on Multiphase Flow/CMF 2010, Tampa, FL USA, 30 May–4 June.

8

Summary

In order to improve the performance of DPIs, the present thesis proposes surface engineering of glass beads as model carrier for DPIs. These surface modified glass beads should help to tailor interparticle interactions in DPI formulations, which on the one hand means, drug adhesion on the carrier surface for handling, dosing and transport, and on the other hand, drug detachment of the model API particles, spray dried salbutamol sulphate, from the carrier during inhalation. As the adhesion forces between the drug and the carrier largely depend on the surface chemistry of the interacting particles as well as on the contact area between drug and carrier, and as the contact area in turn depends on the surface roughness of the interacting partners, surface engineering might be an appropriate means to impact adhesion forces between the drug and the carrier in DPIs and thus the performance of DPIs.

This thesis showed that the surface roughness of glass beads, intended for the use as carrier in dry powder inhalers, can be successfully modified. Mechanical treatment in a ball mill with quartz and tungsten carbide as grinding materials and grinding times of 4 hours and 8 hours led to surfaces with roughnesses in the nanometer scale. Depending on the hardness of the grinding material and the grinding time the surface roughness was more or less pronounced. Nevertheless, surface modification did not change the particle size and shape of the glass beads, ensuring that interparticle interactions were impacted by surface roughness modification only and not influenced by other changes like size and shape. For characterizing the changes of surface topography that have been generated by the ball mill processing, the surface roughness determination via atomic force microscopy (AFM) and the determination of the specific surface area via gas adsorption have proven to be suitable.

Additionally performed plasma etching studies showed that mechanical surface processing of the glass beads by plasma for 1min led to glass bead surfaces

that showed a higher specific surface area and a higher surface roughness than the glass beads processed in a ball mill.

As besides surface topography also surface chemistry influences interparticle interactions, also chemical surface modification was performed. Studies on chemical surface modification showed that by treating glass beads with different silanes, hydrophobic glass beads could be prepared.

Studies on the FPF of mixtures with spray dried salbutamol sulphate and surface modified glass beads using the same surface coverage of API ($30\% \pm 5\%$) showed that surface modified glass beads lead to slightly higher FPFs compared to untreated glass beads. The model API, salbutamol sulphate, was spray dried, because spray dried particles exhibit a spherical shape ensuring that interparticle interactions and thus drug detachment are independent from the orientation of the API particle on the carrier surface and thereby independent from the shape of the API particle. The increase in FPF for physically modified glass beads was attributed to the introduced surface roughnesses on the surface of modified glass beads. Due to these roughnesses the contact area between API and carrier decreases and further interparticle interactions were decreased. Consequently, drug detachment was facilitated and the FPF increased. The evaluation of surface characteristics of physically modified glass beads on the FPF showed that there is a quite good correlation between surface roughness and FPF. It was concluded that the higher the surface roughness of the carrier particles the higher is the FPF. Additionally, it was possible to demonstrate that drug detachment from surface modified glass beads is more reproducible than from untreated glass beads. This was indicated by lower standard deviations for the FPFs delivered from surface modified glass beads and attributed to the irregular, non-standardized surface roughness of untreated glass beads.

Investigations of the FPF delivered from chemically modified glass beads showed that the FPF for chemically modified glass beads is significantly lower compared to the FPF for untreated and physically modified glass beads of the same surface coverage. This was explained by the formation of API clusters on the surface of chemically modified glass beads. It is claimed that these clusters were formed as a result of rather strong cohesion forces between

salbutamol sulphate particles, which exceeded the adhesion forces between salbutamol sulphate particles and chemically modified glass beads. As a result API particles were detached as particle agglomerates instead of single particles. API particles trapped in these agglomerates impacted in the upper airways and were not able to reach the deep lung, which was also reflected in the low FPFs of chemically modified glass beads.

Studies on the influence of surface coverage on the FPF revealed that higher surface coverages also led to higher FPFs as more API particles were present on the glass beads surface. Plots of the FPF versus the surface coverage however showed that the slope of the resulting lines differed from each other depending on the carrier material used. This was attributed to the energy distribution of sites of contact between the API and the carrier that is different and individual for each carrier modification and thus each carrier type. Summing up, these findings exposed that when studying the performance of DPIs, the surface coverage has to be taken into account. This is especially true as the amount of API that is used for preparing the API carrier mixtures does not necessarily equal the amount of API adhering on the carrier surface because of API losses on the walls of mixing vessels or inhaler walls during mixing, handling and dosing. So the true surface coverage can differ notably from the targeted calculated surface coverage.

Besides statistical analysis of the fluid stresses acting on fine particles attached to a carrier particle during their way through the inhaler based on CFD (macro simulation) the determination of the detachment rate of the fine drug particles from the surface of one carrier (micro simulations) was described. For the simulation of the detachment rate that might occur through sliding, lift-off or rolling, the opposing particle-particle interactions and some material properties (friction coefficient and surface energy) were needed. The measurements of particle - particle, here glass bead - salbutamol sulphate interactions were performed via atomic force microscopy (AFM) and showed that the adhesion force between the two particles could be reduced by the use of surface modified rough carrier particles. This was attributed to the reduced contact area between the glass beads and salbutamol sulphate particles, which goes together with the introduction of surface roughnesses on the glass

beads surfaces. Reduced contact areas consequently led to lower interparticle interactions.

Numerical studies of particle detachment via sliding, lift-off and rolling revealed that lift-off can never occur and that rolling detachment has a higher probability than sliding detachment for all the differently modified carrier particles tested. Results of these calculations also showed that the highest detachment probability was reached for glass beads treated with tungsten carbide for 8h. Glass beads treated with tungsten carbide for 8h were the roughest carrier particles tested in this study and showed also the lowest adhesion force to salbutamol sulphate among all carrier particles tested. Thus, these results prove that by carrier surface modification interparticle interactions and consequently drug detachment from the carrier can be tailored as glass beads treated with tungsten carbide for 8h also show the highest FPF among all ball mill treated glass beads.

9

Conclusion and outlook

The fact that physical surface modification leads to glass beads with different shades of roughness and that the surface roughness can be correlated with the in vitro respirable fraction (FPF), make glass beads an ideal carrier for tailoring the performance of DPIs in the therapy of asthma and chronically obstructive pulmonary diseases. The higher the introduced surface roughness the lower is the adhesion force between carrier and salbutamol sulphate. Consequently drug detachment is facilitated and the corresponding in vitro respirable fraction is increased.

With respect to chemical surface modification, the FPF for chemically modified glass beads decreases compared to untreated glass beads. It is proposed that the adhesion force between chemically modified glass beads and salbutamol sulphate is weaker than the cohesion force between the API particles. However, this does not increase the FPF, but decreases it, as salbutamol sulphate particles are not detached as single particles but as particle agglomerates instead. API particles are trapped in these agglomerates, impact in the upper airways and thus are not able to reach the deep lung, which is reflected in the low FPFs of formulations containing chemically modified glass beads. To allow a correlation between surface chemistry and the in vitro respirable fraction certainly further studies are required to test drug detachment from chemically modified glass beads with different shades of chemical surface modification. This means an ascending or descending sequence of surface hydrophobicities or/and surface energies.

Moreover it would be beneficial to check whether the correlations found in this study are still true when other API particles or different inhaler geometries are used. The purpose of the study in collaboration with the research group of Prof. Sommerfeld was therefore to develop a drug detachment model that can finally be used to optimise and design new efficient inhaler geometries. The implementation of the results for the detachment probability of a single particle

(micro simulations) into the macro-scale simulations is part of future work. Based on this, finally a drug detachment model for Lagrangian calculation of the entire device using OpenFOAM1 will be developed. The resulting detachment model will be validated based on in vitro respirable fraction (FPF) data obtained from impactor experiments. The final goal would be the development of a platform, so that on the one hand, when knowing the inhaler geometry and the API, the appropriate or ideal carrier for the formulation can be selected, or on the other hand the most suitable inhaler geometry for a given carrier - API mixture can be selected to achieve highest lung deposition. This platform should help to bring the development of formulations used in DPIs on a scientific level.

10

Appendix

10.1 Curriculum vitae

Sarah Zellnitz

Born on June 27th 1985, Deutschlandsberg, Austria

Austrian citizen

Phone: +43 650 6486631

E-Mail: sarah.zellnitz@rcpe.at

EDUCATION

Since 07/2010	Doctoral Program in Natural Science Graz University of Technology, Graz, Austria Thesis: Glass beads as model carrier in dry powder inhaler Supervisor: Prof. Nora A. Urbanetz
30/09/2009	obtaining the Austrian pharmacist's diploma
10/2008 – 09/2009	Aspirant Pharmacy Zur St. Anna, Graz, Austria
10/2003 – 06/2008	Diploma study Pharmacy University of Graz, Austria With distinction Thesis: Formol releasing agents and their relation to allergic contact dermatitis Supervisor: Prof. Reinhold Wintersteiger
09/2007 – 03/2008	Studies via the Erasmus exchange program Université of Montpellier ¹ , Institute of Toxicology, France
09/1995 – 06/2003	Gymnasium St. Veit/Glan School leaving examination, with distinction

PROFESSIONAL EXPERIENCE

Since 07/2012	Research Center Pharmaceutical Engineering GmbH Researcher (Area II, Products and Formulations)
07/2010 – 06/2012	Graz University of Technology, Institute for Process and Particle Engineering Project manager of the DFG (German research foundation) program SPP 1486 “Partikel im Kontakt“
12/2009 – 03/2010	Edelweiß Pharmacy, Schladming, Austria Pharmacist
10/2008 – 09/2009	Pharmacy/Apotheke zur St. Anna, Graz, Austria Aspirant
07/2007	Pharmacy/Baerenapotheke, St.Veit/Glan, Austria Internship
07/2006	Pharmacy/Baerenapotheke, St.Veit/Glan, Austria Internship
07/2005	Pharmacy/Baerenapotheke, St.Veit/Glan, Austria Internship
07/2004	Pharmacy/Baerenapotheke, St.Veit/Glan, Austria Internship
08/2003	Kaerntner Sparkasse, St. Veit /Glan, Austria Internship

DISTINCTIONS

09/2011	Lesmueller Posterpreis at the Joint Meeting of the Austrian and German Pharmaceutical Societies (oedphg 2011, Innsbruck, Austria)
---------	---

10.2 List of publications

10.2.1 Research papers

Zellnitz S., Redlinger-Pohn J.D., Schroettner H., Kappl M., Urbanetz N.A., Preparation and characterization of physically modified glass beads used as model carriers in dry powder inhalers. *International Journal of Pharmaceutics*, 2013, 447, 132-138

Littringer E.M., **Zellnitz S.** Hammernik K., Adamer V., Friedl H., Urbanetz N.A., Spray drying of aqueous salbutamol sulfate solutions using the Nano Spray Dryer B-90 – The impact of process parameters on particle size. *Drying Technology*, 2013, 31, 1346–1353

Cui Y., Schmalfuß S., **Zellnitz S.**, Sommerfeld M., Urbanetz N.A., Towards the optimisation and adaptation of dry powder inhalers. *International Journal of Pharmaceutics*, 2014 in press

Zellnitz S., Schroettner H., Urbanetz N.A., Influence of surface coverage on the fine particle fraction: investigating surface modified glass beads as model carriers in dry powder inhalers. *Powder Technology*, submitted for publication

Zellnitz S., Schroettner H., Urbanetz N.A., Influence of surface characteristics of modified glass beads as model carriers in dry powder inhalers (DPIs) on the aerosolization performance. *Drug Development and Industrial Pharmacy*, submitted for publication

10.2.2 Application notes

Zellnitz S., Redlinger-Pohn J.D., Urbanetz N.A., Characterization of physically modified glass beads as potential model carriers in DPIs. *The microReport from Micromeritics Instrument Corporation*, 2013, online

10.2.3 Conference proceedings

Zellnitz S., Redlinger-Pohn J.D., Schroettner H., Urbanetz, N.A.: Enhancing the performance of dry powder inhalers by tailoring Interparticle forces via surface modification of carrier and active. – in: *Conference Proceedings, Joint Meeting of the Austrian and German Pharmaceutical Societies*. Innsbruck, 09.2011, 281

Zellnitz S., Redlinger-Pohn J.D., Schroettner H., Urbanetz, N.A.: The importance of interparticle interactions for the performance of dry powder inhalers. – in: *Conference Proceedings, 8th European Congress of Chemical Engineering*. Berlin, 09.2011

Zellnitz S., Redlinger-Pohn J.D., Schroettner H., Urbanetz, N.A.: Tailoring interparticle interactions to improve the performance of dry powder inhalers. – in: *Conference Proceedings, International Congress of Pharmaceutical Engineering*. Graz, 09.2011, 10-11

Zellnitz S., Redlinger-Pohn J.D., Schroettner H., Urbanetz, N.A.: Improving the performance of dry powder inhalers by tailoring interparticle interactions. – in: Conference Proceedings, Drug Delivery to the Lungs 22. Edinburgh, 12.2011, 205-208

Zellnitz S., Schroettner H., Urbanetz, N.A.: Chemical surface modification of glass beads used as model carriers for dry powder inhalates. – in: Conference Proceedings, 8th World Meeting on Pharmaceutics, Biopharmaceutics and Pharmaceutical Technology. Istanbul, 03.2012

Redlinger-Pohn J.D., **Zellnitz S.**, Schroettner H., Urbanetz, N.A.: Mechanically treated glass beads as surface modified carrier particles for dry powder inhalates. – in: Conference Proceedings, 8th World Meeting on Pharmaceutics, Biopharmaceutics and Pharmaceutical Technology. Istanbul, 03.2012

Zellnitz S., Schroettner H., Urbanetz N.A.: Optimierung von Pulverinhalatoren über oberflächenmodifizierte Trägersysteme. – in: 8. Minisymposium der Verfahrenstechnik – Book of Abstracts. Linz, 05.2012, 168-172

Zellnitz S., Redlinger-Pohn J.D., Schroettner H., Kappl M., Urbanetz N.A.: Modifying the fine particle fraction of dry powder inhalers by carrier surface modification. – in: Conference Proceedings, 12th International Conference on Pharmacy and Applied Physical Chemistry. Graz, 05.2012

Zellnitz S., Redlinger-Pohn J.D., Schroettner H., Kappl M., Urbanetz N.A.: Surface optimized model carrier systems for pulmonary drug delivery. – in: Conference Proceedings, 20th International Congress of Chemical and Process Engineering. Prag, 08.2012

Zellnitz S., Redlinger-Pohn J.D., Schroettner H., Kappl M., Urbanetz N.A.: Glass beads as alternative carrier systems for dry powder inhalers – in: conference proceedings, 7th International Conference for Conveying and Handling of Particulate Solids. Friedrichshafen, 09.2012, online

Zellnitz S., Redlinger-Pohn J.D., Schroettner H., Kappl M., Urbanetz N.A.: Mechanical modification of glass beads used as model carrier particles in dry powder inhalers. – in: Conference Proceedings, Drug Delivery to the Lungs 23. Edinburgh, 12.2012, 261-264

Zellnitz S., Redlinger-Pohn J.D., Schroettner H., Kappl M., Urbanetz N.A.: Characterization of physically modified glass beads as potential carrier particles in dry powder inhalates – in: 9. Minisymposium der Verfahrenstechnik – Book of Abstracts. Leoben, 04.2013, 262-265

Zellnitz S., Redlinger-Pohn J.D., Schroettner H., Kappl M., Urbanetz N.A.: Surface modified model carrier particles for the use in dry powder inhalates – in: Conference Proceedings, International Congress on Particle Technology. Nuernberg, 04.2013

Zellnitz S., Schroettner H., Kappl M., Urbanetz N.A.: Preparation of adhesive mixtures of surface modified glass beads as model carriers in dry powder inhalers and spray dried salbutamol sulphate – in: Conference Proceedings, AIChE Annual Meeting 2013. San Francisco, 11.2013

Zellnitz S., Schroettner H., Kappl M., Urbanetz N.A.: Understanding the mixing behavior of mechanically modified glass beads as model carriers in DPIs and salbutamol sulphate. – in: Drug Delivery to the Lungs 24. Edinburgh, 12.2013, 267-270

Zellnitz S., Schroettner H., Kappl M., Urbanetz N.A.: Tailoring drug delivery to the lung by using modified glass beads as model carrier. – in: Site specific and controlled delivery. Kiel, 02.2014, 21

Zellnitz S., Schroettner H., Kappl M., Urbanetz N.A.: Investigation of surface modified glass beads as potential carriers in dry powder inhalers. – in: 23rd Scientific Congress of the Austrian Pharmaceutical Society – Book of abstracts. Graz 04.2014, 77

10.2.4 Conference participation – invited oral presentations

Zellnitz S., Redlinger-Pohn J.D., Schroettner H., Urbanetz, N.A.: Interparticle Interactions in Dry Powder Inhalers – in: SPP 1486 “Particle in contact“ AFM-Workshop. Mainz, 09.2011 Zellnitz, S.; Urbanetz, N.A.: The importance of interparticle interactions for the performance of dry powder inhalers – in: SPP “Particle in contact” Kick off Meeting. Frankfurt, 12.2010

10.2.5 Conference participation –oral presentations

Zellnitz S., Urbanetz N.A.: The importance of interparticle interactions for the performance of dry powder inhalers – in: SPP 1486 “Particle in contact” Kick off Meeting. Frankfurt, 12.2010

Zellnitz S., Redlinger-Pohn J.D., Schroettner H., Urbanetz, N.A.: Interparticle Interactions in Dry Powder Inhalers – in: SPP “Particle in contact“ AFM-Workshop. Mainz, 09.2011

Zellnitz S., Redlinger-Pohn J.D., Schroettner H., Kappl M., Urbanetz N.A.: Glass beads as alternative carrier systems for dry powder inhalers – in: 7th International Conference for Conveying and Handling of Particulate Solids (CHOPS2012). Friedrichshafen, 09.2012

Zellnitz S., Schroettner H., Kappl M., Urbanetz N.A.: Preparation of adhesive mixtures of surface modified glass beads as model carriers in dry powder inhalers and spray dried salbutamol sulphate – in: American Institute of Chemical Engineers (AIChE) Annual Meeting 2013. San Francisco, 11.2013

10.2.6 Conference participation - poster presentations

Zellnitz S., Redlinger-Pohn J.D., Schroettner H., Urbanetz, N.A.: Enhancing the performance of dry powder inhalers by tailoring Interparticle forces via surface modification of carrier and active. – in: Joint Meeting of the Austrian and German Pharmaceutical Societies (oedphg 2011). Innsbruck, 09.2011

Zellnitz S., Redlinger-Pohn J.D., Schroettner H., Urbanetz, N.A.: The importance of interparticle interactions for the performance of dry powder inhalers. – in: European Congress of Chemical Engineering (ECCE2011). Berlin, 09.2011

Zellnitz S., Redlinger-Pohn J.D., Schroettner H., Urbanetz, N.A.: Tailoring interparticle interactions to improve the performance of dry powder inhalers. – in: International Congress of Pharmaceutical Engineering (ICPE2011). Graz, 09.2011

Zellnitz S., Redlinger-Pohn J.D., Schroettner H., Urbanetz, N.A.: Improving the performance of dry powder inhalers by tailoring interparticle interactions. – in: Drug Delivery to the Lungs (DDL22). Edinburgh, 12.2011

Zellnitz S., Schroettner H., Urbanetz, N.A.: Chemical surface modification of glass beads used as model carriers for dry powder inhalates. – in: 8th World Meeting on Pharmaceutics, Biopharmaceutics and Pharmaceutical Technology. Istanbul, 03.2012

Redlinger-Pohn J.D., Zellnitz S., Schroettner H., Urbanetz, N.A.: Mechanically treated glass beads as surface modified carrier particles for dry powder inhalates. – 8th World Meeting on Pharmaceutics, Biopharmaceutics and Pharmaceutical Technology. Istanbul, 03.2012

Zellnitz S., Schroettner H.; Urbanetz N.A.: Optimierung von Pulverinhalatoren über oberflächenmodifizierte Trägersysteme. – in: 8. Minisymposium der Verfahrenstechnik. Linz, 05.2012 (oral poster presentation)

Zellnitz S., Redlinger-Pohn J.D., Schroettner H., Kappl M., Urbanetz N.A.: Modifying the fine particle fraction of dry powder inhalers by carrier surface modification. – in: 12th International Conference on Pharmacy and Applied Physical Chemistry (PhandTA12). Graz, 05.2012 (oral poster presentation)

Zellnitz S., Redlinger-Pohn J.D., Schroettner H., Kappl M., Urbanetz N.A.: Impacting interparticle interactions in carrier-based dry powder inhalers (DPIs) by carrier particle surface modification. – in: International Fine Particles Research Institute (IFPRI) Meeting. Ludwigsburg, 06.2012

Zellnitz S., Redlinger-Pohn J.D., Schroettner H., Kappl M., Urbanetz N.A.: Surface optimized model carrier systems for pulmonary drug delivery. – in: 20th International Congress of Chemical and Process Engineering. Prag, 08.2012

Zellnitz S., Redlinger-Pohn J.D., Schroettner H., Kappl M., Urbanetz N.A.: Mechanical modification of glass beads used as model carrier particles in dry powder inhalers. – in: Drug Delivery to the Lungs (DDL23). Edinburgh, 12.2012

Zellnitz S., Redlinger-Pohn J.D., Schroettner H., Kappl M., Urbanetz N.A.: Characterization of physically modified glass beads as potential carrier particles in dry powder inhalates – in: 9. Minisymposium der Verfahrenstechnik. Leoben, 04.2013

Zellnitz S., Redlinger-Pohn J.D., Schroettner H., Kappl M., Urbanetz N.A.: Surface modified model carrier particles for the use in dry powder inhalates – in: International Congress on Particle Technology (PARTEC). Nuernberg, 04.2013

Zellnitz S., Schroettner H., Kappl M., Urbanetz N.A.: Understanding the mixing behavior of mechanically modified glass beads as model carriers in DPIs and salbutamol sulphate. – in: Drug Delivery to the Lungs (DDL24). Edinburgh, 12.2013

Zellnitz S., Schroettner H., Kappl M., Urbanetz N.A.: Tailoring drug delivery to the lung by using modified glass beads as model carrier. – in: Controlled release society (CRS) local chapter meeting – site specific and controlled delivery. Kiel, 02.2014

Zellnitz S., Schroettner H., Kappl M., Urbanetz N.A.: Investigation of surface modified glass beads as potential carriers in dry powder inhalers. – in: 23rd Scientific Congress of the Austrian Pharmaceutical Society. Graz 04.2014, 77

*Presenting authors are underlined.